2024

Epithelial remodeling and microbial dysbiosis in the lower respiratory tract of vitamin A-deficient mouse lungs

BOSTON UNIVERSITY

ARAM V. CHOBANIAN & EDWARD AVEDISIAN SCHOOL OF MEDICINE

Dissertation

EPITHELIAL REMODELING AND MICROBIAL DYSBIOSIS IN THE LOWER RESPIRATORY TRACT OF VITAMIN A-DEFICIENT MOUSE LUNGS

by

KILONI QUILES

B.S., University of Massachusetts Boston, 2018

Submitted in partial fulfillment of the

requirements for the degree of

Doctor of Philosophy

2024

Approved by

First Reader

Felicia Chen, M.D.
Associate Professor of Medicine

Second Reader

W. Evan Johnson, Ph.D.
Director, Professor of Medicine

DEDICATION

I would like to dedicate this work to my incredibly patient spouse Jens and our fur-baby Chewi. I'd also like to dedicate this to the true inspiration of my journey, my hometown community, family, and friends who have lost their quality of life from lack of access to adequate healthcare and affordable treatment. You are the ones who influenced my career choices and continue to be the "why" behind my work. To those who have passed away before I could finish and to those who are still with me today, this is truly in dedication to you.

ACKNOWLEDGMENTS

I would like to acknowledge all the help and support received by my two advisors, Dr. Felicia Chen and Dr. W. Evan Johnson. I would also like to thank Dr. Sènégal Carty for all of her support and assistance during the preparation of this dissertation. Special thanks to Dr. Andrew Lunel-Tilton for his assistance with immunohistochemistry, Dr. Michael Kirber and the Microscopy core for their assistance with imagery and videomicroscopy. Special thanks to Dr. Nick Crossland, Hans, and Aiofe from the National Emerging Infectious Diseases Laboratories (NEIDL) Comparative Pathology Laboratory for their histology work. Yuriy O.Alekseyev, Ashley Leclerc, Nickolas Gorham, and Christopher Williams from the BU Sequencing core were incredibly helpful in optimizing our samples for bulk sequencing. I would also like to acknowledge the Boston University Division of Graduate Medical Sciences, the Boston University Medical Campus (BUMC) Pulmonary Center, and the Computational Biomedicine Department for the training and support to accomplish this dissertation.

EPITHELIAL REMODELING AND MICROBIAL DYSBIOSIS

IN THE LOWER RESPIRATORY TRACT OF

VITAMIN A-DEFICIENT MOUSE LUNGS

KILONI QUILES

Boston University Aram V. Chobanian & Edward Avedisian School of Medicine, 2024

Major Professor: Felicia Chen M.D., Assistant Professor of Medicine

Note that at the time of submission, parts of the following section were under review at Science Translational Medicine. They were also available as a preprint at BioRxiv: https://doi.org/10.1101/2024.06.21.600110

ABSTRACT

While the lung was once believed to be sterile, research now shows that transient microbial communities exist within healthy lungs and are often dysregulated in patients suffering from malnourishment, respiratory infections, and disease. According to the World Health Organization, vitamin A deficiency (VAD) is a major public health issue in low-income communities and many developing countries, while additional studies have shown dietary VAD leads to various lung pathologies. The inability to parse vitamin A-mediated mechanisms from other metabolic mechanisms in humans with pathogenic endotypes, as well as the lack of data investigating how VAD affects the lung microbiome, remains a significant gap in the field. To address this unmet need, we compared molecular, metatranscriptomic, and morphometric data to identify how dietary VAD affects the lung as well as the lung microbiome. Our research shows structural and functional alterations in

host-microbe-diet interactions in VAD lungs compared to vitamin A-sufficient (VAS) lungs; these changes are associated with epithelial remodeling, a breakdown in mucociliary clearance, microbial imbalance, and altered microbial colonization patterns after 8 weeks of vitamin A-deficient diet. These findings confirm vitamin A is critical for lung homeostasis and provide mechanistic insights that could be valuable for the prevention of respiratory infections and disease.

TABLE OF CONTENTS

LIST OF TABLES

LIST OF FIGURES

LIST OF ILLUSTRATIONS

LIST OF ABBREVIATIONS

ALDH ..... Aldehyde dehydrogenase

ALDH1A1 ..... Aldehyde dehydrogenase 1 family member A1

ARDS ..... Acute respiratory distress syndrome

BAL ..... Bronchoalveolar lavage

BALF ..... Bronchoalveolar lavage fluid

BUMC ..... Boston University Medical Campus

CC ..... Ciliated cells

CFU ..... Colony forming units

ChEA ..... ChIP-X Enrichment Analysis

COPD ..... Chronic obstructive pulmonary disease

DAMP ..... Damage-associated molecular pattern

DEG ..... Differentially expressed gene

dnRAR ..... Dominant-negative retinoic acid receptor α

E2F4 ..... Transcription factor E2F4

EPS ..... Extracellular polymeric substrate/substance

FDR ..... False discovery rate

FISH ..... Fluorescence in-situ hybridization

FOXJ1 ..... Forkhead box protein J1

FOXM1 ..... Forkhead box protein M1

GO ..... Gene ontology

GP ..... Gram-positive

H&E ..... Hematoxylin and eosin

iCre .....Inducible Cre-recombinase enzyme

IHC ..... Immunohistochemistry

IPF .....Idiopathic pulmonary fibrosis

IT..... Intratracheal

JUN .....Jun proto-oncogene

LRAT .....Lecithin retinol acyltransferase

LRT ..... Lower respiratory tract

MCC .....Mucociliary clearance

MT .....Microbial transplant

NEIDL ..... National Emerging Infectious Disease Laboratories

Nkx2.1 .....NK homeobox 1

NLR ..... NOD-like receptor

OTU ..... Operational taxonomic unit

PAMP .....Pathogen-associated molecular pattern

PCoA..... Principle coordinate analysis

PCP .....Planar cell polarity

PCR ..... Polymerase chain reaction

PRR .....Pattern recognition receptor

QC ..... Quality control

qRT-PCR ..... Quantitative real-time polymerase chain reaction

QS ..... Quorum sensing

R26 ..... ROSA26 locus

RA ..... Retinoic acid

RAD ..... Retinoic acid deficiency/retinoic acid deficient

RAR ..... Retinoic acid receptor

RARE ..... Retinoic acid response element

RIN ..... RNA Integrity Number

RLR ..... Retinoic acid-inducible gene-I like receptor

RNAseq ..... Ribonucleic acid sequencing

RNA ..... Ribonucleic acid

rRNA ..... Ribosomal ribonucleic acid

RXR ..... Retinoid X receptor

SCFA ..... Short chain fatty acids

TB ..... Tuberculosis

TF ..... Transcription factor

TLR ..... Toll-like receptor

UV ..... Ultraviolet

VAD ..... Vitamin A deficiency/vitamin A-deficient

VADD ..... Vitamin A deficiency-associated disorders

VADMT ..... Vitamin A-deficient microbial transplant

VAS ..... Vitamin A sufficient

VASMT ..... Vitamin A-sufficient microbial transplant

WHO ..... World Health Organization

Note that at the time of submission, parts of the following section were under review at Science Translational Medicine. They were also available as a preprint at BioRxiv: https://doi.org/10.1101/2024.06.21.600110

INTRODUCTION

SECTION 1: Vitamin A

1.1 Overview

Vitamin A is an essential micronutrient in all vertebrate animals, including humans. It cannot be created endogenously and therefore must be ingested through diet.[1] The two major dietary forms of vitamin A are preformed vitamin A (retinol, retinyl esters) and provitamin A carotenoids (such as alpha- and beta-carotene); preformed vitamin A is derived from animal products such as meat, eggs, and dairy, while provitamin A carotenoids are derived from plant foods and are converted to retinol in the body.[1,2] Dietary vitamin A is absorbed by the small intestine and circulates as retinol in the body, where it is then taken into the cells.[3]

All-trans retinoic acid (RA), the bioactive metabolite of vitamin A, is essential for reproduction,[4] embryonic development and growth,[5] vision,[6] and immunity[7] in mammals. Studies have shown serum and liver vitamin A levels do not accurately reflect the bioavailability of RA in the tissue.[8] This is because the concentration of RA is tightly regulated at both the tissue and cellular levels. When the tissue has sufficient or excess RA, the retinol is converted to retinyl ester for storage, a process mediated by lecithin retinol

acyltransferase (LRAT).[9] However, when there is a deficiency of RA (RAD), the oxidation of retinol to RA occurs, with a key step mediated by aldehyde dehydrogenase (ALDH).[10] RA then enters the nucleus where it binds to retinoid X receptor (RXR) and retinoic acid receptor (RAR) heterodimer known as the retinoic acid response element (RARE) to mediate transcriptional activity (Illustration 1).[11-12]

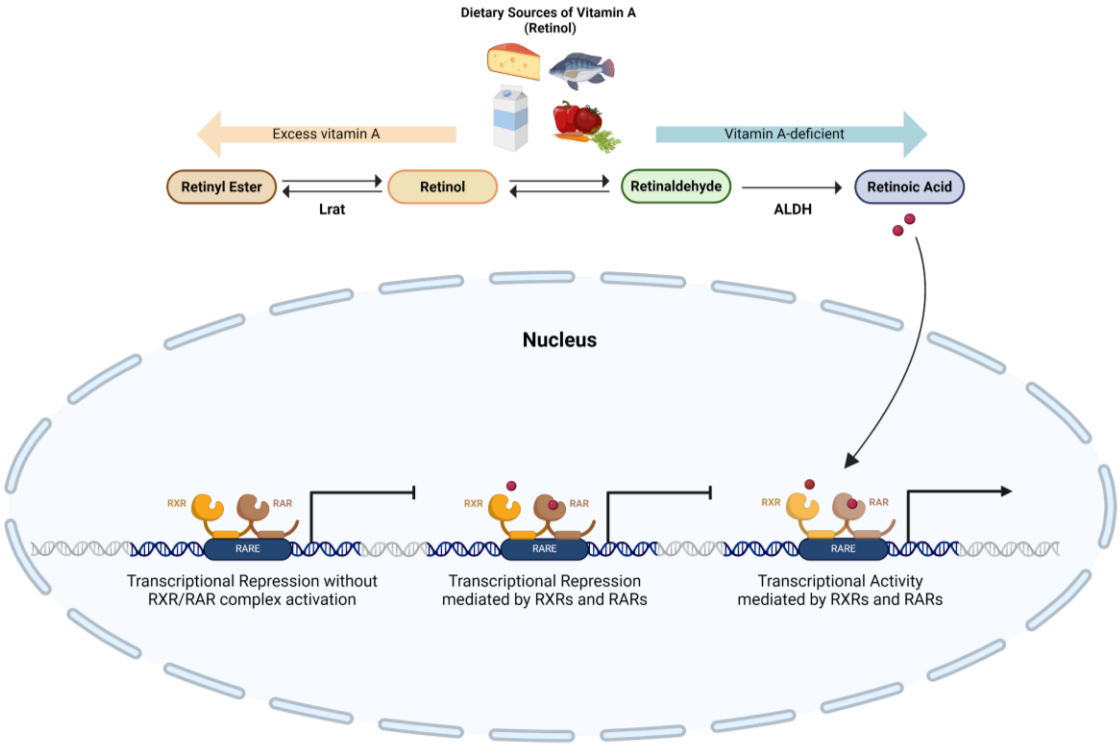

Illustration 1: Metabolic pathway of vitamin A.

In a VAD setting, retinol is converted to RA. RA enters the nucleus and binds to RAR/RXR heterodimers to activate transcription of the target gene. In the VAS setting, retinol is converted to retinyl ester by LRAT and stored within the cell. Illustration created using Biorender.

1.2 Epidemiology

Vitamin A deficiency (VAD), combined with protein malnutrition, is the most common nutritional disorder in the world.[8] According to the World Health Organization (WHO), VAD primarily affects low-income communities and developing countries, two demographics where recurrent respiratory infections are common, and malnutrition is widespread.[8,13-15] Low vitamin A intake greatly raises the risk of VAD-associated disorders (VADD) such as xerophthalmia, worsened infection, and mortality.[16-18] VAD patients often suffer from diarrhea, respiratory diseases, and other inflammatory disorders, which lowers the endogenous vitamin A level further by (1) reducing intake due to anorexia and malabsorption, (2) decreasing the level of transport proteins, and (3) excess excretions via the urinary and gastrointestinal tracts, further heightening the risks of VADD.[8,19]

1.3 Respiratory Manifestations

It is well-documented that vitamin A plays an essential role in the maintenance of mucociliary differentiation of the tracheobronchial tree in vertebrates, including humans.[20-22] Chronic VAD in humans predisposes the host to chronic obstructive pulmonary disease (COPD), asthma, idiopathic pulmonary fibrosis (IPF), and respiratory infections such as tuberculosis (TB), influenza, measles, and SARS-CoV-2.[8,23-28] A major clinical challenge is the inability to fully reverse the epithelial damage, infection risk, and mortality rate in patients with vitamin A supplementation alone.[29-31] In some cases, malnourished patients given excess vitamin A can cause a cytotoxic condition known as hypervitaminosis A in patients.[8] leading to symptom exacerbation and a worsened prognosis overall.[32]

Conversely, respiratory infections have been shown to deplete vitamin A serum levels and retinoid stores in patients,[8] effectively inducing VAD independent of diet.[33]

Additionally, there are associations between the composition and diversity of the lower respiratory tract (LRT) microbiome and idiopathic pulmonary fibrosis (IPF), asthma,[34] acute respiratory distress syndrome (ARDS),[35] COPD,[36] lung cancer,[37] and SARS-CoV-2-induced lung damage.[38] These findings suggest that the LRT microbial microenvironment may trigger, predispose, or exacerbate lung pathogenesis. Thus, identifying alternative therapeutic targets would not only impact the long-term health of patients, but may also be an effective prevention and control strategy for the transmission of respiratory infections to the greater public.

SECTION 2: Lung

2.1 Overview

Descending from the trachea, the airway branches into an increasingly intricate network of bronchi leading into the airspaces of the LRT.[39] Maintaining the proximal and distal airway structure is a major component regulating healthy airway function in adults. RA acts directly or indirectly to influence cellular proliferation, differentiation, and patterning of the respiratory system; these mechanisms tightly regulate tissue determination, branching morphogenesis, and alveolarization.[40] The airways are lined by a pseudostratified epithelium, which plays a major role in mucociliary clearance (MCC), a critical innate defense mechanism responsible for maintaining homeostasis in the lung.[41]

In addition to airway clearance, the epithelium maintains the mechanical barrier of the airway. Adhesion and tight junctions bind epithelium together to form the physical-mechanical barrier responsible for preventing microbial invasion and lung infection.[42] Smoking, malnutrition, and bacterial infections are just a few ways that airway barrier function can be aberrated, leading to permeability of the epithelium, a loss of cellular polarity, a reduction in ciliary beat frequency, and a subsequent loss of proper MCC mechanics.[43-44] Specifically, chronic VAD can lead to squamous metaplasia of the airway epithelium that predisposes humans to respiratory infections and disease.[31] With dietary VAD becoming a global phenomenon in disparate communities, exploring RA-mediated mechanisms responsible for epithelial remodeling, embryonic lung development, and adult lung health remains an unmet need.

2.2 Lung Components of Immunity

2.2.1 Epithelium in Innate and Adaptive Immunity

Increasing evidence suggests the lung epithelium play an essential role in both innate and adaptive immune responses.[45] As the first line of defense against pathogens and other insults, the airway epithelium performs multiple functions simultaneously: barrier integrity, cell-cell sensing and signaling, mucosal immunity, and microbial clearance.[45-46] Proliferation in the airway is largely quiescent in healthy adult lungs but is markedly increased in patients with COPD, cystic fibrosis, and cancer; increased proliferation causes epithelial remodeling that impairs these critical functions and leads to a breakdown in lung structure and function.[47-48] Epithelium also expresses molecules that modify the immune landscape in the lungs by triggering B- and T-cell activation and differentiation.

Dysregulation of these mechanisms often leads to lung inflammation and injury over time.[49]

2.2.2 Localized vs. Distal Immune Responses

While immune activation can be triggered locally in the lung as previously described, it can also be activated by distal signals from the gut where over 70% of the body's total immune response occurs; signaling peptides such as short-chain fatty acids travel to the lung to modify the local immune landscape via the gut-lung axis.[50] Gut dysbiosis is one of the factors found in patients with developing asthma and other respiratory conditions.[51-53] Fecal transplants of healthy gut microbes into mice with *S.pneumoniae* lung infections both alleviated the infection and lowered cytokine levels in the lung, illustrating how the gut microbiome can distally modify lung immunity.[54-55]

2.2.3 Quorum Sensing

Another method of modifying localized immune responses is through quorum sensing (QS). When growth conditions change, such as a loss of nutrients or an increase in oxidative stress, bacteria and fungi secrete molecules into the extracellular space that activate signaling pathways to alter host immunity and cellular gene expression.[56] QS permits bacteria to communicate as a community, signaling behaviors such as planktonic-to-sessile adherence, biofilm formation, and antibiotic resistance.[57-58]

2.2.4 Pathogen Detection

In addition to the MCC, lung epithelial cells can control or kill microbes by releasing antimicrobial peptides into the airways following activation of pattern

recognition receptors (PRRs) by pathogen-associated molecular patterns (PAMPs) or damage-associated molecular patterns (DAMPs).[59] PAMPs are derived from microbes and are largely pro-inflammatory signaling molecules that cause localized tissue inflammation and injury in response to infection.[60] DAMPs are host-derived molecules released from damaged, dying, or tumor cells.[61] DAMPs can activate an immune response like an infection but without the microbial insult, a phenomenon that often exacerbates the severity of existing lung infections.[62-64] DAMPs are common in patients who recently suffered excessive cellular stress, damage, and aberrant remodeling to the tissue, but can also be found in response to hypoxia or ischemia.[65-67]

PRRs are found on innate immune cells, epithelial cells, and fibroblasts.[68-69] Some of the most common PRRs include membrane-bound toll-like receptors (TLRs), intracellular NOD-like receptors (NLRs) and intracellular retinoic acid-inducible gene I-like receptors (RLRs).[70] Once ligands bind to PRRs, a signaling cascade triggers changes in gene transcription and post-translational modification in host cells that often alter cellular structure and function. Despite extensive research, most mechanisms responsible for PRR selectivity and activation by QS signaling peptides are still being investigated.

2.2.5 Role of Airway Epithelium in Maintaining MCC

Animal models deficient in vitamin A display respiratory epithelial hyperplasia followed by squamous metaplasia.[71] Similarly, airway epithelial culture in-vitro in medium free of RA loses the pseudostratified mucociliary epithelium and possesses a stratified, squamous morphology.[72] The loss of pseudostratified mucociliary epithelium is also a

hallmark of several respiratory diseases characterized by epithelial injuries, repair defects, tissue remodeling, and altered MCC.[73-74]

The two main epithelial cell types in the LRT are secretory cells and ciliated cells (CCs). At the bronchoalveolar transition sites in the human airway, club cells (formerly called Clara cells) replace the function of goblet cells in mucin production, a major component of epithelial barrier integrity and microbial defense.[75] Club cells are non-ciliated cells capable of mucus (bronchial feature) and surfactant (alveolar feature) production, and are the major secretory cells in the intraparenchymal airways.[75-76] Secretory cells secrete a mucinous layer that protects the apices of the airway epithelium by trapping the inhaled particles, potential pathogens, and commensal microbes within the mucin. CCs facilitate the transport of microbes, particles, and other pollutants proximally to expel these substances, a process known as the mucociliary escalator and a major component of MCC mechanics in the lung.[74]

TUBB4A and CC10 proteins are both critical for maintaining lung homeostasis through MCC mechanisms.[77] Several studies have found secretory protein CC10 expression up-regulated in obstructive lung diseases and down-regulated in restrictive lung diseases, making CC10 an important biomarker for lung health and disease.[78] Likewise, expression of nuclear FOXJ1 and ciliary TUBB4A proteins are key regulators of motile ciliogenesis in the airway epithelium.[79-80]

2.2.6 Planar Cell Polarity and Ciliogenesis

Planar cell polarity (PCP) is a ubiquitously conserved mechanism in eukaryotes that is maintained by many factors. Desmosomes, tight junctions, and adherens junction complexes are a few components that aid in maintaining barrier integrity while permitting signaling between the epithelium along the airway.[81] Cytoskeletal components maintain structural integrity and help define the apical and basal regions of the cell.[82] When barrier integrity is lost, junction complexes cannot maintain cell polarity effectively, leading to a disruption in cellular organization and division.[83]

2.2.7 Respiratory Infections and Malnutrition

Malnourishment, either in the form of undernourishment or obesity, alters the host immune response and increases the risk of infections.[84] Pneumonia and acute lower respiratory infections continue to be major causes of childhood mortality worldwide, especially in malnourished children from developing countries.[85-86] Likewise, malnourishment has been shown to alter both innate and adaptive immune responses in humans, with VAD specifically associated with the development and severity of asthma, pneumonia, COPD, TB, lung cancer, measles, influenza, and SARS-CoV-2 infection.[8,24-28,87] Despite the strong correlation between VAD and the increased risk and severity of respiratory infections, the mechanisms driving this vulnerability are still unclear and warrant further study.

SECTION 3: Lung Microbiome

3.1 Overview

A healthy lung microbiome is maintained through a careful balance of immigration and elimination.[88] In this way, the lung is a unique microenvironment due to the transient nature of its microbial communities. However, when MCC is impaired, the microbes cannot be expelled effectively, providing a permissive niche for pathogenic microbial colonization and biofilm formation.[89-90] The subsequent dysbiosis may cause further epithelial injury, leading to chronic diseases.

While the field of *microbiomics* - or the study of the microbiome as a discipline - is still rapidly developing, new insights continue to support associations between the diversity and composition of the lung microbiome and the health of adult lungs in humans. Unfortunately, investigating changes in microbial composition in the human LRT is expensive, invasive, and relatively difficult. Sputum samples and nasal swabs are the most common forms of collection for respiratory microbiome analysis but are not representative of the LRT specifically as the upper respiratory tract microbes are also present in these samples.[91] The “gold standard” sampling method is to extract lung tissue from the patient for sequencing, a technique that is invasive, painful, risky, and challenging to control for covariables such as differences in collection sites, demographics, and patient cohorts. Combined with factors such as genetic background and lifestyle, reproducibility of patient-derived microbiome research quickly becomes a dubious task.[92-93] Creating standards in microbiome research that leverage reproducible models such as in-vitro organoids or in-

vivo animal models will help standardize the field and reduce technical bias in microbiome results.

3.2 Lung Microbiome and Respiratory Disease

3.2.1 Lung Microbiome in Patients with Disease or Infection

It has been well-characterized that infectious agents impair lung function and repair mechanisms in malnourished patients, but these studies fail to account for more complex host-microbe and microbe-microbe interactions, leaving the mechanisms involved in these interactions largely unknown.[94] Several studies highlight the role that common pathogens and commensals play in health and disease, but few have investigated the relationship between diet, microbial abundance, and lung pathogenesis. Especially within the LRT where microbial abundance is low, understanding the dynamic flux of microbial activity is imperative to uncovering biomarkers for lung infection and disease, which holds tremendous potential for early clinical diagnostics.[95]

3.2.2 Biofilms and Lung Pathogenesis

Several host- and microbe-derived factors carefully regulate microbial adherence, colonization, and invasion/infection in the lung, such as the mucosal immune system, signaling peptides within the airway, bacteriocins, and bacteriophage.[96-101] In hostile conditions such as nutrient deprivation, hypoxia, or inflammatory cell activation, bacteria can form a colony that collectively produces a protective outer shell to protect from antimicrobial substances and to preserve nutrients and energy; this shell is often called an extracellular polymeric substrate or substance (EPS).[102-104]

Biofilms create group dynamics in mixed microbial communities that are both functionally and structurally complex.[105] While several definitions of biofilms exist, for this dissertation we refer to the 2002 Donlan and Costerton definition: "a microbially derived sessile community characterized by cells that are irreversibly attached to a substratum or interface or each other, embedded in a matrix of extracellular polymeric substances (EPS) that they have produced, and exhibit an altered phenotype concerning growth rate and gene transcription."[106]

Chronic or recurrent infections caused by multidrug-resistant pathogens continue to be a significant public health burden and a major cause of morbidity and mortality in hospitalized patients. These pathogens are challenging to eradicate due to their resistance to conventional antibiotics and their ability to form biofilms.[107-108] Biofilm formation is the primary mechanism bacteria utilize to evade the host immune system and antibiotic treatment; once formed, the EPS outer shell is notoriously difficult to destroy.[109] Biofilm-derived bacteria are reprogrammed to break off from the original biofilm and seek another location within the host tissue for invasion, adherence, and colonization; this behavior contributes to inflammation and persistent infections in patients over time.[110-111] Therefore, understanding the mechanisms that trigger biofilm formation in the lung by variably abundant microbes would have great clinical relevance for patient health outcomes.

3.3 Lung Microbiome in Mouse Models

Accurately characterizing host-microbe-diet interactions in humans is difficult. Patients with one vitamin deficiency are often deficient in others and factors like genetics

and lifestyle influence microbial variability, leading to complications and batch effects in downstream analysis.[112-113] The microbiome of each person is unique, containing a consortium of microbes that differs even between siblings or offspring.[114-115] Compositional complexity and inter-microbial dynamics of the microbiome influence the function and structure of adult lungs in ways that require further study. However, experimental standards have yet to be established in the field. There is currently a wide variety of experimental and computational approaches to microbiome research with few gold standards or core principles, leading to discordance in human datasets.[116]

A well-controlled mouse model can overcome most of these challenges. By administering a custom diet to isogenic littermates, we can isolate the functional and morphological effects of dietary VAD on the lung without undue environmental or genetic influence. Here, we used a combined metatranscriptomic, morphometric, and functional approach to explore changes to the host lung epithelium as well as characterize the microbial milieu of the VAD mouse lungs.

Note that at the time of submission, parts of the following section were under review at Science Translational Medicine. They were also available as a preprint at BioRxiv: https://doi.org/10.1101/2024.06.21.600110

MATERIALS AND METHODS

Housing and Dietary Modulation

Wild-type C57BL/6J female mice were purchased from Jackson Laboratory at 7-9 weeks of age (catalog # 000664). Female mice were used exclusively for the preliminary study to minimize in-fighting and potential injury during transit or during the required 1-week acclimation period following arrival to our animal facility, which would minimize the potential for a compromised immune system. Female mice also allowed us to co-house mice shipped in different cages, which would enable us to control for cage effects in our preliminary study.[117] We also used female mice to remove sex effects from the preliminary results, which is another covariate that could have skewed our findings.

Mice were purchased from Jax as littermates to minimize genetic drift as another covariate. Four mice were shipped in each cage; following the acclimation period, mice were separated evenly into each arm of the study and housed with a female from a different cage to ensure any variation in the microbiome due to cage effects was shared evenly between the two dietary treatments. Cage localization and variation in microbes on the cages themselves can drastically affect the outcome of lung microbiome research.84 Considering these findings, we changed the cage, food, water, and bedding as well as

rotated the cages in the rack every 2-3 days so that each cage was never 1) next to the same cages or 2) in the same location on the rack more than once throughout the entire study.

We provided each cage with a custom research diet created by Envigo® that was either vitamin A-sufficient (VAS) or VAD (Catalog # TD.91280 and TD.86143). The chow was sterilized, irradiated, and vacuum-sealed to prevent microbial contamination. After the mice had undergone the desired period of dietary modulation, the mice were euthanized and their lungs extracted. The left lobe of each lung was paraffin embedded for histology and immunohistochemistry (IHC), while the right lobes were homogenized for mixed host-microbe bulk RNAseq (Illustration 2).

RNA Isolation and Extraction

The following protocol was designed by our lab to achieve mixed RNA samples with a higher microbiome RNA yield than previously published techniques. To do so, we tested many approaches and combined portions of three separate protocols for maximum results; a portion of our modified GentleMACS® (Miltenyi Biotec, catalog # 130-096-427) technique created by our lab for cell sorting and whole lung digest, a portion of the QiaShredder® (Qiagen, catalog # 79656) tissue disruption and homogenization protocol to maximize mammalian RNA extraction, and a portion of the PureLink® RNA extraction (Thermo Fisher/Invitrogen, catalog # 12183018A) and DNase Digest (Thermo Fisher/Invitrogen, catalog #s 12185010 and 18068015) for maximum 16S and mixed microbiome sample RNA integrity. The following is our novel mixed host-microbe RNA extraction protocol:

Preparation

Mice were euthanized using isoflurane with cervical dislocation as a secondary method. To ensure minimal cross-contamination, dissection tools were sterilized in 100% ethanol for one hour before placing in a surgical tray. Dissection supplies and pre-aliquoted sterile solutions were placed in a metal surgical tray, the tray sealed in a transparent bag, and processed through a ThermoFisher CL-1000 ultraviolet (UV) crosslinker once (catalog # 95-0174-01, serial # 061608-001). Without opening the bag, items were turned over and processed through the UV crosslinker again. The supplies remained in the sealed transparent bag until it was time for lung extraction. The bag was sterilized with 70% ethanol before placing it in a fume hood to open for use.

Extraction

Lungs were extracted using sterile forceps and dissecting scissors. The trachea and as much of the connective tissue as possible were removed from the LRT while the sample was still within the thoracic cavity to minimize contamination. The left lobe was placed in a canonical tube containing 4% paraformaldehyde and placed on ice. The right lobe was placed in a 1.5mL Eppendorf tube, previously sterilized in the surgical tray, containing 1mL of RNAlater (Thermo Fisher/Invitrogen, catalog # AM7024) and placed on ice. The left lobes were stored in a 4°C refrigerator until the next day.

Whole Lung Tissue Disruption and Homogenization

Each lobe that was previously placed in RNAlater was transferred to a GentleMACS® M-tube (Miltenyi Biotec, catalog # 130-093-236) with 1.2 mL of RLT buffer from the Qiagen® RNeasy mini kit (catalog # 74104). 24 μL 2M DTT was added to the tube, and then homogenized using the GentleMACS^{TM} Octo-dissociator (Miltenyi Biotec, catalog # 130-096-427). Two programs were used that are pre-programmed and standard for this machine; the "m_lung_01_01" setting was run once, followed by two rounds of "RNA_01_01". The M tubes were then centrifuged at 15,000 rpm for 2 minutes. Up to 650 μL of the supernatant was transferred into a QiaShredder spin column by Qiagen® (catalog # 79656), keeping the M tubes on ice. QiaShredder columns were centrifuged at 12,000 x g for 2 minutes before adding 50 μL of RNA-free water directly onto the spin column and centrifuging for another 2 minutes at 12,000 x g. The flow-through tubes were capped and placed on ice between each transfer of the spin column.

Pellet Disruption and Homogenization

100 μL of lysozyme solution was added to the M tubes and vortexed to resuspend the pellet. 8 μL of 1% SDS solution was added before vortexing and transferring the samples to Eppendorf tubes. Using a 21-gauge needle, we rapidly filled and expelled a 1 mL syringe 15-20 times to ensure the bacterial cell walls had been denatured. The tubes were then centrifuged at 12,000 x g for 2 minutes at room temperature before transferring the supernatant to a clean RNA-free microcentrifuge tube.

RNA Extraction

250 μL of 100% ethanol was added to each tube and vortexed briefly. Each sample was transferred into a spin cartridge with a collection tube from the PureLink® RNA extraction kit and centrifuged at 12,000 x g for 15 seconds at room temperature. The flow-through was discarded but not the collection tube. 350 μL of Wash Buffer I was added to the column to repeat the previous step once before discarding and replacing the collection tube. We were sure to use only one spin cartridge per sample tube collected from the homogenization steps. Even though fewer spin cartridges could reduce contamination and the potential for sampling bias, performing too many centrifuges with the same spin cartridge will clog the membrane and dramatically reduce the RNA yield.

DNA Digest

80 μL of DNase Digest solution from the PureLink® DNase digest protocol was added to each spin cartridge and incubated for 15 minutes at room temperature. 500 μL of Wash buffer II was added to each spin column and centrifuged for 15 seconds at 12,000 x g. Flow-through was discarded from the collection tube before repeating the previous step. The spin cartridge was placed into a clean 1.5 mL Eppendorf tube for its final elution and collection phase. 40 μL of RNA-free water was added to the center of the spin column before incubating for 1 minute followed by centrifugation at 12,000 x g for 1 minute. Another 40 μL of RNA-free water was added around the edges of the spin column and the previous incubation and spin steps were repeated once per spin cartridge. Each spin column collected from the same sample was placed into the same Eppendorf collection tube for the

elution stage. Each collection tube was vortexed to combine elutions well before verifying the RNA yield and quality using a Nanodrop^{TM} spectrophotometer.

Using the protocol outlined above, the RNA we collect averages a perfect nucleic acid 260/280 ratio of 2.0-2.1, and an excellent RNA Integrity Number (RIN) of 9.1-9.9. Our designed protocol is exhaustive, requiring an entire day for extraction and three separate RNA processing kits plus additional reagents. However, our downstream analysis results indicate these extra steps lead to higher yields and RINs than other protocols we've tried.

Host-Microbe Total RNA Sequencing (RNAseq)

Sample Selection and Sequencing Depth

To ensure the best quality data, we extracted RNA from 18 samples after 3 weeks (9 VAS and 9 VAD) and 23 samples after 8 weeks of dietary modulation (11 VAS and 12 VAD) before submitting them to the Boston University Microarray and Sequencing Resource (BUMSR) Core Facility for quality control (QC) analysis. The 10 samples at 3 weeks and 14 samples at 8 weeks with the best quality and yields were approved for further processing and library preparation, with 260/280 scores ranging from 2.0 to 2.1 and yields from 40.4 ng/μL to 284.6 ng/μL. To increase the sequencing depth of the microbiome in our mixed samples, BUMSR performed mouse rRNA depletion prior to sequencing. Next Generation total RNA sequencing was performed using the Illumina NextSeq2000. Samples underwent two sequencing runs using a P2 flow cell for the first run and a P3 flow cell for the second run to increase sequencing depth. Each run repeated for 200 cycles with

100 x 100 base pair paired-end reads. The final sequencing depth was approximately 1.77 billion read pairs, ranging from 60.7 to 86.9 million reads for each of the 24 samples collected (Table 1).

Sequence Pre-processing and Alignment

Raw FastQ files of single paired-end reads were trimmed based on minimum Illumina phred scores of 33 using the Trimmomatic package version 0.36.[118-120] The trimmed sequences were aligned to bacterial, fungal, viral, and miscellaneous microbial gene indices downloaded from Refseq[121] while filtering out samples that also aligned to human and mouse gene indices from Refseq. Rsubread was used to align the same sequences to the mouse gene index mm10.[122] Raw RNA sequences feature counts and the pre-processing and sequence alignment code written by our lab is available on our Github repository.[123]

RNAseq Data Analysis

Raw read counts were loaded into two R-based Shiny Apps for preliminary data analysis: for the microbiome, Animalcules[124] version 1.4.0 in RStudio version 4.0.2, and for the host, Single Cell Toolkit[125] version 1.9.1 in RStudio version 4.1.1. Within the Single Cell Toolkit platform, the host RNAseq read counts were normalized using the Limma R/Bioconductor software package,[126] version 3.44.3 in Animalcules and version 3.48.3 in Single Cell Toolkit. Alpha and beta diversity plots were generated in MicrobiomeAnalyst.[127-129] *P*-values for diversity plots were calculated in the app using the

Wilcoxon Rank Sum Test with continuity correction model. BatchQC[128] was used to normalize feature counts using Combat and DESeq2.[130-132]

Paraffin-Embedding and Sectioning Lung Tissue

Left lobes were fixed in a 4% paraformaldehyde solution overnight at 4°C. We then paraffin-embedded the lungs by clearing the tissues in serial dilutions of ethanol and xylene and processing the tissues in a 60°C vacuum oven with paraffin wax for 3 hours. The tissues were left to harden at room temperature before storing in the 4°C fridge until sectioning. Paraffin-embedded tissues were sectioned into 5 μm tissue slices using a microtome. The tissues were left in a 37°C oven overnight to cure before storing in a 4°C fridge until staining.

Immunohistochemical Staining

Protocols for each stain were followed using the guidelines specified by their respective manufacturers; SCGB1A1/CC10 from Santa Cruz Biotech (1:1200, catalog # sc-365992), TUBB4A from Invitrogen (1:1500, catalog # AA10), FOXJ1 from Thermo Fisher Scientific (1:1500, catalog #14-9965-80), Ki-67 from Invitrogen eBioscience (1:200, lot # 1935015), Crumbs from the Varelas laboratory at Boston University (1:1000), Scribble from Santa Cruz Biotech (1:500, catalog # 11049), and E-cadherin from Abcam (1:500, catalog # ab40772).

All secondary antibodies were diluted to 1:500: Donkey anti-rabbit from Jackson Immuno Research (lot # 138314) for CC10, Crumbs and E-cadherin, donkey anti-goat from

Life Technologies (lot # 1627966) for Scribble, and donkey anti-mouse from Thermo Fisher (catalog # A21202) for FOXJ1, TUBB4A, and Ki-67.

Fluorescence In-Situ Hybridization

For fluorescence in-situ hybridization (FISH), we used the RNAscope® 2.5 High-Definition Detection Kit (RED) from ACD Bio (catalog # 322350) and followed the manufacturer instructions for formalin-fixed paraffin-embedded tissues to visualize retinoic acid receptor-ɣ (*RARg*) transcript expression (catalog # 463118). After the hybridization steps, we blocked the tissues in donkey serum (1:200) for 45 minutes before staining with TUBB4A (1:1500) overnight.

Genetic Mouse Model Generation

To create our RA knockdown mouse model, we purchased genetically engineered mice on a C57B/J6 background from Jackson Laboratories.[133] Male mice with a heterozygous tamoxifen-inducible Cre recombinase located in the endogenous Nk2 homeobox 1 (*Nkx2.1*) promoter region were bred with female mice containing a *loxP*-flanked STOP codon upstream of a dominant-negative retinoic acid receptor-α (*dnRAR*) gene in the Rosa26 (R26) locus. The resulting progeny contained a tamoxifen-inducible lung epithelium-specific RAD mutation.[134-135]

These mice underwent daily intraperitoneal injections of tamoxifen (Sigma-Aldrich, catalog # T5648-1G) for 5 days. Tamoxifen doses were 20 mg/mL of corn oil, or 5 μL per gram of body weight. After injections, the mice underwent a mandatory observation period of 3 days in the separate animal facility designated for tamoxifen

injections to ensure they did not experience adverse side effects and to allow the tamoxifen to be externally secreted away from the general mouse population. After the isolation period, the mice were moved to the general mouse facility where they remained for the duration of the study. Lungs were collected at 8 weeks and 19-20 weeks using the same protocol as the dietary model (Illustration 2, 19-20 week data not shown).

Ciliary Function Assay

The tissue collection, processing, and imaging protocol for the ex-vivo tracheal analysis of ciliary motility is published and publicly available by Jove.[136] We used a Nikon wide-field deconvolution epifluorescent microscope at the BUMC Cellular Imaging Core Facility. We used 0.20 μm Fluoresbrite® carboxylate microspheres from Polysciences, catalog number 09834-10. Video footage of microsphere motility was recorded at 250 frames per second in accordance with the above-mentioned Jove protocol. The videos of equal time length were then processed in the Nikon NIS Viewer package and composite images of each video file were generated to measure the distance traveled by each bead using Fiji/ImageJ software.[137] A minimum of 100 beads were measured for each arm of the study.

Morphometric Analysis

Formalin-fixed paraffin-embedding tissues were processed into 5μm sections and stained using hematoxylin and eosin (H&E) or IHC with CC10 and TUBB4A antibodies to visualize the airway epithelium (n = 10). Tissues were imaged at 40x, 63x, and 100x depending on the quality of the image and tissue section. Ciliated cells and secretory cells

were counted using QuPath cell detection and annotation software.[138] Epithelial cell ratios were measured by dividing the number of each cell type by the total number of epithelia. Hyperplastic regions were also calculated from the 8-week VAS and VAD samples using QuPath. Using the drawing function from the toolbar, I manually selected and annotated hyperplastic and non-hyperplastic regions of interest in the airway epithelium. The total area of each classification was measured in μm^2 (3-4 mice per arm and 3-4 images per sample, n = 7) and compared between diets. Hyperplastic ratios were measured by dividing the hyperplastic area by the total area measured per image. The statistical significance of both findings was determined using the student's T-test.

Gram Stain and Colony-Forming Unit Quantification

Formalin-fixed paraffin-embedded tissues were sent to the National Emerging Infectious Diseases Laboratories (NEIDL) Pathology Comparative Laboratory (NPCL). The laboratory of Nick Crossland used a standard Gram stain on 5-μm thick sections before imaging using a whole-slide scanner. Gram-stained sections were visually analyzed on QuPath to count the number of bacterial colony-forming units (CFU) on each whole tissue section (n = 8).

Real-Time polymerase chain reaction (PCR)

Total RNA was extracted using the previously mentioned extraction protocol and processed using the Invitrogen™ Superscript™ III First-Strand Synthesis system for RT-PCR (catalog # 18080051). Samples were reverse transcribed using the manufacturer's instructions. Each cDNA sample was then mixed with TaqMan®, a mouse β-actin

endogenous VIC-labeled control probe from Thermo Fisher (catalog #s 4444557 and 4352341E), and the Thermo Fisher FAM-labeled probe of interest per batch: early secretory marker Scgb3a2 (Mm00504412_m1), late secretory marker Scgb1a1 (Mm00442046_m1), early ciliary marker Foxj1 (Mm01267279_m1), and late ciliary marker Tubb4a (Mm00726185_s1). 20μL of sample mix per well was plated in triplicate into a flat-bottom 96-well plate and analyzed using a QuantStudio3^{TM} real-time PCR system by Thermo Fisher (catalog # A28566) for the Ct Standard Curve (ΔΔCt).

Bronchoalveolar lavage (BAL) Microbial Extractions

After 8 weeks of dietary modulation, BAL donor mice were euthanized with isoflurane (Sigma, catalog # 792632) in an induction chamber. The trachea was exposed using sterile scissors and forceps. 20-gauge sterile catheters (BD Angiocath^{TM}, Ref # 381134) were inserted into the stoma made in the exposed mouse trachea (Supplemental Figure 3). We collected 500 μL of BAL fluid (BALF) after administering 700 μL of sterile PBS (Gibco, catalog # 14190144) with a sterile syringe (BD, Ref # 309602). This step was repeated once more for a total sample collection of 1mL. Samples were centrifuged at 12,000 x g for 2 minutes at 4°C before removing the upper 900 μL of supernatant. Samples were vortexed briefly before performing a live/dead cell stain using Trypan Blue (Thermo Fisher, catalog # 15250061) and following the manufacturer's instructions. Cell counts were performed using a Corning® Cytosmart^{TM} cell counter (catalog # 6749) with the gating size set to 0-11 μm. Cell counts were performed in triplicate, vortexing the filtered BAL briefly between each run. The final cell counts and cell sizes were averaged and graphed using the Cytosmart^{TM} Technologies software that comes standard with the

machine. Samples were kept on ice until the instillation stage. The average live cell concentration extracted using this protocol was approximately 1.5 x 10^6 cells/mL.

Intratracheal Microbial Transplants

BAL recipient mice were anesthetized with isoflurane inside an induction chamber. Mice were kept in the chamber until their heartbeat slowed and were immobile but not deceased. The recipient mice were mounted on a rodent intubation stand (Braintree Scientific, SKU # RIS 100) suspended by their incisors using string, and secured to the stand by the tail. The tongue was held with sterile forceps out of the mouth and gently pulled to one side while 100 μL of the donor BAL was administered intratracheally (IT) using a 100 μL pipette and sterile pipette tip. The mouse would then aspirate the microbial transplant (MT) for several seconds but no more than 30 seconds; the IT instillation was considered successful once the mouse was breathing normally. We found the MT predominantly infiltrated the left lobe and the proximal regions of the right lobe using this approach (data not shown).

Note that at the time of submission, parts of the following section were under review at Science Translational Medicine. They were also available as a preprint at BioRxiv: https://doi.org/10.1101/2024.06.21.600110

RESULTS

CHAPTER ONE: VAD ALTERS LUNG FUNCTION AND MORPHOLOGY

Establishing VAD in mouse lungs

For the purposes of this study, we define "chronic VAD" as maintaining an adult mouse on a VAD diet for 8 weeks.[139] We maintained 8-week-old wild-type C57BL/6J mice on a VAS or VAD diet for 8 weeks before extracting both lobes of the lung for bulk RNA sequencing and histology/IHC analysis (Illustration 2). Since serum vitamin A levels do not accurately represent RA bioavailability in the lung, we opted to measure the RNA expression of two enzymes that are critically involved in the vitamin A metabolic process, lecithin retinol acyltransferase (*Lrat*) and aldehyde dehydrogenase 1 family memberA1 (*Aldh1a1*) (Illustration 1).[9-10]

When the body is deficient in vitamin A, retinyl esters stored within the cells are metabolized back into retinol, oxidized into retinaldehyde by alcohol dehydrogenase enzyme, and then converted to RA by ALDH enzymes.[10] The expression of LRAT is down-regulated and ALDH1A1 is up-regulated to facilitate the biosynthesis of RA (Figure 1A).[140] These transcriptional changes indicate the vitamin A pathway is altered to favor retinol-to-RA biosynthesis, but further evidence is required to make that conclusion.

We next assessed changes in gene expression of known vitamin A targets to see if VAD lungs showed a reduction in vitamin A signaling. A heatmap depicting the level of expression (LogCPM) of vitamin A target genes cluster VAS and VAD samples separately (Figure 1B).[141-148] Expression of these vitamin A target genes was also down-regulated in VAD lungs overall compared to the VAS lungs, indicating that VAD leads to reduced vitamin A pathway activation.

Finally, genes down-regulated in VAD compared to VAS lungs ($p < 0.05$) were analyzed against gene sets from the ChIP-X Enrichment Analysis (ChEA) transcription factor target database.[149] Gene sets associated with RARs and RXRs were found highly enriched in our samples (Figure 1C).[150] These findings provide further support that the mouse lungs are deficient in vitamin A signaling after dietary vitamin A deprivation for 8 weeks.

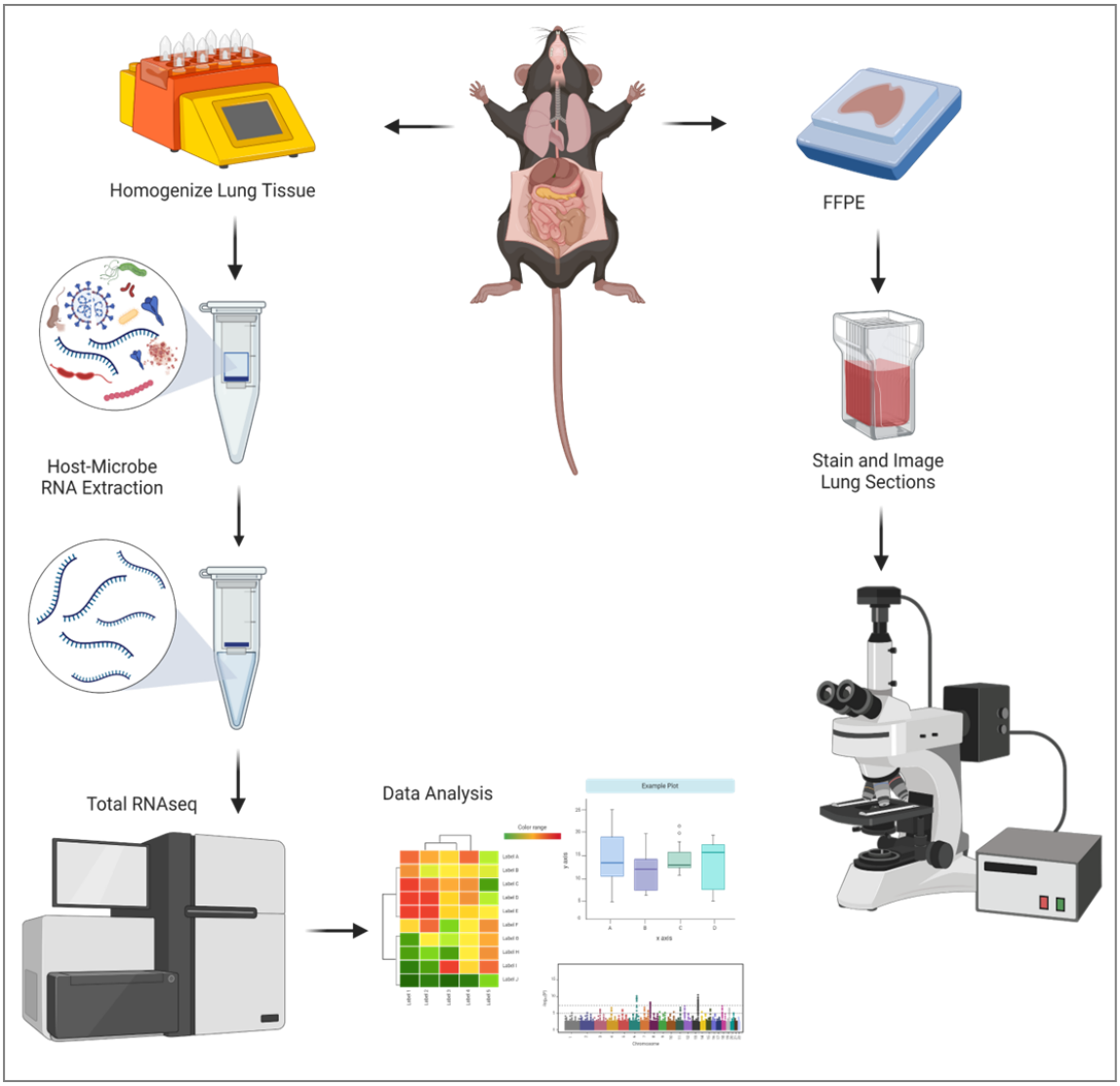

Illustration 2. Schematic of the sample collection workflow for VAD studies.

Adult wild-type C57BL/6J mice were maintained on a VAS or VAD diet for 8 weeks. Both lobes of the lung were used for bulk RNA sequencing, histology, and IHC. Figure was created using BioRender.

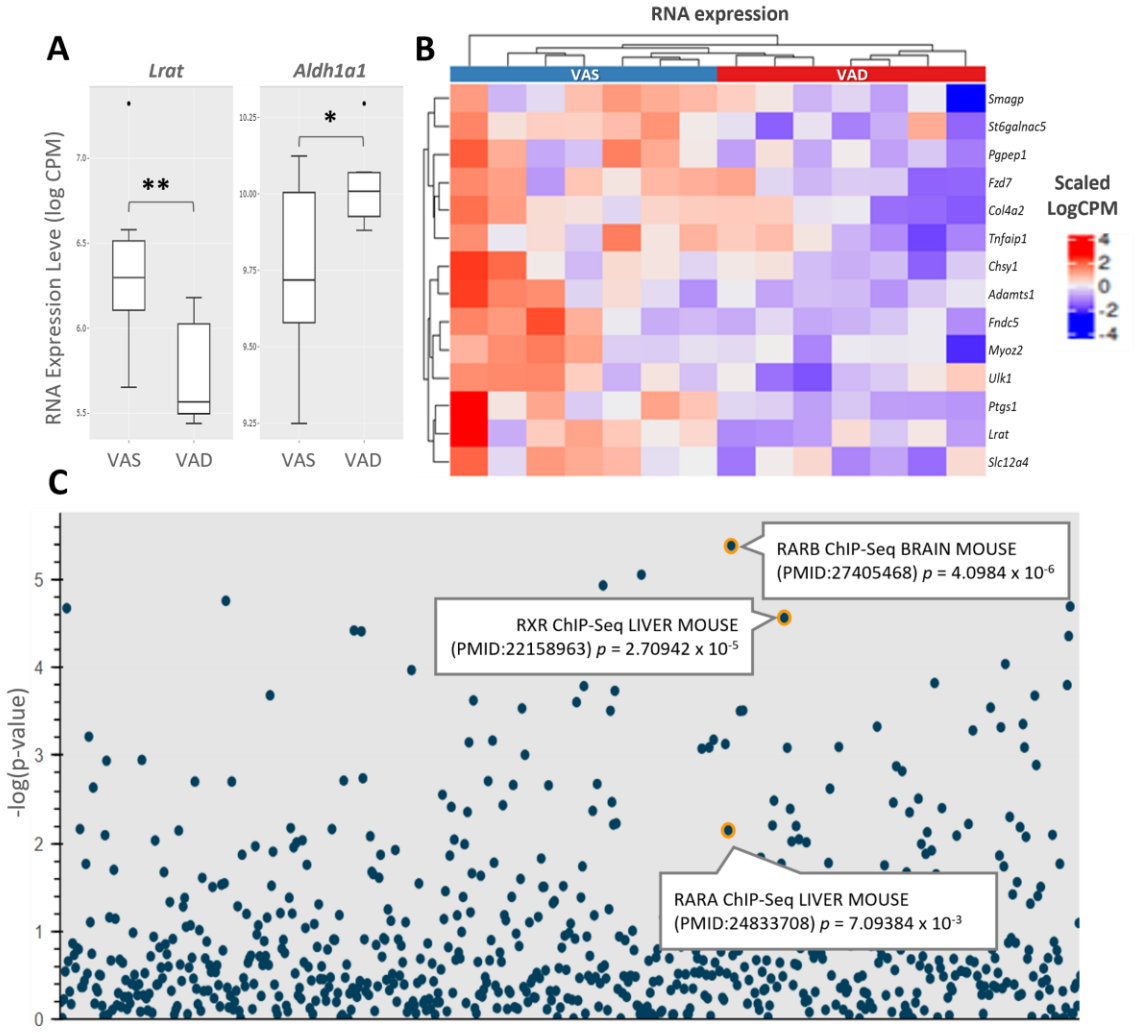

Figure 1. Transcriptional confirmation of vitamin A deficiency in adult mouse lungs after 8 weeks of dietary modulation.

(**A**) Gene expression of *Lrat* and *Aldh1a1*, two indicators of tissue vitamin A status. *P*-values = 0.009 and 0.036 respectively. (**B**) Heatmap of vitamin A targets from literature in VAS and VAD mouse lungs. (**C**) Manhattan plot of ChEA gene sets. Each point indicates one term from the ChEA 2022 gene set. The y-axis represents the –log(*p*-value) of the enrichment between the input gene set and the ChEA term gene set. The input gene set used included all down-regulated genes in VAS lungs at 8 weeks with a *p*-value < 0.05 (n=14). All mouse RNA sequencing files were annotated and processed using SingleCell Toolkit version 1.9.1 on Rstudio version 4.1.1.

Genes differentially up-regulated by VAD are enriched in epithelial and immune cells

To determine which cell types were most affected by host VAD status, we compared the genes that were up-regulated in VAD lungs ($p < 0.05$) with gene signatures from the Tabula Muris single-cell transcriptome database.[151] The tSNE clustering of the cell ontology classifications from over 20 different mouse organs and tissues showed our genes enriched in the lung epithelium, ectodermal epithelial stem cells, myeloid cells, and lung-derived macrophages. This data provides evidence that epithelium and immune cells are the primary cell types affected in the lung by VAD (Figure 2A).

Pro-proliferation gene signatures are enriched in VAD lungs

We next analyzed the up-regulated VAD genes using ChEA to perform transcription factor (TF) enrichment analysis.[149] Our results showed that target transcripts of pro-proliferation factors forkhead box protein M1 (FOXM1), jun proto-oncogene (JUN), and transcription factor E2F4 (E2F4) were highly enriched in our VAD samples (Figure 2B),[152-154] indicating that dietary VAD alters the transcriptional landscape of the LRT to increase cellular proliferation.

FOXM1 is considered an oncogenic TF and is found highly up-regulated in many forms of cancer.[155-156] Once activated, FOXM1 translocates into the nucleus where it promotes cell cycle progression, proliferation, differentiation, and in some cases tumorigenesis.[157-158] Likewise, the JUN and E2F pathways are also found up-regulated in the VAD lungs and have been linked to tumorigenesis in human and mouse studies.[159-162]

These results suggest that dietary VAD leads to an increase in proliferation and activation of pro-oncogenic pathways in the LRT (Figure 2C).[157] Interestingly, genes associated with ciliary motility and cellular replication from literature were also differentially expressed in VAD lungs (Figure 2C). These results provide evidence that VAD-induced proliferation is triggered by signals of a real or perceived breakdown in ciliary and cellular repair mechanisms, or that an increase in proliferation leads to a change in cellular turnover that compromises the structure and function of the epithelium.

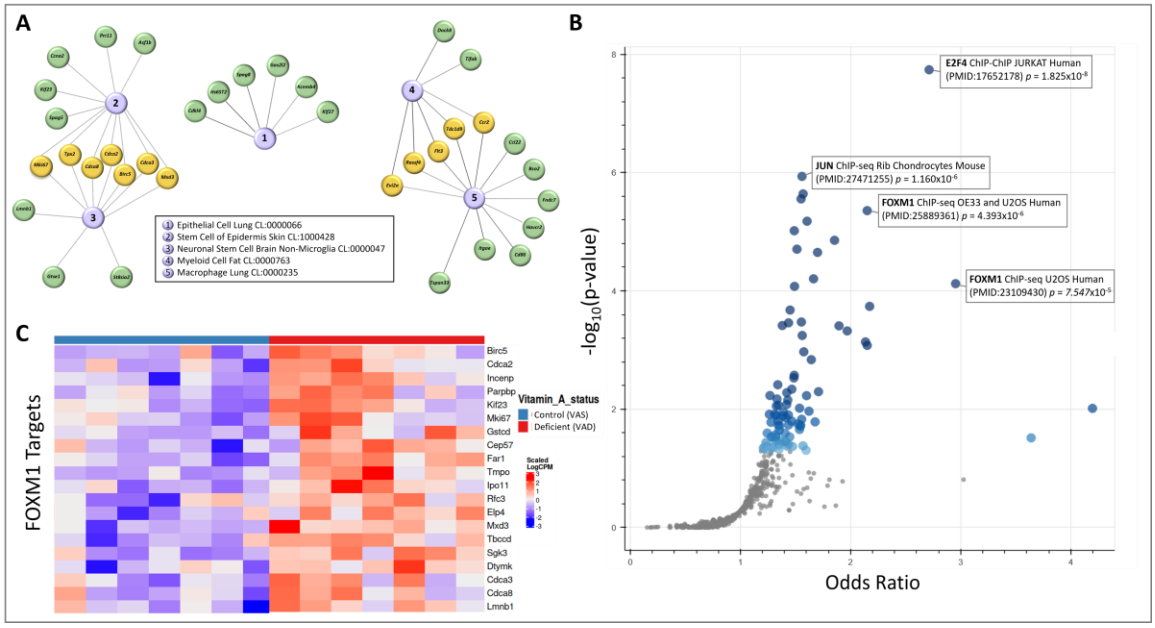

Figure 2. Gene set and TF enrichment analyses show an increase in proliferation signatures and a decrease in replication and ciliary motility in VAD lungs.

(**A**) Enrichr KG cluster map depicting five major nodes and three major clusters of gene signatures from the Tabula Muris mouse model transcriptome database. The input gene set used included all up-regulated genes in VAD lungs at 8 weeks with a *p*-value < 0.05 (n = 14). (**B**) Volcano plot showing targets of pro-proliferation transcriptional factors FOXM1, JUN, and E2F4 enriched in VAD lungs at 8 weeks ($p < 0.05$, n=14). (**C**) Heatmap of FOXM1 target genes gathered from literature. Gene expression is calculated as the log of the total read counts per million reads (LogCPM).

VAD diet leads to epithelial remodeling in adult mouse lungs

To determine if the VAD transcriptional signature translates to morphological changes in the lung, we next performed histological analysis of the airways in the LRT of VAS and VAD lungs. Our results show airway epithelial remodeling in the VAD mouse lungs (right) compared to the VAS controls (left) (Figures 3A-F). The observed VAD-induced airway remodeling is characterized by epithelial denudation and cellular debris, thickening of the smooth muscle layer, focal hyperplasia, and an increased number of epithelial cells expressing proliferation marker Ki-67 in both the large (Figures 3G-H) and small airways (Figures 3I-J) of the LRT.[163]

Further, quantification of *Mki67* expression (the transcript for Ki-67 protein) (Figure 3K) and $Ki67^{+}$ airway epithelial cells (Figure 3L) both support increased proliferation in VAD airway epithelium. These results were consistent with previous studies showing that vitamin A/RA pathway inhibition promotes proliferation in mouse and human lung epithelial organoids.[164] Taken together, these findings confirm an increase in the proliferation of airway epithelial cells in VAD lungs.

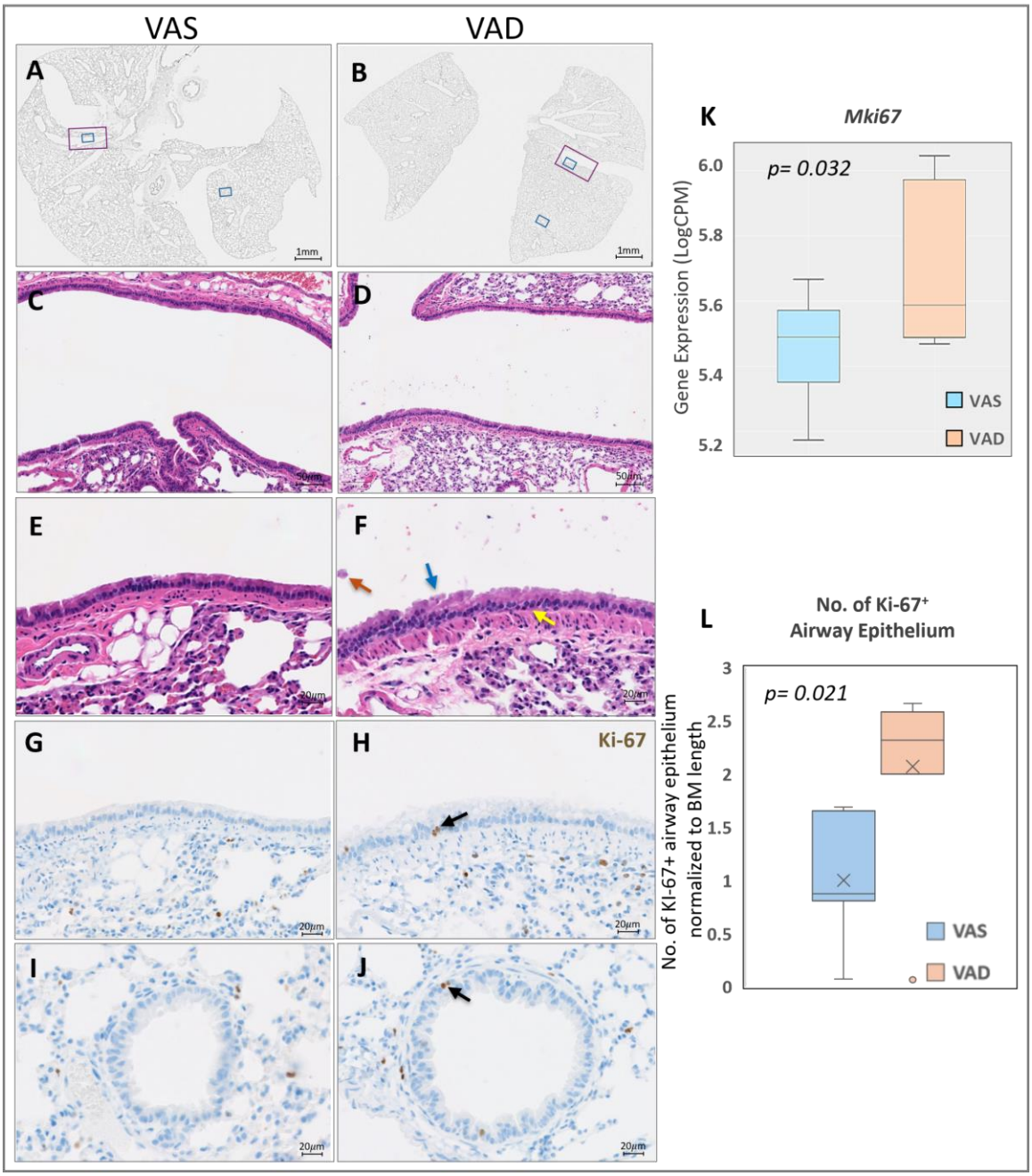

Figure 3. Increased proliferation and epithelial remodeling are observed in VAD airways after 8 weeks.

(**A-J**) Histology staining of VAS and VAD lungs. (**A,B**) Whole lung scans showing regions of image analysis in the proximal (**E-H**) and distal (**I,J**) regions of the LRT. H&E (**C-F**) and Ki-67 (**G-J**) staining of VAS (left) and VAD (right) lungs. Hyperplasia in the VAD airway is indicated by the blue arrow. The orange arrow points to a sloughed-off airway

epithelial cell. Thickening of the basement membrane is indicated by the yellow arrow. Ki-67^+ airway epithelial cells are indicated by the black arrows. Photos taken at 50 μm (**C-D**) and 20 μm (**E-J**) magnification. Boxplots of (**K**) *Mki67* RNA expression and (**L**) $Ki67^+$ cell counts in the airways and in VAS and VAD lungs at 8 weeks, *p-values* = 0.032 and 0.021 respectively (n = 14).

Increased proliferation leads to focal hyperplasia and an increased proportion of secretory cells in VAD airways

To further characterize the epithelial proliferation in VAD airways, we manually annotated and quantified hyperplastic regions in the large airways using QuPath.[138] VAD airways were found to have a marked increase in focal hyperplasia compared to VAS airways (Figures 4A-B, n = 10). Quantitative analysis illustrates a greater than 6x the proportion of focal hyperplasia of the VAD airway compared to controls (Figure 4C, p = 0.000196). These results confirm that dietary VAD leads to proliferation and epithelial remodeling in the airway of the LRT.

We next wanted to determine if VAD-induced epithelial remodeling favors a particular cell type. Since the two most abundant epithelial cells in the mouse LRT airway are secretory and ciliated cells,[74] we started by collecting whole lung samples for RT-PCR analysis of secretory markers *Scgb1a1* and *Scgb3a2* and ciliated cell markers *Foxj1* and *Tubb4a*. The levels of both secretory cell markers were significantly up-regulated in VAD lungs while the levels of the ciliary cell markers were unchanged by VAD (Figure 4D). Quantitative cell counts of secretory ($CC10^+$) and ciliated ($TUBB4A^+$-) cells in the airways also showed an increase in the proportion of secretory cells relative to ciliated cells in VAD lungs (Figure 4E). These results suggest that airway hyperplasia in VAD lung is driven by the proliferation of the secretory cells, consistent with a prior report that RA signaling inhibition of adult human and mouse lung epithelial organoids results in the proliferation of secretory cells.[164]

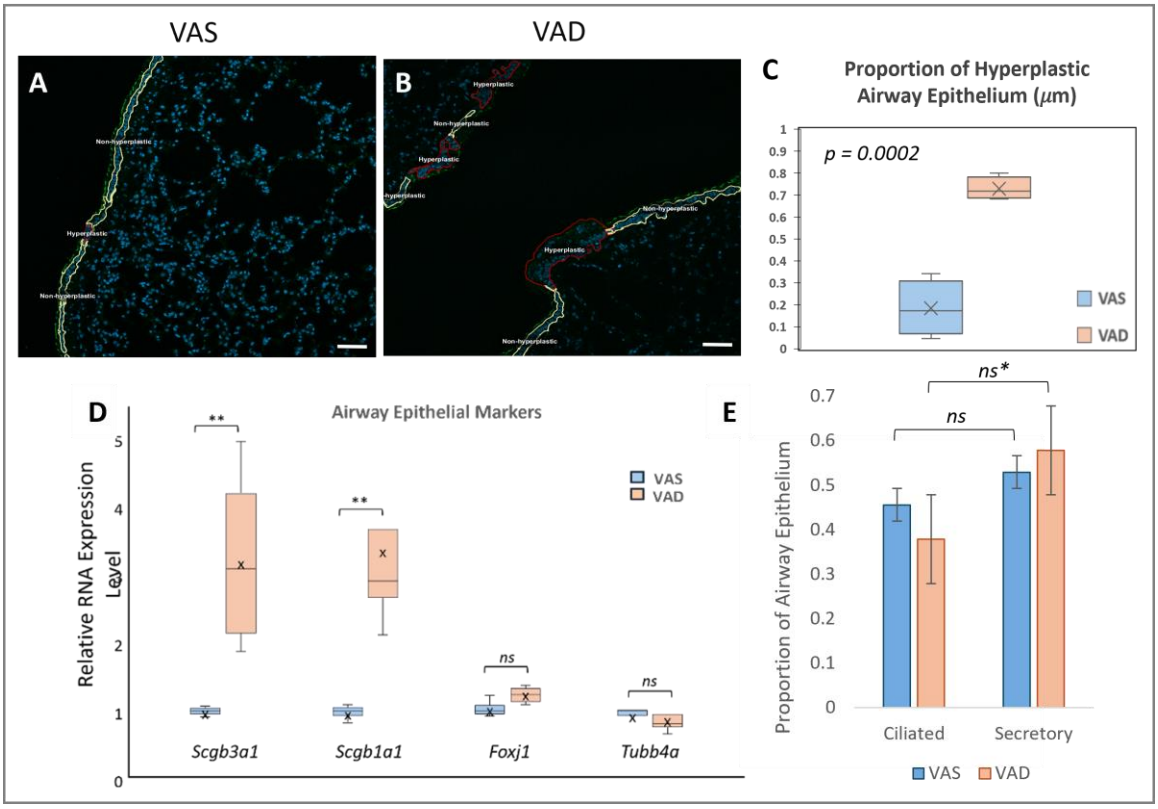

Figure 4. Proliferation and epithelial remodeling favor secretory cells in VAD lungs.

(**A-C**) Quantification of hyperplastic airway epithelium in VAS (**A**) and VAD (**B**) lungs. (**C**) Hyperplastic ratios were quantified using QuPath. Scale bar in A and B: 50 μm. (**D**) Gene expression of secretory (***Scgb1a1*** **and** ***Scgb3a2***) and ciliary (***Foxj1, Tubb4a***) markers in VAS and VAD mouse lungs (n = 14). ** = $p < 0.01$. "*ns*" = not significant. (**E**) Proportion of ciliated and secretory cells normalized to the total number of epithelium quantified within the airway of the LRT in VAS and VAD lungs. The y-axis represents the actual proportion of total airway epithelium where 1 = 100%. *P*-values = 0.26 (VAS) and 0.07 (VAD) respectively. ***ns**** = near significance.

Dietary VAD alters airway ciliary pathways and morphology

Next, we performed gene set enrichment analysis of all differentially expressed genes in VAD lungs at 8 weeks (n = 14, 619 genes with $p < 0.05$). The dataset was converted using a mouse-to-human orthologous analysis pipeline built into the Reactome data analysis toolkit.[165] The top three significant pathways from the Reactome 2022 database correlated to VAD status involved cilia assembly and trafficking (Figure 5A).

Of note, these same pathways were the most enriched whether we used a gene set with all differentially expressed genes (DEGs) including down-regulated genes (Figure 5A), or if we restricted our input gene set to only the up-regulated genes in the VAD lung (Figure 5B). These findings provide robust evidence of a cilia-specific gene signature present in VAD lungs that implicates ciliary dysfunction as a byproduct. Interestingly, the same Reactome enrichment analysis of genes up-regulated by VAD also showed enrichment for cell cycle pathways such as “Mitotic prometaphase”, “M phase”, “Cell cycle, mitotic”, and “Cell cycle” (Figure 5B), providing further evidence that dietary VAD leads to a hyperproliferative phenotype in the LRT.

Using the mouse-to-human orthologous pathway generator and disease pathway analysis toolkit by Reactome,[165] we showed that genes with increased expression in VAD lungs are enriched for Reactome terms relevant to striated and smooth muscle actin contraction (Figure 5C, olive = $p < 0.05$, yellow = $p < 0.01$). Actin-myosin complexes form actomyosin, a motorized protein mechanism that regulates the cytoskeletal integrity and ciliary function of the cell.[166] Disruption of the subapical actin filaments prevents

polarization and a metachronal beating pattern, leading to ciliary dysmorphism.[167] These results support the hypothesis that VAD-induced airway remodeling may have a profound effect on airway smooth muscle contractility.

To identify whether RAR expression is dysregulated in CCs, we performed a dual fluorescence in-situ hybridization and immunohistochemical (FISH-IHC) staining of paraffin-embedded lung tissues. We co-stained the RNA of RAR-β and RAR-ɣ (β data not shown) with ciliary protein marker TUBB4A and nuclear marker DAPI (Figures 5D-E). This approach enables us to determine whether RA receptors are present in CCs.

TUBB4A expression in control lungs was clearly defined at the apical surface of the pseudostratified airway epithelium (Figure 5D). TUBB4A encodes tubulin protein that is a major component of ciliary motility.[80] In VAD lungs, TUBB4A expression was lost sporadically throughout VAD airways but predominantly at sites of hyperplasia and epithelial dysmorphism (Figure 5E). Taken together, these data suggest that VAD leads to focal regions of airway epithelial remodeling characterized by hyperplasia, secretory cell proliferation, and ciliary dysmorphism.

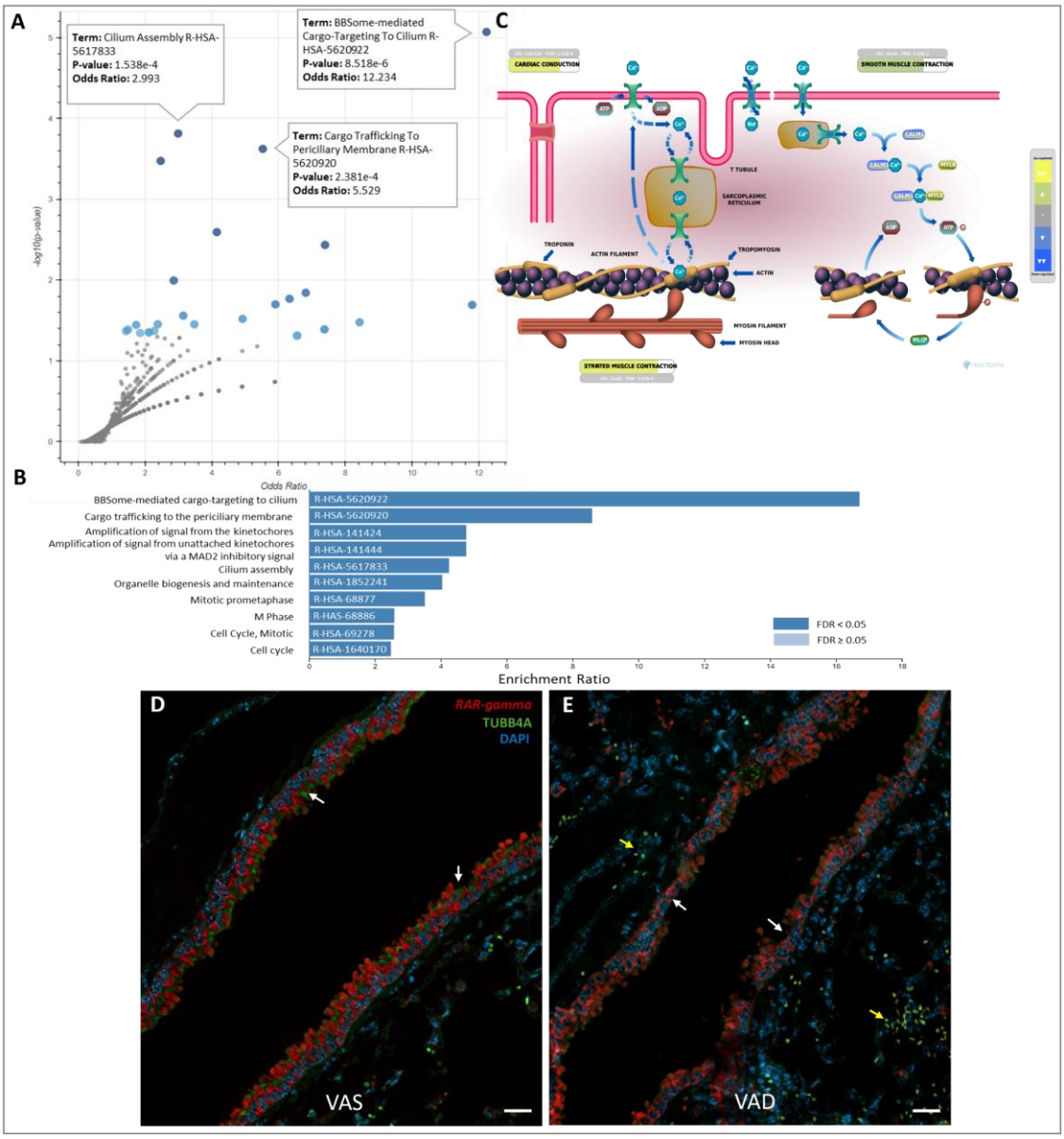

Figure 5. Cilia dysfunction is observed in VAD lungs.

(**A**) Volcano plot of the top pathways from the Reactome 2022 database altered in VAD lungs. The input dataset included all DEGs with $p < 0.05$ (n = 619). (**B**) Barplot showing the top 10 enriched pathways from the Enrichr Reactome database using only genes up-regulated in VAD lungs with $p < 0.05$. (**C**) Mouse-to-human orthologous pathway analysis of bulk RNAseq using the Reactome pathway and image generator. The depicted pathways are associated with striated and smooth muscle actin contraction, and any mechanisms highlighted in yellow are significantly up-regulated in VAD lungs ($p < 0.05$). (**D,E**) FISH of retinoic acid receptor-ɣ (*Rarg*) RNA expression co-stained with ciliary protein marker TUBB4A and nuclear marker DAPI in VAS (**D**) and VAD (**E**) lungs. Scale bar = 50 μm.

White arrows point to regions of TUBB4A expression (**D**) and absence of TUBB4A expression (**E**) in the VAS and VAD airways.

VAD leads to cilia dysfunction, a loss of apical protein expression, and a breakdown in MCC in the airway

The structure and function of the CCs are imperative for proper MCC, the primary innate defense mechanism in the airway.[168] To determine whether the VAD-induced morphologic and transcriptional changes affect ciliary function, we performed an ex-vivo ciliary motility assay to visualize the cilia-driven flow in VAS and VAD airways (Supplemental Figure 2).[136]

Briefly, tracheal explants were extracted and immediately placed in Petri dishes containing L15 media with 20 μl/ml of 0.2-μm fluorescent microspheres; this microsphere size is representative of most small particles, microbes, and other pollutants our lungs commonly trap and expel under homeostatic conditions. Each petri dish was recorded using a Nikon Deconvolution Wide-Field Fluorescence Microscope (B15D) equipped with a camera and video acquisition software to measure the cilia-driven flow. Video frames were concatenated to create still images, allowing us to measure the velocity and distance traveled by individual beads (Figures 6A-H, green lines). A minimum of 100 beads were measured for each arm of the study.

On VAS trachea, the fluorescent beads are observed moving in a smooth, concerted motion in a largely singular direction, indicating that cilia-driven propulsion in the VAS trachea is intact (Figures 6A-D). Conversely, the beads exposed to VAD tracheas (Figures 6E-H) were propelled with a significant reduction in velocity (Figure 6I, $p < 0.00001$), directionality, and distance traveled (Figure 6J) of fluorescent microspheres over the same period of time, indicating ciliary dysfunction in the VAD airway.

IHC expression of secretory epithelial cell marker CC10, the protein product of the transcript *Scgb1a1* normally expressed within the secretory granules of club cells, is normally located at the apical portion of the cytoplasm (Figure 6K). CC10 apical protein expression was significantly reduced in the hyperplastic region of the VAD airway (Figure 6L). Likewise, apical ciliary marker TUBB4A, a protein normally expressed in the cilia of CCs (Figure 6M), was also found reduced or absent in regions of the VAD airway (Figure 6N).[78,169-170] These findings confirm that dietary VAD leads to epithelial remodeling characterized by a loss of apical protein expression of both major cell types and ciliary dysfunction in the intraparenchymal airways, leading to a breakdown in MCC.

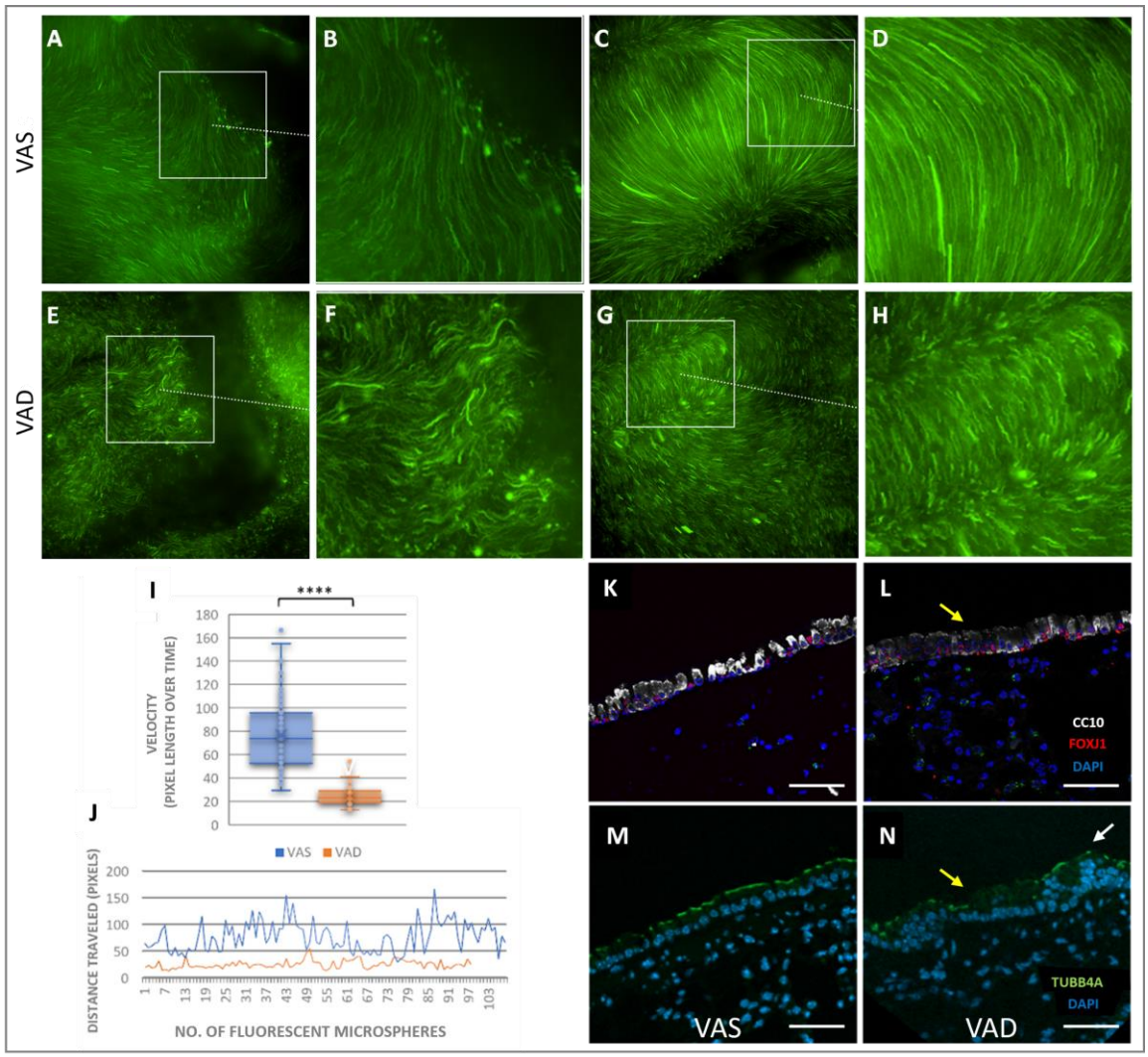

Figure 6. VAD leads to a loss of MCC.

(**A-H**) Composite images of fluorescent microsphere motility in the trachea of VAS and VAD lungs from a cross-sectional (**A-B, E-F**) and anterior (**C-D, G-H**) view at 20x magnification. (**I-J**) Fluorescent microsphere velocity (**I**) and overall distance traveled (**J**) in VAS and VAD lungs, $p < 0.00001$, t-value = 17.70024. (**K-N**) Immunohistochemical staining of airway epithelium. Secretory cells were visualized using CC10 while (CCs) were visualized using both nuclear FOXJ1 and cilia-specific TUBB4A. Yellow arrows indicate regions of reduced expression of the apical proteins CC10 and TUBB4A. White arrow points to a region of focal hyperplasia.

VAD leads to a loss of cell polarity in the airways

The major mechanism responsible for MCC maintenance through apical/basal protein segregation in the airway epithelium is planar cell polarity (PCP).[82-83] PCP is a two-phase process in the lung. The first phase establishes polarity along the tissue axis via PCP complex-mediated cell-cell communication. During phase two, CCs remodel their cytoskeletal structure to orient their cilia towards the airway. The cilia polarizing step not only polarizes the CCs but the entire epithelium.[171] Therefore, a loss of polarity in the intraparenchymal airway epithelium of VAD lungs also leads to a loss of barrier integrity and cell division orientation. Importantly, loss of polarity is a known hallmark of epithelial metaplasia and cancer, and previous reports have identified that the disruption of the apical-basal polarity precedes hyperplasia and epithelial stratification in mouse lung and breast cancer models.[172-173]

The loss of the apical regionalization of CC10 in the VAD airway epithelium is highly suggestive of PCP loss. To determine whether these changes represent a loss of polarity in the airway, paraffin-embedded tissues were fluorescently stained for expression of Keratin 8 - a marker for cytoskeletal keratin expression in epithelial cells – as well as apical-localized Crumbs and basolateral-localized Scribble (Figures 7A-D). While Scribble expression was largely consistent between the two diets, increased Crumbs expression was observed at hyperplastic loci of the proximal airways (Figures 7E-F) while a reduction or dysregulation of Crumbs expression was observed in the distal airways (Figures 7G-H) of VAD lungs.

Changes in Crumbs expression provide strong evidence that VAD interrupts cell polarity mechanisms in the airway. Based on this data and considering the role CCs play in establishing polarity in the airway, we hypothesize that CCs are one of the primary host cells affected by dietary VAD status. Once cilia function is affected, the lung can no longer clear pathogens and pollutants effectively, potentially leading to infections and disease. It is still unclear whether the observed changes in epithelial morphology are mediated by local or distal signals (e.g., via the gut-lung axis).

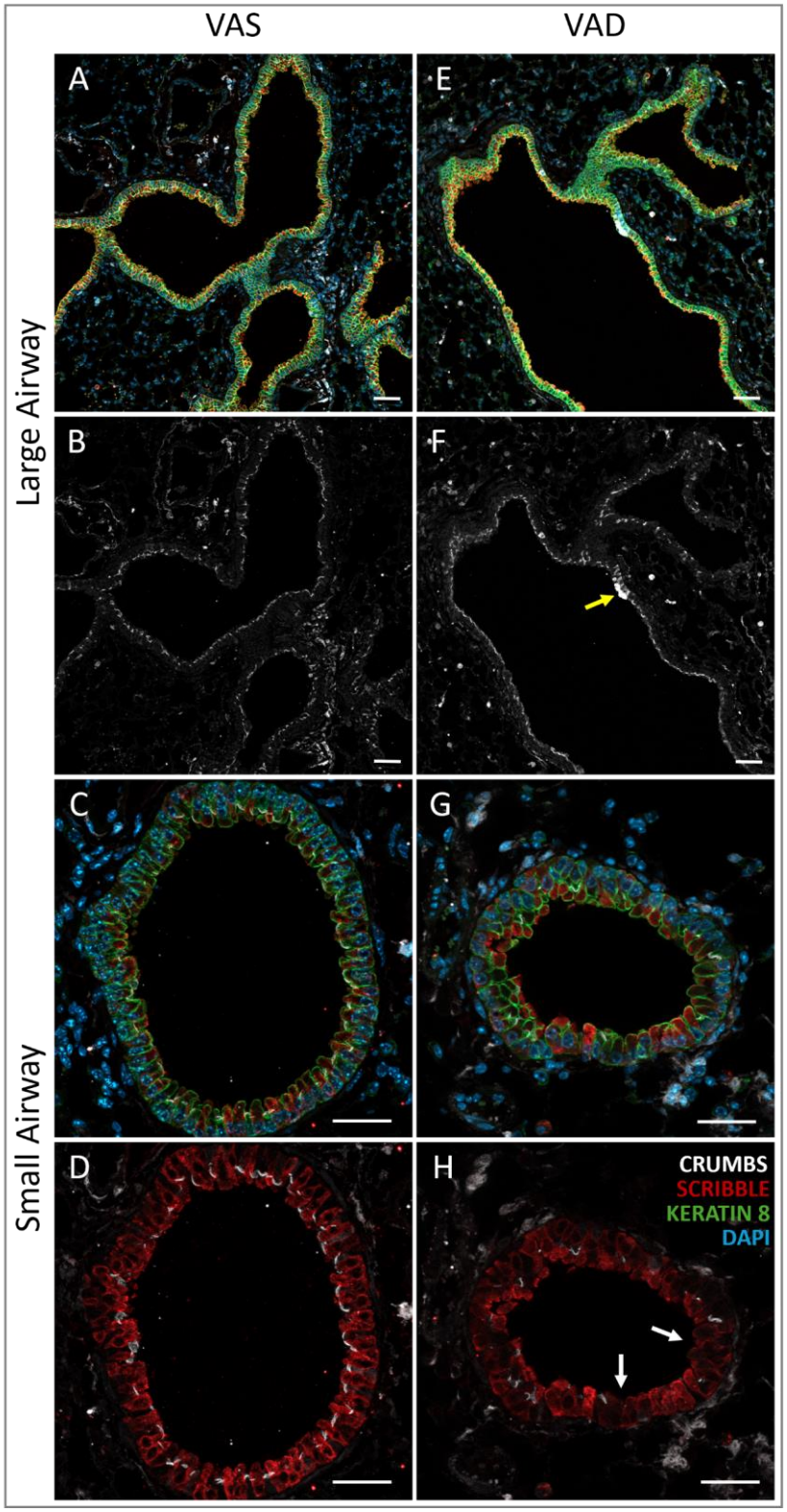
VAS
VAD
Large Airway
Small Airway
A
E
B
F
C
G
D
H
CRUMBS
SCRIBBLE
KERATIN 8
DAPI

Figure 7. VAD alters expression of cell polarity complexes in the distal airway.

Immunofluorescent staining of the VAS (**A-D**) and VAD (**E-H**) airways at 8 weeks taken at 20x (**A-B, E-F**) and 60x (**C-D, G-H**) magnification. Epithelial cytoskeletons were visualized using Keratin 8, apical and basolateral protein complexes were visualized using Crumbs and Scribble respectively. The yellow arrow points to a region of increased Crumbs expression in the large airway. White arrows indicate reduced Crumbs expression in the small airway. Scale bars = 50 μm (**A-B, E-F**) and 20 μm (**C-D, G-H**) respectively.

VAD-induced epithelial remodeling is caused by localized RAD

To create a lung epithelium-specific RAD mouse model, we crossed male C57B/6J mice carrying a copy of a tamoxifen-inducible cre recombinase knocked into the lung epithelium-specific *Nkx2.1* promoter (*Nkx2.1 iCre ERT2*) to female C57B/6J mice homozygous for a *loxP*-flanked STOP codon upstream of a dominant-negative retinoic acid receptor gene in the R26 locus (*flox-flox dnRAR R26*) (Figure 8A). Administering tamoxifen to Cre-positive mice homozygous for floxflox dnRAR R26 for five days created mice whose RAR-mediated signaling is knocked down specifically in the lung epithelium. Tamoxifen-injected Cre-negative littermates were used as control. By only comparing Cre-positive and Cre-negative littermates, this model allows us to simultaneously control for diet, age, sex, batch, and cage effects. Lungs were harvested 8 weeks after tamoxifen injections.

The airways of tamoxifen-injected, Cre-positive mice exhibited a phenotype similar to the dietary VAD models, including focal regions of epithelial hyperplasia and the loss of TUBB4A expression at the apical surface of the airway epithelium (Figures 8B-E, data not shown). Since the dietary and the genetic models both exhibited similar morphologic and molecular changes, there is strong evidence to suggest that these changes are due to the direct effect of vitamin A/RA deficiency on airway epithelium and are independent of distant signals such as the gut-lung axis. We conclude that RA signaling in the lung epithelium is required for proper ciliary function, epithelial integrity, and MCC.

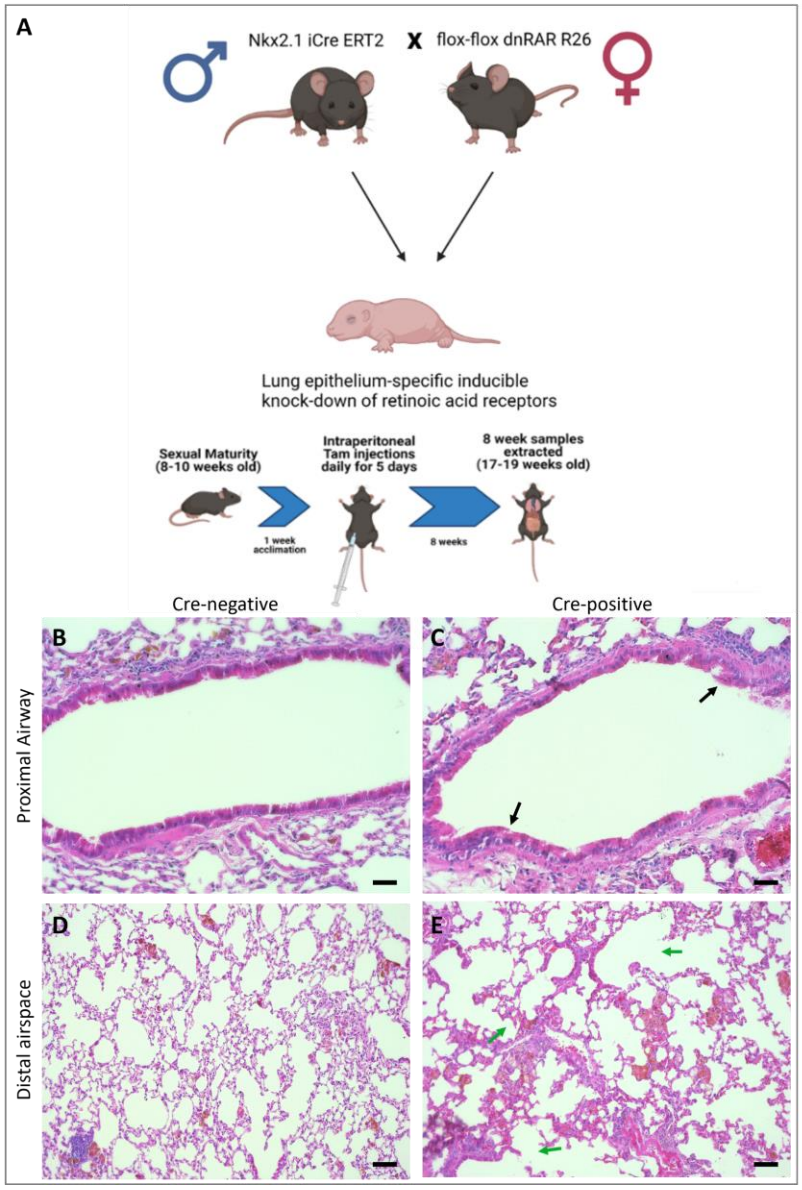

Figure 8. Localized RAD leads to remodeling in the proximal and distal lung.

(A) Generation of a genetic mouse model to inducibly knock down RA signaling in the lung epithelium. Image created using BioRender. (**B-E**) H&E staining of the proximal airway and distal airspace in Cre-negative (**B,D**) and Cre-positive (**C,E**) mouse lungs. Black scale bars = 50 μm magnification. Black arrows indicate regions of hyperplasia. Green arrows indicate alveolar enlargement and thickening near small airway passages.

CHAPTER TWO: VAD LEADS TO MICROBIAL DYSBIOSIS AND BACTERIAL COLONIZATION

Sequencing depth and quality scores of RNAseq data

To date, there have been few longitudinal studies focusing on compositional changes to the lung microbiome over the course of a disease, and even fewer that have identified how diet directly affects lung health over time. Longitudinal microbiome data from humans also tend to contain large batch effects due to the variability in cohorts, geographic location, extraction techniques, patient involvement, and environmental exposures.[174]

Our lab decided to use our dietary mouse model to create a pseudo-longitudinal study of lung microbiome changes in a VAD setting by collecting whole lung samples at the 3-week and 8-week timepoints for host and microbiome RNA sequencing. After trimming and aligning, we filtered low abundance sequences from VAS and VAD cohorts using SingleCelltoolkit.[175] Reads that aligned to both mouse and human indices were discarded as potential contamination in the samples. Microbiome reads were then checked for quality prior to data analysis (Figure 9, Table 2).

All samples submitted for sequencing received a secondary QC check by the BUMSR Core Facility. All RNA samples received a 260/280 score of 2.01-2.11, confirming the samples were of the highest quality and purity.

Run 1 Sequencing Summary	**All Reads in Millions**			

Sample Name	Total Reads Obtained (M)		Metric	Reads (M)
1VAD 3wk	155.06		Minimum	121.70
1VAS_3wk	121.70		Maximum	155,06
2VAD_3wk	136.18		Mean	136.32
2VAS_3wk	136.24		Total	1090.52
3VAD 3wk	138.93			
3VAS 3wk	136.77			
4VAD 3wk	135.89			
4VAS 3wk	129.75			

Run 2 Sequencing Summary			**All Reads in Millions**			
Sample Name	Reads Obtained P2 Run (M)	Reads Obtained P3 Run (M)	Total Reads Obtained (M)		Metric	Reads (M)
VAS1_3wk	17.76	49.86	67.62		Minimum	60.70
VAS2_3wk	17.71	49.56	67.27		Maximum	86.86
VAS3_3wk	15.67	45.03	60.70		Mean	73.97
VAS4_3wk	21.48	57.79	79.28		Total	1775.21
VAS5_3wk	20.47	54.24	74.71			
VAD1_3wk	18.80	49.41	68.21			
VAD2_3wk	16.18	46.50	62.67			
VAD3_3wk	21.88	55.47	77.35			
VAD4_3wk	16.47	45.36	61.83			
VAD5_3wk	17.55	49.17	66.72			

VAS2_8wk	18.44	49.34	67.78			
VAS3_8wk	21.80	55.78	77.58			
VAS4-8WK	23.20	57.56	80.76			
VAS5-8WK	25.37	60.77	86.14			
VAS7-8WK	20.04	55.84	75.87			
VAS9-8WK	25.98	60.88	86.86			
VAS10-8WK	19.34	50.81	70.15			
VAD2-8WK	22.35	55.97	78.33			
VAD3-8WK	23.03	57.61	80.64			
VAD4-8WK	21.07	53.40	74.47			
VAD5-8WK	19.67	54.70	74.37			
VAD7-8WK	23.42	57.08	80.49			
VAD8_8wk	21.94	55.37	77.31			
VAD10_8wk	23.68	54.41	78.09			

Table 1. Total RNA sequencing Bioanalyzer read counts per sample.

Metric	**Value**
Number of Samples	32
Number of Genes	15678
Average number of reads per sample	37929725
Average number of genes per sample	15654
Samples with <1700 detected genes	0
Genes with no expression across all samples	0

Table 2. Microbiome RNA sequencing yield and read quality.

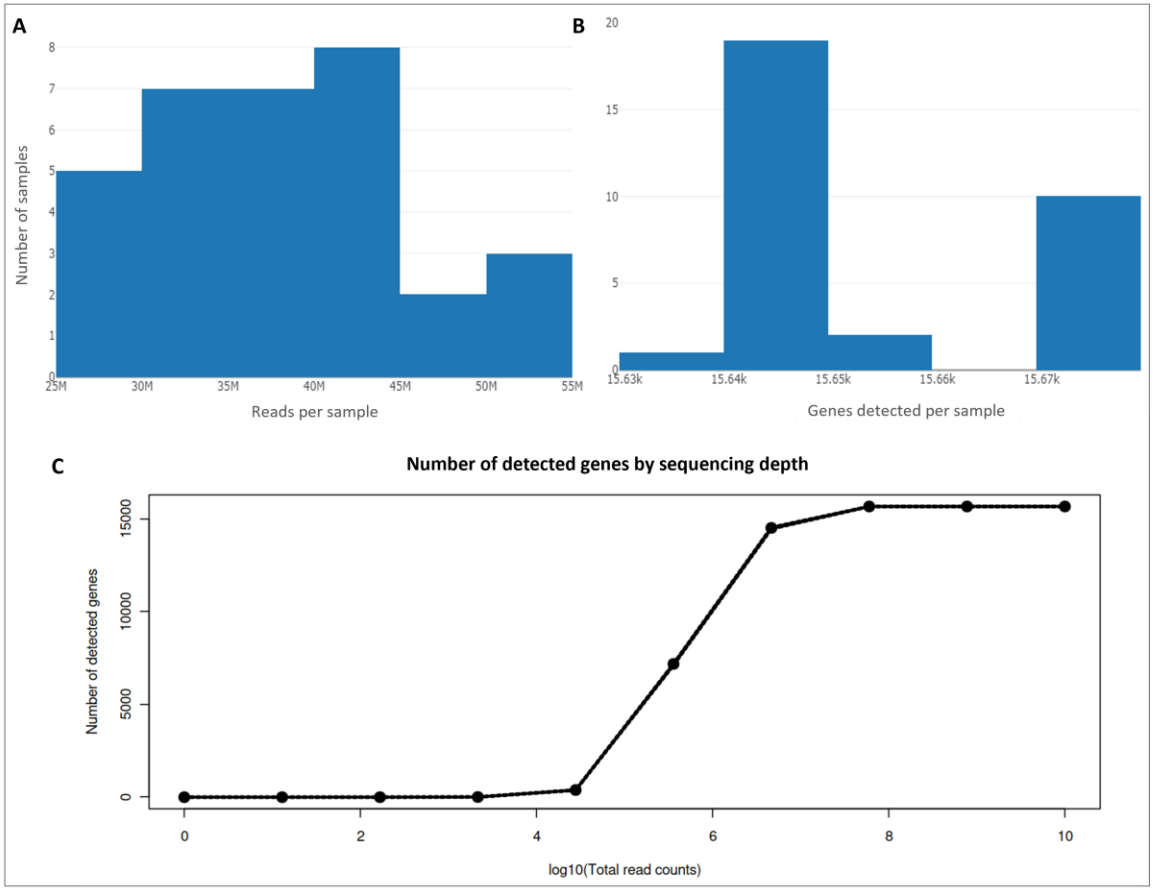

Figure 9. Quality and depth of RNA sequencing data.

RNA sequencing depth and genes detected per sample (n = 32). (**A-B**) Bar plots of the (**A**) number of reads per sample in millions and the (**B**) number of genes detected per sample in tens of thousands. (**C**) The logarithmic curve of read counts versus the number of genes detected per log10 read count.

VAD leads to microbial dysbiosis in the LRT

VAD alters alpha and beta diversity after 8 weeks

Alpha diversity, or the measurement of diversity *within* samples (Figure 10A),[176] was performed on bacterial read counts at the phylum level using the Mann-Whitney/Kruskal-Wallis statistical test. VAD samples exhibited a near-significant increase in alpha diversity compared to controls ($p = 0.072$), indicating an increase in the diversity of bacterial communities found within VAD lung samples. Beta diversity, or the measurement of diversity *between* samples,[177] was performed on bacterial transcripts using the Bray-Curtis dissimilarity index (Figure 10B) and showed VAS and VAD cohorts clustered separately with a *p*-value of 0.01. These results provide evidence of a statistically significant shift in bacterial composition in VAD lungs at 8 weeks.

VAD-induced dysbiosis alters the relative abundance of bacteria and fungi

To see if the observed shift in bacterial composition translated to an increase in bacterial gene expression, we quantified the 16S ribosomal RNA (rRNA) expression within VAS and VAD lungs using RT-PCR. 16S rRNA is a sequence found in all bacteria and is commonly measured as a gold standard for determining bacterial burden.[178] Briefly, RT-PCR is a method of quantifying the number of sequence copies within a sample. By amplifying the bacterial 16S rRNA within each sample, we are able to quantify the total bacterial content and calculate the bacterial load within a group of samples.[179] RT-PCR results from whole lung homogenates (n = 8) did not show a significant change in bacterial burden ($p = 0.42$, Figure 10C) between VAS and VAD lungs, but these findings do not identify functional shifts in the VAD lung microbiome over time.

Today, microbiome researchers often calculate the relative abundance of microbes within a host tissue instead of actual abundance, as these values can be more functionally relevant to predict dysbiosis and disease progression over time; parametric models like DESeq2 use negative binomial distributions applied to normalized data to minimize hidden confounding factors from sample fractions.[180] By applying DESeq2 with false discovery rate (FDR) correction to our Log-transformed RNA read counts at 8 weeks (n = 14), we determined that both bacteria and fungi exhibited significant shifts in relative abundance (p = 0.025 and 0.020 respectively, Figure 10D). Specifically, we observed a relative decrease in fungi and a relative increase in bacteria at 8 weeks. These findings could indicate the presence of a polymicrobial crosstalk between fungi and bacteria that is modified in a VAD context.

It is worth noting that we were unable to measure alpha and beta diversity in the fungi because there were only two major phyla extracted from all 32 samples, which are too few to perform the calculation.

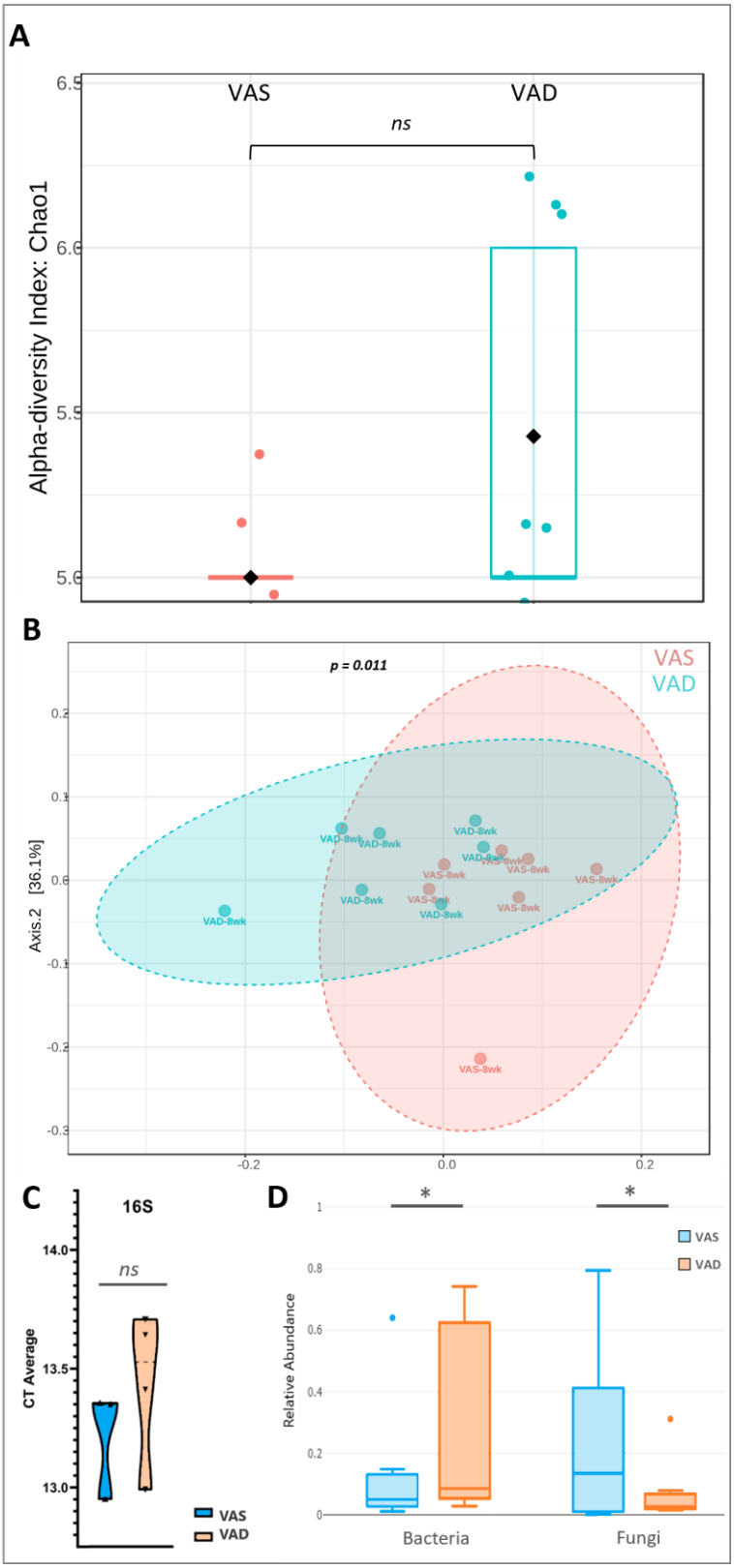
A
VAS
VAD
ns
Alpha-diversity Index: Chao1
6.5
6.0
5.5
5.0
B
p = 0.011
VAS
VAD
Axis.2 [36.1%]
0.2
0.1
0.0
-0.1
-0.2
-0.3
-0.2
0.0
0.2
VAD-8wk
VAS-8wk
C
16S
ns
CT Average
14.0
13.5
13.0
VAS
VAD
D
*
*
Relative Abundance
1
0.8
0.6
0.4
0.2
0
VAS
VAD
Bacteria
Fungi

Figure 10. VAD alters the microbial composition of the LRT.

(**A**) Alpha diversity barplot of bacterial transcripts at the phylum level from VAS and VAD lungs at 8 weeks using Mann-Whitney/Kruskal-Wallis statistical method, $p = 0.07$ (n = 14). (**B**) Beta diversity expressed by principal coordinate analysis (PCoA) plot of bacterial transcripts at 8 weeks using the Bray-Curtis dissimilarity index and PERMANOVA statistical method, $p = 0.01$. (**C**) RT-PCR violin plot of 16S rRNA expression represented by CT Average (y-axis, "CT" = cycle threshold, n = 8) and (**D**) RNAseq boxplots (n = 14) of bacterial and fungal relative abundance in VAS and VAD lungs, $p = 0.025$ and 0.020 respectively.

Stepwise changes in microbial gene expression suggest QS in VAD lungs

Although the relative bacterial burden increased in VAD lungs over time (Figure 11A), major shifts in bacterial composition were not evident until week 8 at the phylum level (Figure 11B) ($p = 0.0255$).[181] Meanwhile, the relative abundance of Ascomycota - a fungal phylum known to be beneficial for human health - plummeted as early as week 3 and maintained the same level of relative abundance at week 8 (Figure 11C) ($p = 0.0203$).[182-184]

To determine the functional relevance of the compositional changes in VAD lungs over time, the bacterial meta database BacDive was used to annotate the RNA read counts of whole lung samples collected at 3 weeks and 8 weeks (n = 32).[185] BacDive compiles strain-level research data from culture collection databases and primary literature to provide taxonomic classifications for over 90% of defined bacterial species. BacDive taxonomic classifications like antibiotic resistance are sourced from the Chemical Entities of Biological Interest database.[186] VAS samples at 3 weeks and 8 weeks were combined to represent the control lung cohort (n = 16), and any differences in the relative abundance of VAS microbes between these two time points at the phylum level were insignificant (data not shown). Combined VAS samples will serve as time 0 in our quasi-longitudinal analysis, while VAD samples reflect changes after 3 weeks and 8 weeks of dietary VAD. We also classify “low abundance bacteria” as bacteria with less than 1% relative abundance in our VAS cohort (“Other” in Figure 11B).

The relative abundance of bacteria classified as antibiotic-resistant is largely depleted at week 8 (Figure 11D). This change in bacterial composition could be due to the

increased relative proportion of rare and low-abundant bacteria in VAD lungs that have yet to be classified as functionally relevant to human health (Figure 11B). Another possibility is that microbes with known antibiotic-resistant potential may become transcriptionally quiescent in the VAD lung, a QS-mediated mechanism commonly associated with stress response and biofilm formation.[187-188]

Aerobic bacteria were overabundant at the 8-week timepoint in the VAD lung (Figure 11E, outer ring). Since vitamin A is an antioxidant,[189] these results suggest chronic VAD may lead to an increase in oxidative stress within the lung, which in turn could lead to the preferential selection of oxygen-tolerant microbes. We also observed an increase in the relative abundance of gram-negative bacteria compared to gram-positive (GP) bacteria in VAD lungs at 8 weeks. As mentioned previously, changes in microbial transcription are often regulated by the QS signaling mechanism.[190] A reduction in transcriptional activity could suggest selective enrichment of gram-negative bacteria, transcriptional quiescence of gram-positive bacteria, or a combination of the two (Figure 11F).

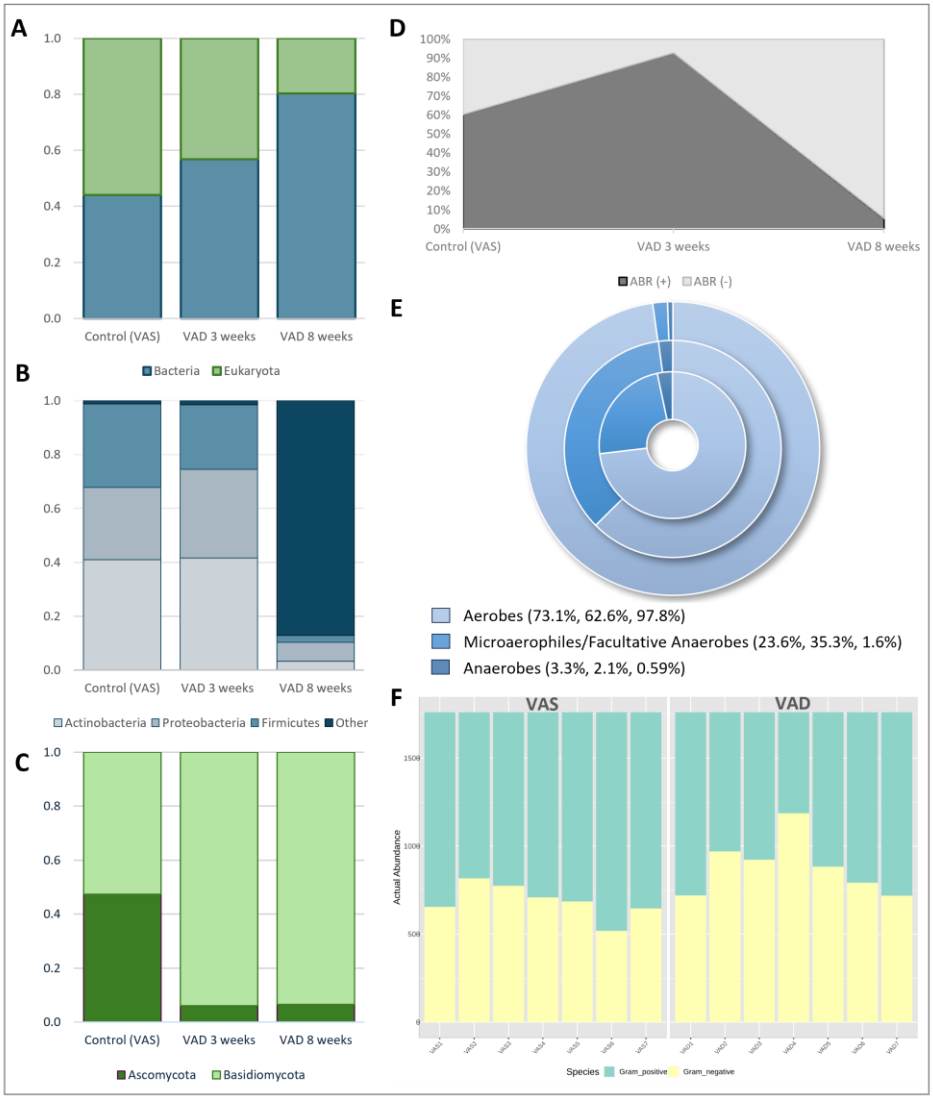

Figure 11. Changes in bacterial and fungal gene expression implicate QS mechanisms.

(**A-C**) Relative abundance barplots of Bacteria and Fungi in VAS (n = 18) and VAD lungs at 3 weeks (n = 9) and 8 weeks (n = 7) at the phylum level. Y-axis represents the overall microbial abundance where 1.0 = 100% of RNA transcripts. All bacteria with less than 1% abundance in VAS lungs were grouped into 'Other'. (**D**) Stacked proportion chart showing changes in relative abundance of antibiotic-resistant (ABR^+) and non-antibiotic-resistant (ABR^-) bacteria in VAD lungs over time (n = 32). (**E**) Stacked doughnut abundance plots of bacterial oxygen tolerance in VAS (inner ring), VAD at week 3 (middle ring) and VAD at week 8 (outer ring) lungs. Listed percentages represent proportions of bacteria by oxygen tolerance in VAS (left), 3 week VAD (middle), and 8 week VAD (right) lungs. (**F**) Stacked bar chart showing actual abundance of gram-positive and gram-negative bacterial

transcripts at 8 weeks (n = 14). Classifications of antibiotic resistance (**D**), oxygen tolerance (**E**), and gram status (**F**) were manually annotated from BacDive.

Microbial classification and gene signature analysis indicate early dysbiosis and an increase in low-abundant microbes in VAD lungs

To determine how VAD-induced lung dysbiosis influences the localization and colonization of bacteria within the LRT, we analyzed our 8-week RNAseq samples using MicrobiomeAnalyst[191], a metacoder analysis package used to depict taxonomic differences between the VAS and VAD microbial communities.[192] Our data shows that *Pseudomonadota* and *Deinococcota* are predominantly found in the VAD lung (Figure 12A, blue), two phyla known for their pathogenic and extremophilic potential .[193-194] Extemophilic microbes can survive in some of the harshest conditions such as starvation, extreme temperatures, and radiation.[195] In fact, *Deinococcota* is known for being able to synthesize its own carotenoids such as deinoxanthin, aiding its survival during hostile and nutrient-depleted circumstances.[194]

Our analysis also revealed that VAD lungs are more enriched with Gammaproteobacteria, the class of bacteria known to include many common gram-negative lung "pathogens" in humans (Figure 12A).[196-198] Gammaproteobacteria are capable of using inflammatory byproducts such as reactive oxygen and nitrogen species as nutrients to survive in harsh environments.[199-202] In addition, Gammaproteobacteria are known to produce molecules that promote a cyclical inflammatory processes in the host,[203] leading to chronic infection.

On the other hand, the commensal *Bacillota* phylum is predominantly expressed in the VAS lung (Figure 12A, red), suggesting that chronic VAD leads to a reduction in the

relative abundance of commensal bacteria at the phylum level and favors bacterial population with higher pathogenic potential.

The diversity and composition of fungi in VAD lungs were also altered at 8 weeks (Figures 11C, 12B), although more data is needed to fully characterize why Ascomycota transcriptional activity is nearly ablated in VAD lungs and maintains inactivity at 8 weeks (Figure 11C). It's also important to note these findings on relative abundance represent the functional activity of the lung microbiome more so than absolute microbial counts and can be equally indicative of functional changes fungi and other microbes may employ to preserve resources and become metabolically inactive.[190]

To analyze microbiome data at the genus level, we used the BatchQC[130] Shiny App R package to correct our raw read counts for unidentified batch and covariate effects that could skew our results. Using the app, we first normalized the genus-level log-transformed read counts using DESeq2,[180] followed by Limma[126] for differential expression analysis (Figure 12C, Table 3). Our volcano plot depicts the *p*-value (x-axis) and significance value (y-axis) for the compositional changes of each genus in VAS and VAD lungs at 8 weeks.

Of the six microbes that met the significance threshold, Saprochaete from the Ascomycota phylum was the only fungi significantly altered (green dot). We also observed an increase in Methylobacterium expression from the *Pseudamonadota* phylum, a species known for healthcare-associated infections.[204] Additionally, VAD led to an increase in transcriptional activity of low-abundant microbes as well as pathobionts such as *Planctomycetes* at 8 weeks (Figure 12D),[181] confirming that VAD alters microbial

composition and transcriptional activity in both fungal and bacterial communities in the airway.

GENUS	**LOG_2FC**	***P*-VALUE**
Saprochaete	-5.98601	0.002504
Cognaticolwellia	-2.90527	0.024646
Pseudoruegeria	-1.24726	0.026923
Methylobacterium	0.789777	0.026969
Tepidiphilus	-2.75174	0.028844
Nitratireductor	-2.75155	0.02885
Wickerhamomyces	-2.61494	0.033349
Borrelia	-2.21635	0.052371
Herbaspirillum	0.69555	0.0642
Microbacterium	-0.75251	0.072397

Table 3. Differential gene expression of microbes at the genus level.

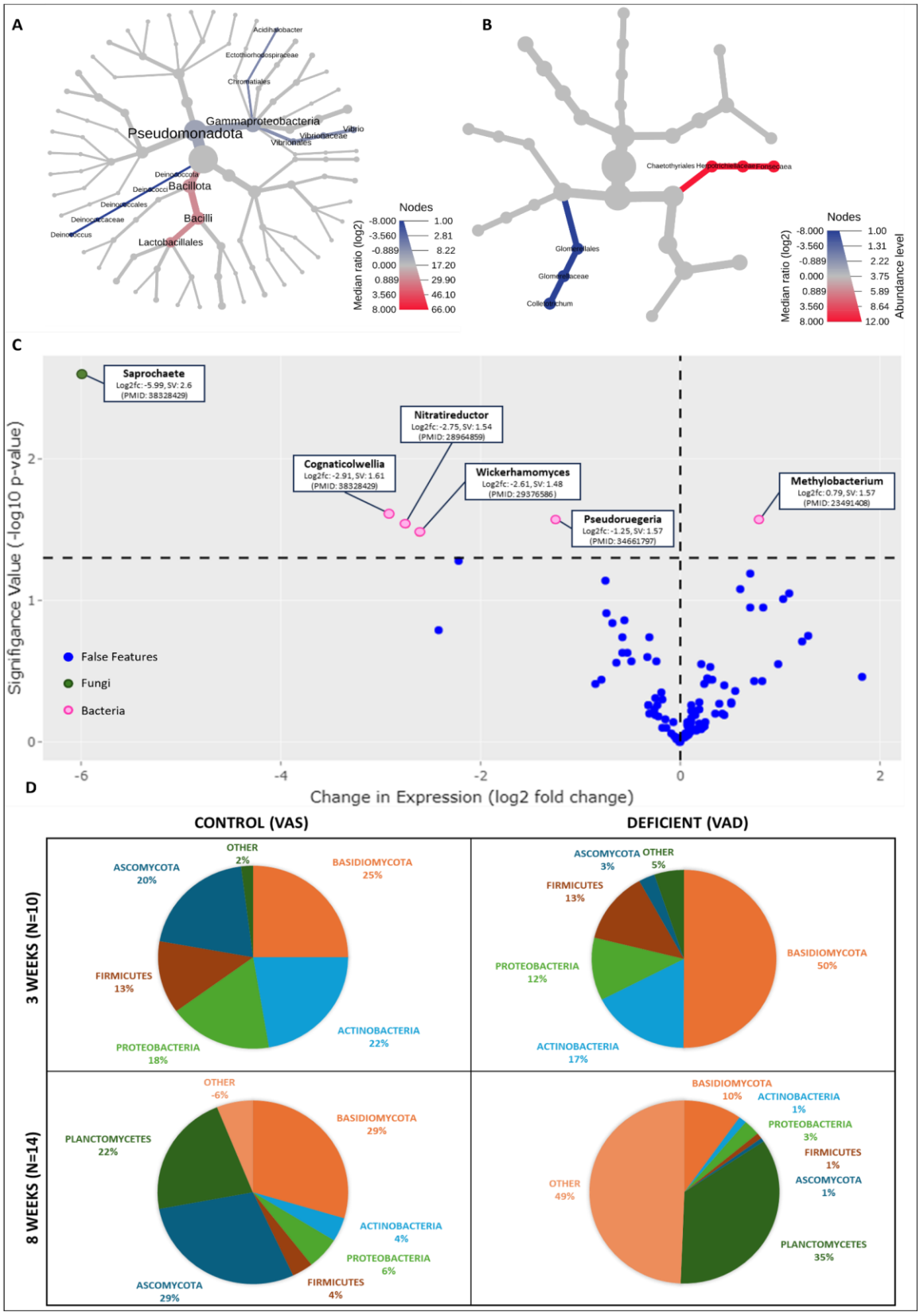
A
Acidithiobacter
Ectothiorhodospiraceae
Chromatiales
Gammaproteobacteria
Pseudomonadota
Vibrionaceae
Vibrionales
Vibrio
Deinococcota
Deinococci
Bacillota
Deinococcales
Deinococcaceae
Deinococcus
Bacilli
Lactobacillales
Nodes
Median ratio (log2)
-8.000 1.00
-3.560 2.81
-0.889 8.22
0.000 17.20
0.889 29.90
3.560 46.10
8.000 66.00
B
Chaetothyriales
Glomerellales
Glomerellaceae
Colletotrichum
Nodes
Median ratio (log2)
-8.000 1.00
-3.560 1.31
-0.889 2.22
0.000 3.75
0.889 5.89
3.560 8.64
8.000 12.00
Abundance level
C
Saprochaete
Log2fc: -5.99, SV: 2.6
(PMID: 38328429)
Nitratireductor
Log2fc: -2.75, SV: 1.54
(PMID: 28964859)
Cognaticolwellia
Log2fc: -2.91, SV: 1.61
(PMID: 38328429)
Wickerhamomyces
Log2fc: -2.61, SV: 1.48
(PMID: 29376586)
Methylobacterium
Log2fc: 0.79, SV: 1.57
(PMID: 23491408)
Pseudoruegeria
Log2fc: -1.25, SV: 1.57
(PMID: 34661797)
Signifigance Value (-log10 p-value)
False Features
Fungi
Bacteria
Change in Expression (log2 fold change)
D
CONTROL (VAS)
DEFICIENT (VAD)
3 WEEKS (N=10)
8 WEEKS (N=14)
OTHER 2%
ASCOMYCOTA 20%
BASIDIOMYCOTA 25%
FIRMICUTES 13%
ACTINOBACTERIA 22%
PROTEOBACTERIA 18%
ASCOMYCOTA 3%
OTHER 5%
FIRMICUTES 13%
BASIDIOMYCOTA 50%
PROTEOBACTERIA 12%
ACTINOBACTERIA 17%
OTHER -6%
BASIDIOMYCOTA 29%
PLANCTOMYCETES 22%
ACTINOBACTERIA 4%
PROTEOBACTERIA 6%
ASCOMYCOTA 29%
FIRMICUTES 4%
BASIDIOMYCOTA 10%
ACTINOBACTERIA 1%
PROTEOBACTERIA 3%
FIRMICUTES 1%
ASCOMYCOTA 1%
OTHER 49%
PLANCTOMYCETES 35%

Figure 12. VAD encourages an increase in low-abundant, potentially more pathogenic microbes in the airway.

(A) Heat tree of bacterial operational taxonomic unit (OTU) median ratios and (**B**) fungal relative abundance at the genus level calculated using the Metacoder app in MicrobiomeAnalyst. Blue = enriched in VAD lungs ($p < 0.05$). Red = enriched in VAS lungs ($p < 0.05$). (**C**) Volcano plot of microbes at the phylum level differentially expressed in VAD lungs using BatchQC version 1.99.02 on RStudio version 4.3.1. (**D**) Pie charts of bacteria and fungi taxonomic abundance after 3 weeks and 8 weeks of dietary modulation at the phylum level.

VAD encourages bacterial colonization in the LRT

While changes in gene expression can indicate changes in microbial abundance, significant alterations in gene expression within a particular taxa can also indicate a functional shift from a *planktonic* or non-adherent state to a *sessile* or adherent state (Illustration 3).[205] To determine whether the VAD-induced dysbiosis translates to changes in lung colonization patterns, we analyzed bacterial Gram stains of the mouse airway after 8 weeks of dietary modulation (Figures 13A-H). We observed 3-dimensional biofilm-like structures containing gram-positive bacteria in VAD lungs (Figures 13C-D, black arrows). Importantly, there were biofilm-like structures found in VAS lungs as well, but the size and quantity were fewer compared to VAD lungs (Figure 13I, histology data not shown). We also observed a large cohort of planktonic gram-negative bacteria along the VAD airway epithelium with no visible signs of colonization (Figure 13D, green arrows), although more evidence is needed to make that determination. These results indicate that gram-positive bacteria may have a distinct VAD-associated stress response in the lung that differs from gram-negative bacteria.

VAD reprograms gram-positive bacteria to invade and colonize the airway

To determine causality in relation to lung-microbe interactions, we wanted to investigate whether the microbiome can rescue or exacerbate the VAD and VAS lung phenotypes respectively. To that end, we extracted the lung microbiome from mice maintained on diets for 8 weeks and administered daily IT instillations of filtered BALs from VAS and VAD lungs into VAD and VAS mouse lungs respectively for 3 weeks (Supplemental Figure 3). It is important to note that while our extraction technique

removed larger host and immune cells, signaling molecules and immune cells smaller than 10μm such as leukocytes could not be removed from the samples using our extraction and IT protocol.[206] Therefore, our daily MTs contained the microbes and smaller signaling molecules found within the airway of the LRT.

Interestingly, early signs of invasion and colonization by gram-positive bacteria were observed in VAS lungs exposed to VAD microbial transplants for 3 weeks (VAS + VADMT; Figures 13E-F). VAD lungs receiving VAS microbial transplants also showed evidence of biofilm formation (VAD + VASMT; Figures 13G-H), although these structures may have persisted from the 8-week time point when the IT MTs began. While further validation with more repeats and saline-injected controls are still needed, these preliminary results provide evidence that dietary VAD reprograms the GP bacterial consortium to enable invasion and colonization in an otherwise healthy lung with an intact immune system. These findings provide further evidence that VAD provides a permissive niche for infection in the LRT of adult mouse lungs.

The VAD microbiome may be involved in PRR and disease pathway activation in the lung

An increase in gram-positive colony-forming units (CFUs) and expression of TLRs, some of the most common PRRs in epithelial cells (Figures 13I-J), was observed in VAD lungs. The most significant increases were observed in TLR5, TLR6, TLR7, and TLR11 gene expression. TLR5 senses flagellin, the major protein in bacterial flagella.[207] TLR5 also creates a complex with TLR4 to promote lung injury-associated MyD88-dependent signaling.[208] Likewise, TLR11 stimulation is also known to initiate the MyD88-

dependent immune pathway through bacterial sensing.[209] TLR6 creates a complex with TLR2 to regulate the innate immune response to gram-positive bacteria and fungi in the lung while TLR7 is involved in viral sensing and metabolic processing.[210-211]

Reactome disease pathway analysis showed TLR5-mediated bacterial flagellin sensing was down-regulated (Supplemental Figure 4) despite an increase in gene expression. TLR5 signaling is critical for orchestrating the mucosal immune response in the airway and is often seen down-regulated in smokers with COPD.[212] Therefore, our data provides strong evidence that VAD causes a disruption in TLR-mediated immune signaling, leading to an inflammatory response.

We also performed Microbe-Disease enrichment analysis using the MicrobiomeProfiler R/Shiny package (Figure 13K).[213] Using the top 20 Gene Ontology (GO) terms generated from our microbiome dataset, the most enriched host disease pathways from our VAD microbiome gene signature were associated with cancer, cell cycle progression, proliferation, and infection. Importantly, our host RNAseq pathway analysis (Figure 2) also indicated these same processes, suggesting host-microbe interactions may be an integral component of regulating cell cycle, differentiation, and tumorigenesis in the lung.

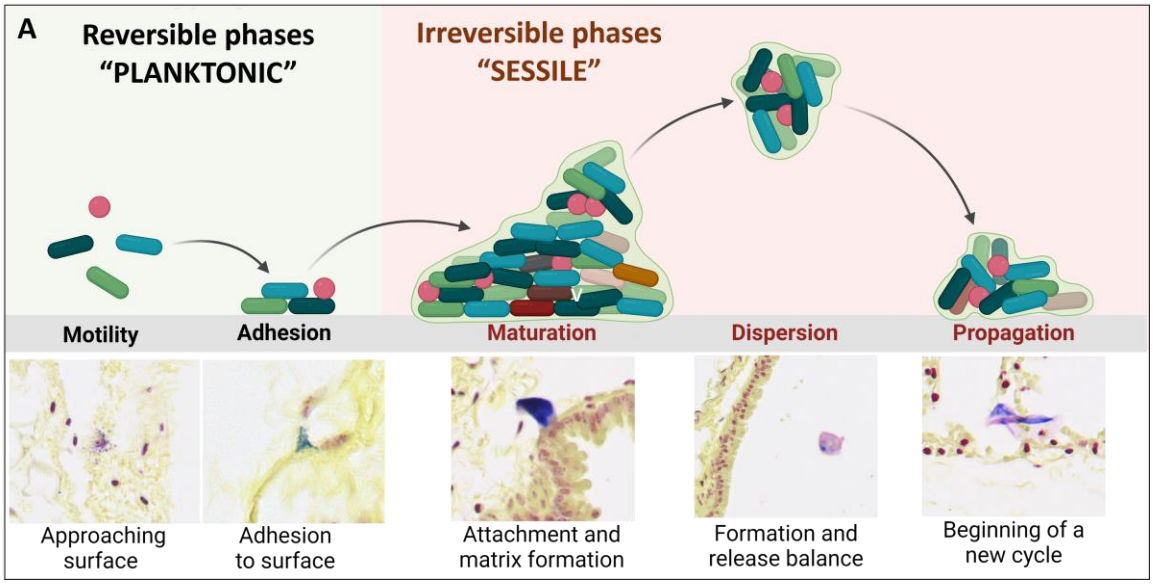

Illustration 3. Biofilm formation in the lung.

Graphical depiction of gram-positive biofilm formation in adult mouse lungs. Illustration created using BioRender.

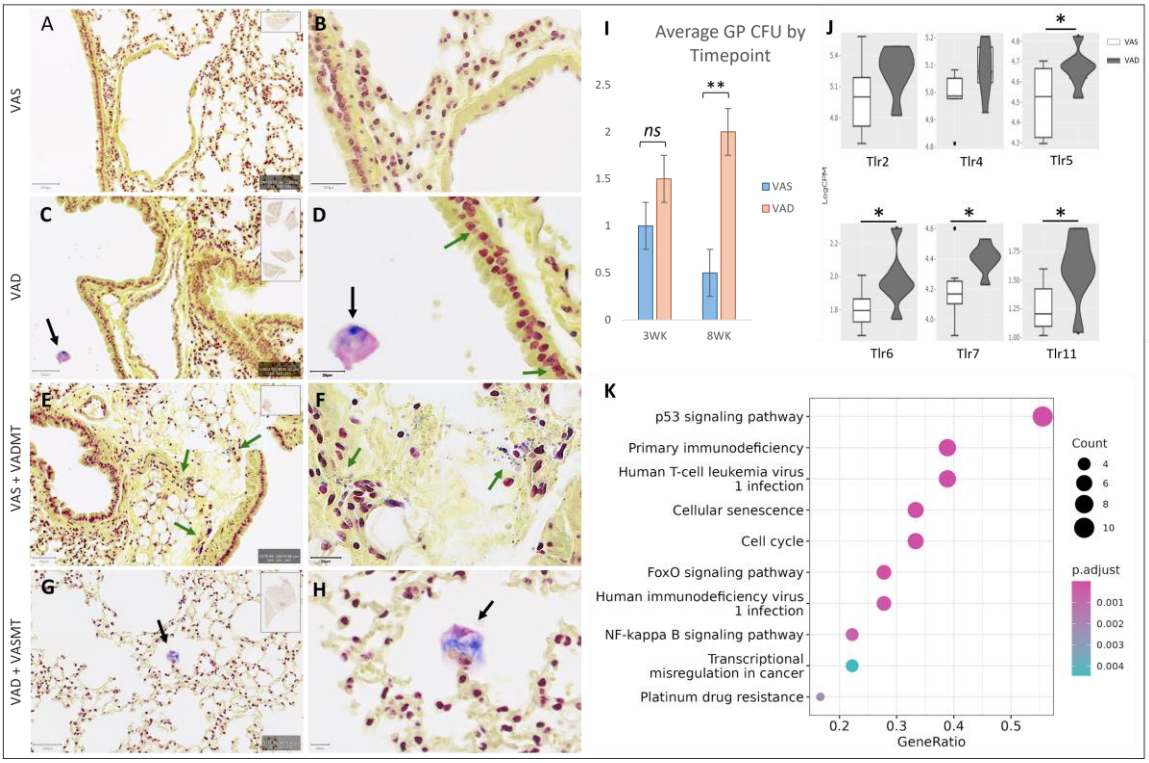

Figure 13. VAD encourages bacterial colonization and biofilm formation in the airway.

(**A-H**) Bacterial (Gram) staining of VAS (**A,B**) and VAD (**C,D**) lungs at week 8. Mice maintained on VAS and VAD diets for 8 weeks were given daily ITinstillation for 3 weeks with BALF from mice maintained on the opposite diet (**E-H**). VADMT = vitamin A deficient microbial transplant. VASMT = vitamin A sufficient microbial transplant. Black arrows indicate 3-dimensional structures containing gram-positive bacteria. Green arrows indicate planktonic or non-colonizing bacteria. Insets within **A**, **C**, **E**, and **G** show the region within the whole lung where the photos were taken. Figures **B**, **D**, **F**, and **H** are magnified photos of **A**, **C**, **E**, and **G**, respectively. (**I**) The average CFU of gram-positive (GP) bacteria found on each whole tissue slide scan, n = 2 for 3 weeks, n = 4 for 8 weeks, *p*-values = 0.42264973 and 0.002022368 respectively. (**J**) TLR gene expression in VAS and VAD lungs at 8 weeks, * = $p < 0.05$. (**K**) The top 20 ranked GO terms from KEGG pathway analysis with Bonferroni correction from VAS and VAD lungs. Figure generated using Microbiome Profiler version 1.0.0 and SingleCell Toolkit version 1.9.1 on RStudio version 4.1.1. 'Gene ratio' is the percentage of total DEGs in the given GO term. 'Count' is the number of genes enriched in a GO term.

Note that at the time of submission, parts of the following section were under review at Science Translational Medicine. They were also available as a preprint at BioRxiv: https://doi.org/10.1101/2024.06.21.600110

DISCUSSION

Many papers have uncovered links between nutritional status of humans and the onset of lung cancer and disease, but there are currently no published studies indicating dietary VAD acts directly on the lung microbiome, nor is there evidence of host-microbe interactions in the lung that are influenced by host vitamin A status. This report is the first to characterize the functional interactions between vitamin A metabolites, the lung, and the lung microbiome. We found that VAD leads to epithelial remodeling, epithelial denudation, a loss of apical protein expression in the airway epithelium, focal hyperplasia, and a breakdown of MCC. These changes illustrate a form of lung injury that is similar to diseases found in humans, although few have looked into the role diet plays in lung disease.

Considering serum retinol levels are not reflective of the RA bioavailability in the lung,[8] our lab aimed to determine whether VAD-induced epithelial remodeling is a local phenomenon. Despite sufficient vitamin A supplied through diet, our Cre-positive mouse model exhibited similar remodeling to our diet model 8 weeks after treatment, confirming the lung epithelium requires RAR activation to maintain lung homeostasis.

Gene sets associated with cilia assembly and trafficking were the most enriched pathways associated with VAD status, suggesting that ciliary dysfunction and a loss of epithelial integrity may occur within the VAD lung. Ciliary dysfunction leads to MCC impairment, one of the first defense mechanisms to prevent microbial residence or infection

in the lung.[58] Ciliary dysfunction is commonly found in patients with primary ciliary dyskinesia and cystic fibrosis (CF), but it can also be observed in patients with lung infection, α1-antitrypsin deficiency (AATD), COPD, and asthma.[59] While research has uncovered evidence suggesting diet influences the severity and progression of pulmonary diseases, the exact mechanisms that determine prognosis in these patients remain largely unknown.

Luckily, the function and structure of cilia-related proteins responsible for proper motility and MCC are evolutionarily conserved and can be easily studied in relation to the human lung using a mouse model.[61] Based on our findings, we propose that chronic VAD predisposes adult mouse lungs to microbial colonization and respiratory infections over time. We hypothesize that CCs are one of the host cells affected by dietary VAD status within the lung. Once ciliary function is affected, the lung can no longer clear pathogens and pollutants effectively.

Microbial dysbiosis leads to increased inflammation, infections, and disease in the human lung.[75] For instance, significant alterations in the abundance of *Pseudamonadota* was observed in patients during COPD exacerbations.[74] Our work provides evidence that dietary vitamin A is important for a healthy lung, while VAD alters the lung epithelium and the microenvironment to create a permissive niche for pathogenic outgrowth and biofilm formation.

Metatranscriptomic analysis showed a reduction in fungal abundance and an increase in relative bacterial abundance in VAD lungs at week 8, primarily consisting of gram-negative bacteria. Histological staining supported these findings, while also

providing evidence of a VA-mediated mechanism that triggers colonization in gram-positive but not gram-negative bacteria, suggesting that vitamin A may be involved in gram-specific QS mechanisms. Transcriptional data confirms changes in fungal composition precede measurable changes to the bacterial consortium in VAD lungs, suggesting that VA-mediated QS mechanisms in the LRT are likely polymicrobial in nature.

Of note, our results are consistent with human studies where bacteria undergo a functional change towards colonization and oral biofilm formation; researchers investigating the development of dental plaque following a meal observed a reduction in the relative abundance of gram-positive bacteria in late biofilm samples, with different molecular pathways activated between early and late biofilm formation.[73] Specifically, KEGG analysis of late biofilm transcripts were enriched for pathways involved in cellular transport, cell motility including pilus and flagella assembly, and DNA/mismatch repair, the same pathways enriched in our mouse dataset (Figures 5A-B, other data not shown). These findings support the hypothesis that chronic VAD shifts the microbial composition of the LRT towards dysbiosis and early pathogenesis. This shift is evidenced by a reduction in the relative abundance of Ascomycota and gram-positive bacteria, as well as an increase in the relative abundance of CFUs and oxygen-tolerant microbes more broadly, predisposing the VAD lung to infectious and inflammatory diseases.

While our MT data provides evidence that bacteria from the VAD airway are prone to epithelial injury by adherence, colonization, and invasion, it is difficult to make determinations without identifying the strains present within these microbes. Future studies

aimed towards isolating bacteria from VAD lungs would allow us to perform species- or strain-level identification, absolute abundance counts, and analysis of the formation and maturation of the extracellular matrix (ECM) over time.

A promising future direction of this work towards detection of respiratory infection is the observed fungal sensitivity to host vitamin A status. Ascomycota, the most abundant fungal phylum found in humans worldwide, dramatically reduced transcriptional activity at our earliest time point in VAD lungs; this change in transcription preceded the hyperplasia and the bacterial biofilm formation. Therefore, future studies investigating the effect of vitamin A status on the lung *mycobiome* may uncover useful and sensitive biomarkers for early detection of airway maladaptive repair and infection in malnourished patients.

APPENDIX

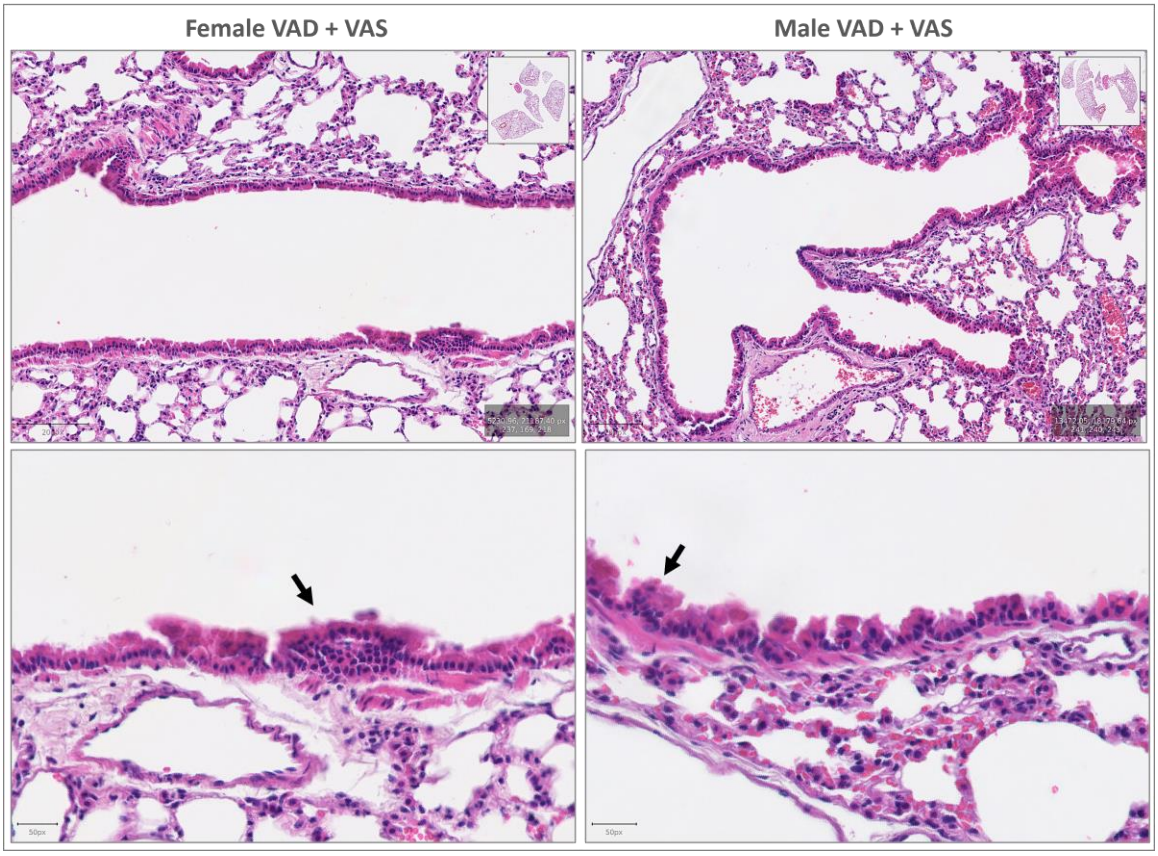

Supplemental Figure 1. Vitamin A supplementation does not repair the epithelial remodeling in VAD lungs.

Adult wild-type C57B/J6 mice were maintained on VAD diets for 8 weeks followed by a normal chow diet for 12 weeks. Whole lungs were extracted and stained with H&E for morphological analysis. Scale bars = 50 μm magnification. Black arrows indicate regions of hyperplasia.

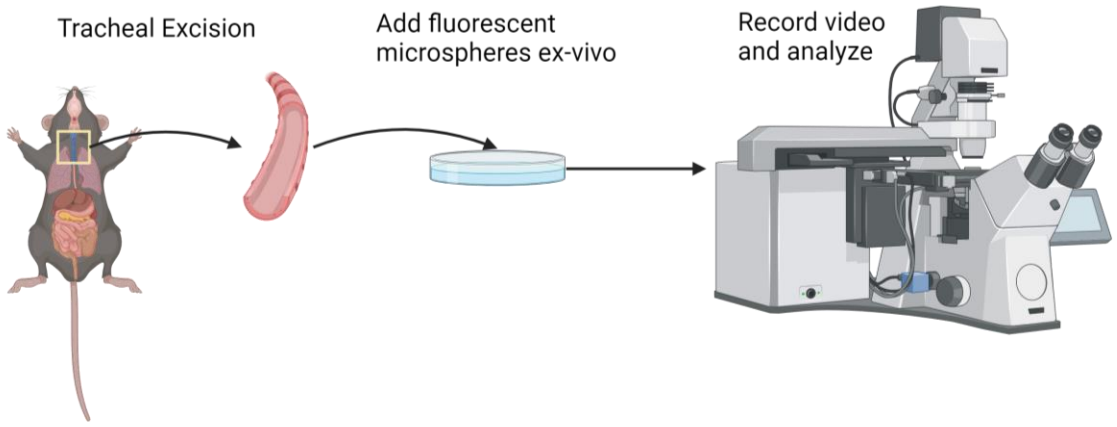

Supplemental Figure 2. Experimental design of the ciliary motility assay.

Illustration created using BioRender.

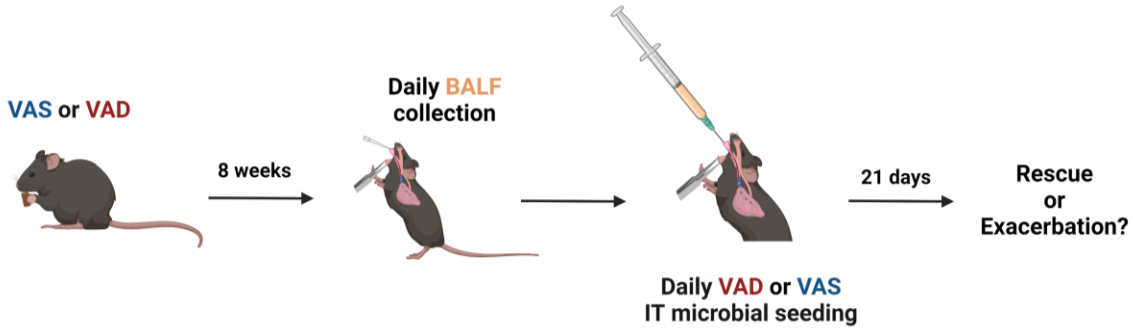

Supplemental Figure 3. Experimental design of the microbial transplant experiment.

Illustration created using BioRender.

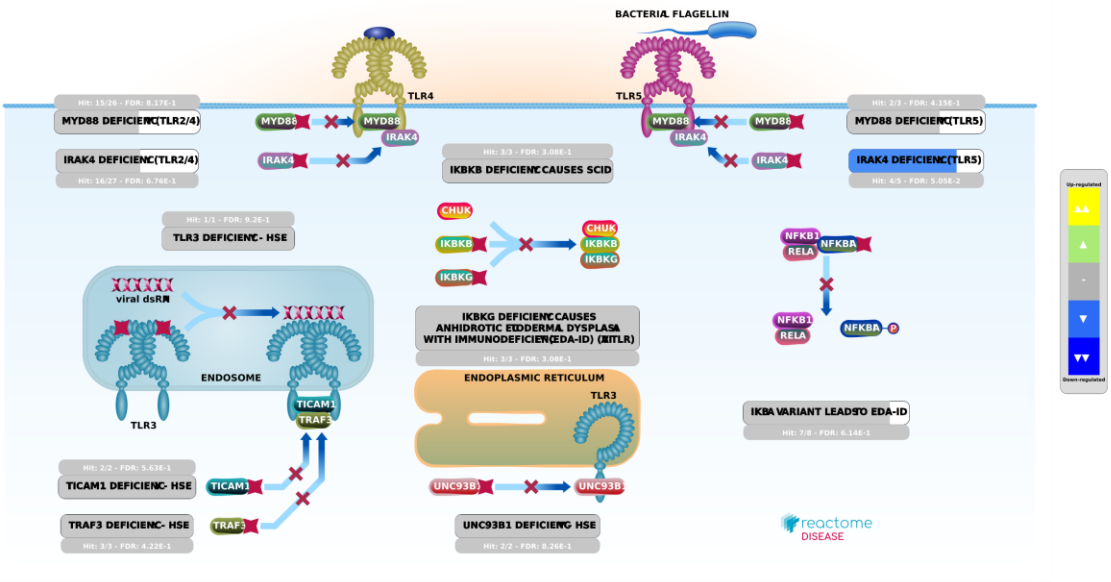

Supplemental Figure 4. Illustration of PRR disease pathway expression in VAD lungs.

Illustration of the bacterial sensing PRR pathway using our full host RNAseq dataset and the pathway analysis and data visualization tools from Reactome

BIBLIOGRAPHY

1. Carazo A, Macáková K, Matoušová K, Krčmová LK, Protti M, Mladěnka P. Vitamin A Update: Forms, Sources, Kinetics, Detection, Function, Deficiency, Therapeutic Use and Toxicity. Nutrients. 2021 May 18;13(5):1703. doi: 10.3390/nu13051703. PMID: 34069881.

2. Dawson MI. The importance of vitamin A in nutrition. Current Pharmaceutical Design. 2000 Feb;6(3):311-25. doi: 10.2174/1381612003401190. PMID: 10637381.

3. Blaner WS, Li Y, Brun PJ, Yuen JJ, Lee SA, Clugston RD. Vitamin A Absorption, Storage and Mobilization. Subcell Biochem. 2016;81:95-125. doi: 10.1007/978-94-024-0945-1_4. PMID: 27830502.

4. Clagett-Dame M, Knutson D. Vitamin A in reproduction and development. Nutrients. 2011 Apr;3(4):385-428. doi: 10.3390/nu3040385. Epub 2011 Mar 29. PMID: 22254103.

5. Clagett-Dame M, DeLuca HF. The role of vitamin A in mammalian reproduction and embryonic development. Annual Review of Nutrition. 2002;22:347-81. doi: 10.1146/annurev.nutr.22.010402.102745E. PMID: 12055350.

6. Saari JC. Vitamin A and Vision. Subcell Biochem. 2016;81:231-259. doi: 10.1007/978-94-024-0945-1_9. PMID: 27830507.

7. Huang Z, Liu Y, Qi G, Brand D, Zheng SG. Role of Vitamin A in the Immune System. Journal of Clinical Medicine. 2018 Sep 6;7(9):258. doi: 10.3390/jcm7090258. PMID: 30200565.

8. Timoneda J, Rodríguez-Fernández L, Zaragozá R, Marín MP, Cabezuelo MT, Torres L, Viña JR, Barber T. Vitamin A Deficiency and the Lung. Nutrients. 2018 Aug 21;10(9):1132. doi: 10.3390/nu10091132. PMID: 30134568.

9. Golczak M, Sears AE, Kiser PD, Palczewski K. LRAT-specific domain facilitates vitamin A metabolism by domain swapping in HRASLS3. Nature Chemical Biology. 2015 Jan;11(1):26-32. doi: 10.1038/nchembio.1687. Epub 2014 Nov 10. PMID: 25383759.

10. Molotkov A, Duester G. Genetic evidence that retinaldehyde dehydrogenase Raldh1 (Aldh1a1) functions downstream of alcohol dehydrogenase Adh1 in metabolism of retinol to retinoic acid. Journal of Biological Chemistry. 2003 Sep 19;278(38):36085-90. doi: 10.1074/jbc.M303709200. Epub 2003 Jul 7. PMID: 12851412.

11. Ross AC. Retinoid production and catabolism: role of diet in regulating retinol esterification and retinoic Acid oxidation. Journal of Nutrition. 2003 Jan;133(1):291S-296S. doi: 10.1093/jn/133.1.291S. PMID: 12514312.

12. Stevison F, Jing J, Tripathy S, Isoherranen N. Role of Retinoic Acid-Metabolizing Cytochrome P450s, CYP26, in Inflammation and Cancer. Advances in Pharmacology. 2015;74:373-412. doi: 10.1016/bs.apha.2015.04.006. Epub 2015 May 27. PMID: 26233912.

13. Ross I, Bick S, Ayieko P, Dreibelbis R, Wolf J, Freeman MC, Allen E, Brauer M, Cumming O. Effectiveness of handwashing with soap for preventing acute respiratory infections in low-income and middle-income countries: a systematic review and meta-analysis. Lancet. 2023 May 20;401(10389):1681-1690. doi: 10.1016/S0140-6736(23)00021-1. Epub 2023 Apr 27. PMID: 37121242.

14. Berman S. Epidemiology of acute respiratory infections in children of developing countries. Reviews of Infectious Diseases. 1991 May-Jun;13 Suppl 6:S454-62. doi: 10.1093/clinids/13.supplement_6.s454. PMID: 1862276.

15. Arthur SS, Nyide B, Soura AB, Kahn K, Weston M, Sankoh O. Tackling malnutrition: a systematic review of 15-year research evidence from INDEPTH health and demographic surveillance systems. Global Health Action. 2015 Oct 29;8:28298. doi: 10.3402/gha.v8.28298. PMID: 26519130.

16. Kheir AE, Dirar TO, Elhassan HO, Elshikh MA, Ahmed MB, Abbass MA, Idris SS. Xerophthalmia in a traditional Quran boarding school in Sudan. Middle East African Journal of Ophthalmology. 2012 Apr-Jun;19(2):190-3. doi: 10.4103/0974-9233.95247. PMID: 22623857.

17. Sherwin JC, Reacher MH, Dean WH, Ngondi J. Epidemiology of vitamin A deficiency and xerophthalmia in at-risk populations. Transactions of the Royal Society of Tropical Medicine and Hygiene. 2012 Apr;106(4):205-14. doi: 10.1016/j.trstmh.2012.01.004. Epub 2012 Feb 11. PMID: 22326691.

18. Ramakrishnan U, Darnton-Hill I. Assessment and control of vitamin A deficiency disorders. Journal of Nutrition. 2002 Sep;132(9 Suppl):2947S-2953S. doi: 10.1093/jn/132.9.2947S. PMID: 12221275.

19. el Bushra HE, Ash LR, Coulson AH, Neumann CG. Interrelationship between diarrhea and vitamin A deficiency: is vitamin A deficiency a risk factor for diarrhea? Pediatric Infectious Disease Journal. 1992 May;11(5):380-4. doi: 10.1097/00006454-199205000-00008. PMID: 1630858.

20. Chai Z, Lyu Y, Chen Q, Wei CH, Snyder LM, Weaver V, Sebastian A, Albert I, Li Q, Cantorna MT, Ross AC. RNAseq studies reveal distinct transcriptional response to

vitamin A deficiency in small intestine versus colon, uncovering novel vitamin A-regulated genes. Journal of Nutritional Biochemistry. 2021 Dec;98:108814. doi: 10.1016/j.jnutbio.2021.108814. Epub 2021 Jul 6. PMID: 34242724.

21. Owusu, S. A. Vitamin A Supplementation: Its Effects on Ontogeny, Lung Development, and Neonatal Lung Injury. 2015.

22. Zachman RD. Role of vitamin A in lung development. Journal of Nutrition. 1995 Jun;125(6 Suppl):1634S-1638S. doi: 10.1093/jn/125.suppl_6.1634S. PMID: 7782917.

23. Paiva SA, Godoy I, Vannucchi H, Fávaro RM, Geraldo RR, Campana AO. Assessment of vitamin A status in chronic obstructive pulmonary disease patients and healthy smokers. American Journal of Clinical Nutrition. 1996 Dec;64(6):928-34. doi: 10.1093/ajcn/64.6.928. PMID: 8942419.

24. Arora P, Kumar V, Batra S. Vitamin A status in children with asthma. Pediatric Allergy and Immunology. 2002 Jun;13(3):223-6. doi: 10.1034/j.1399-3038.2002.00010.x. PMID: 12144646.

25. Pakasi TA, Karyadi E, Wibowo Y, Simanjuntak Y, Suratih NM, Salean M, Darmawidjaja N, van der Meer JW, van der Velden K, Dolmans WM. Vitamin A deficiency and other factors associated with severe tuberculosis in Timor and Rote Islands, East Nusa Tenggara Province, Indonesia. European Journal of Clinical Nutrition. 2009 Sep;63(9):1130-5. doi: 10.1038/ejcn.2009.25. Epub 2009 May 27. PMID: 19471295.

26. Penkert RR, Smith AP, Hrincius ER, McCullers JA, Vogel P, Smith AM, Hurwitz JL. Effect of Vitamin A Deficiency in Dysregulating Immune Responses to Influenza Virus and Increasing Mortality Rates After Bacterial Coinfections. Journal of Infectious Diseases. 2021 May 28;223(10):1806-1816. doi: 10.1093/infdis/jiaa597. PMID: 32959872.

27. Melenotte C, Brouqui P, Botelho-Nevers E. Severe measles, vitamin A deficiency, and the Roma community in Europe. Emerging Infectious Diseases. 2012 Sep;18(9):1537-9. doi: 10.3201/eid1809.111701. PMID: 22932125.

28. Stephensen CB, Lietz G. Vitamin A in resistance to and recovery from infection: relevance to SARS-CoV2. British Journal of Nutrition. 2021 Dec 14;126(11):1663-1672. doi: 10.1017/S0007114521000246. Epub 2021 Jan 20. PMID: 33468263.

29. Bhaskaram P. Micronutrient malnutrition, infection, and immunity: an overview. Nutrition Reviews. 2002 May;60(5 Pt 2):S40-5. doi: 10.1301/00296640260130722. PMID: 12035857.

30. Benn CS, Aaby P, Arts RJ, Jensen KJ, Netea MG, Fisker AB. An enigma: why vitamin A supplementation does not always reduce mortality even though vitamin A deficiency is associated with increased mortality. International Journal of Epidemiology. 2015 Jun;44(3):906-18. doi: 10.1093/ije/dyv117. Epub 2015 Jul 2. PMID: 26142161.

31. Surman SL, Penkert RR, Sealy RE, Jones BG, Marion TN, Vogel P, Hurwitz JL. Consequences of Vitamin A Deficiency: Immunoglobulin Dysregulation, Squamous Cell Metaplasia, Infectious Disease, and Death. International Journal of Molecular Sciences. 2020 Aug 4;21(15):5570. doi: 10.3390/ijms21155570. PMID: 32759702.

32. Zhang Y, Lu Y, Wang S, Yang L, Xia H, Sun G. Excessive Vitamin A Supplementation Increased the Incidence of Acute Respiratory Tract Infections: A Systematic Review and Meta-Analysis. Nutrients. 2021 Nov 26;13(12):4251. doi: 10.3390/nu13124251. PMID: 34959803.

33. Ross AC, Stephensen CB. Vitamin A and retinoids in antiviral responses. FASEB Journal. 1996 Jul;10(9):979-85. PMID: 8801180.

34. Castro-Nallar E, Shen Y, Freishtat RJ, Pérez-Losada M, Manimaran S, Liu G, Johnson WE, Crandall KA. Integrating microbial and host transcriptomics to characterize asthma-associated microbial communities. BMC Medical Genomics. 2015 Aug 16;8:50. doi: 10.1186/s12920-015-0121-1. PMID: 26277095.

35. Dickson RP. The Lung Microbiome and ARDS. It Is Time to Broaden the Model. American Journal of Respiratory and Critical Care Medicine. 2018 Mar 1;197(5):549-551. doi: 10.1164/rccm.201710-2096ED. PMID: 29091746.

36. Mammen MJ, Sethi S. COPD and the microbiome. Respirology. 2016 May;21(4):590-9. doi: 10.1111/resp.12732. Epub 2016 Jan 27. PMID: 26852737.

37. Mao Q, Jiang F, Yin R, Wang J, Xia W, Dong G, Ma W, Yang Y, Xu L, Hu J. Interplay between the lung microbiome and lung cancer. Cancer Letters. 2018 Feb 28;415:40-48. doi: 10.1016/j.canlet.2017.11.036. Epub 2017 Dec 2. PMID: 29197615.

38. Cyprian F, Sohail MU, Abdelhafez I, Salman S, Attique Z, Kamareddine L, Al-Asmakh M. SARS-CoV-2 and immune-microbiome interactions: Lessons from respiratory viral infections. International Journal of Infectious Diseases. 2021 Apr;105:540-550. doi: 10.1016/j.ijid.2021.02.071. Epub 2021 Feb 18. PMID: 33610778.

39. Mettelman RC, Allen EK, Thomas PG. Mucosal immune responses to infection and vaccination in the respiratory tract. Immunity. 2022 May 10;55(5):749-780. doi: 10.1016/j.immuni.2022.04.013. PMID: 35545027.

40. Fernandes-Silva H, Araújo-Silva H, Correia-Pinto J, Moura RS. Retinoic Acid: A Key Regulator of Lung Development. Biomolecules. 2020 Jan 17;10(1):152. doi: 10.3390/biom10010152. PMID: 31963453.

41. Adivitiya, Kaushik MS, Chakraborty S, Veleri S, Kateriya S. Mucociliary Respiratory Epithelium Integrity in Molecular Defense and Susceptibility to Pulmonary Viral Infections. Biology (Basel). 2021 Jan 29;10(2):95. doi: 10.3390/biology10020095. PMID: 33572760.

42. Chegini Z, Noei M, Hemmati J, Arabestani MR, Shariati A. The destruction of mucosal barriers, epithelial remodeling, and impaired mucociliary clearance: possible pathogenic mechanisms of Pseudomonas aeruginosa and Staphylococcus aureus in chronic rhinosinusitis. Cell Communication and Signaling. 2023 Oct 30;21(1):306. doi: 10.1186/s12964-023-01347-2. PMID: 37904180.

43. Heijink IH, Brandenburg SM, Postma DS, van Oosterhout AJ. Cigarette smoke impairs airway epithelial barrier function and cell-cell contact recovery. European Respiratory Journal. 2012 Feb;39(2):419-28. doi: 10.1183/09031936.00193810. Epub 2011 Jul 20. PMID: 21778164.

44. Saint-Criq V, Lugo-Villarino G, Thomas M. Dysbiosis, malnutrition and enhanced gut-lung axis contribute to age-related respiratory diseases. Ageing Research Reviews. 2021 Mar;66:101235. doi: 10.1016/j.arr.2020.101235. Epub 2020 Dec 13. PMID: 33321253.

45. Schleimer RP, Kato A, Kern R, Kuperman D, Avila PC. Epithelium: at the interface of innate and adaptive immune responses. Journal of Allergy and Clinical Immunology. 2007 Dec;120(6):1279-84. doi: 10.1016/j.jaci.2007.08.046. Epub 2007 Oct 18. PMID: 17949801.

46. Leiva-Juárez MM, Kolls JK, Evans SE. Lung epithelial cells: therapeutically inducible effectors of antimicrobial defense. Mucosal Immunology. 2018 Jan;11(1):21-34. doi: 10.1038/mi.2017.71. Epub 2017 Aug 16. PMID: 28812547.

47. Durham AL, Adcock IM. The relationship between COPD and lung cancer. Lung Cancer. 2015 Nov;90(2):121-7. doi: 10.1016/j.lungcan.2015.08.017. Epub 2015 Aug 29. PMID: 26363803.

48. Conese M, Di Gioia S. Pathophysiology of Lung Disease and Wound Repair in Cystic Fibrosis. Pathophysiology. 2021 Mar 10;28(1):155-188. doi: 10.3390/pathophysiology28010011. PMID: 35366275.

49. Moldoveanu B, Otmishi P, Jani P, Walker J, Sarmiento X, Guardiola J, Saad M, Yu J. Inflammatory mechanisms in the lung. Journal of Inflammatory Research. 2009;2:1-11. Epub 2008 Dec 16. PMID: 22096348.

50. Song Z, Meng Y, Fricker M, Li X, Tian H, Tan Y, Qin L. The role of gut-lung axis in COPD: Pathogenesis, immune response, and prospective treatment. Heliyon. 2024 May 3;10(9):e30612. doi: 10.1016/j.heliyon.2024.e30612. PMID: 38742057.

51. Hufnagl K, Pali-Schöll I, Roth-Walter F, Jensen-Jarolim E. Dysbiosis of the gut and lung microbiome has a role in asthma. Seminars in Immunopathology. 2020 Feb;42(1):75-93. doi: 10.1007/s00281-019-00775-y. Epub 2020 Feb 18. PMID: 32072252.

52. Zhuang H, Cheng L, Wang Y, Zhang YK, Zhao MF, Liang GD, Zhang MC, Li YG, Zhao JB, Gao YN, Zhou YJ, Liu SL. Dysbiosis of the Gut Microbiome in Lung Cancer. Frontiers in Cellular and Infectious Microbiology. 2019 Apr 18;9:112. doi: 10.3389/fcimb.2019.00112. PMID: 31065547.

53. Zhang D, Li S, Wang N, Tan HY, Zhang Z, Feng Y. The Cross-Talk Between Gut Microbiota and Lungs in Common Lung Diseases. Frontiers in Microbiology. 2020 Feb 25;11:301. doi: 10.3389/fmicb.2020.00301. PMID: 32158441.

54. Schuijt TJ, Lankelma JM, Scicluna BP, de Sousa e Melo F, Roelofs JJ, de Boer JD, Hoogendijk AJ, de Beer R, de Vos A, Belzer C, de Vos WM, van der Poll T, Wiersinga WJ. The gut microbiota plays a protective role in the host defence against pneumococcal pneumonia. Gut. 2016 Apr;65(4):575-83. doi: 10.1136/gutjnl-2015-309728. Epub 2015 Oct 28. PMID: 26511795.

55. Keskey R, Cone JT, DeFazio JR, Alverdy JC. The use of fecal microbiota transplant in sepsis. Translational Research. 2020 Dec;226:12-25. doi: 10.1016/j.trsl.2020.07.002. Epub 2020 Jul 7. PMID: 32649987.

56. Antonioli L, Blandizzi C, Pacher P, Guilliams M, Haskó G. Rethinking Communication in the Immune System: The Quorum Sensing Concept. Trends in Immunology. 2019 Feb;40(2):88-97. doi: 10.1016/j.it.2018.12.002. Epub 2019 Jan 2. PMID: 30611647.

57. Albuquerque P, Casadevall A. Quorum sensing in fungi--a review. Medical Mycology. 2012 May;50(4):337-45. doi: 10.3109/13693786.2011.652201. Epub 2012 Jan 24. PMID: 22268493.

58. Rollet C, Gal L, Guzzo J. Biofilm-detached cells, a transition from a sessile to a planktonic phenotype: a comparative study of adhesion and physiological characteristics in Pseudomonas aeruginosa. FEMS Microbiology Letters. 2009 Jan;290(2):135-42. doi: 10.1111/j.1574-6968.2008.01415.x. Epub 2008 Nov 21. PMID: 19054076.

59. Leiva-Juárez MM, Kolls JK, Evans SE. Lung epithelial cells: therapeutically inducible effectors of antimicrobial defense. Mucosal Immunology. 2018 Jan;11(1):21-34. doi: 10.1038/mi.2017.71. Epub 2017 Aug 16. PMID: 28812547.

60. Chong DLW, Sriskandan S. Pro-inflammatory mechanisms in sepsis. Contributions to Microbiology. 2011;17:86-107. doi: 10.1159/000324022. Epub 2011 Jun 9. PMID: 21659748.

61. Gong T, Liu L, Jiang W, Zhou R. DAMP-sensing receptors in sterile inflammation and inflammatory diseases. Nature Reviews Immunology. 2020 Feb;20(2):95-112. doi: 10.1038/s41577-019-0215-7. Epub 2019 Sep 26. PMID: 31558839.

62. Pouwels SD, Heijink IH, ten Hacken NH, Vandenabeele P, Krysko DV, Nawijn MC, van Oosterhout AJ. DAMPs activating innate and adaptive immune responses in COPD. Mucosal Immunology. 2014 Mar;7(2):215-26. doi: 10.1038/mi.2013.77. Epub 2013 Oct 23. PMID: 24150257.

63. Land WG. Role of DAMPs in respiratory virus-induced acute respiratory distress syndrome-with a preliminary reference to SARS-CoV-2 pneumonia. Genes and Immunity. 2021 Jul;22(3):141-160. doi: 10.1038/s41435-021-00140-w. Epub 2021 Jun 17. Erratum in: Genes and Immunity. 2022 Dec;23(8):245. doi: 10.1038/s41435-022-00190-8. PMID: 34140652.

64. Bolourani S, Brenner M, Wang P. The interplay of DAMPs, TLR4, and proinflammatory cytokines in pulmonary fibrosis. Journal of Molecular Medicine (Berl). 2021 Oct;99(10):1373-1384. doi: 10.1007/s00109-021-02113-y. Epub 2021 Jul 13. PMID: 34258628.

65. Zhang Q, Kang R, Zeh HJ 3rd, Lotze MT, Tang D. DAMPs and autophagy: cellular adaptation to injury and unscheduled cell death. Autophagy. 2013 Apr;9(4):451-8. doi: 10.4161/auto.23691. Epub 2013 Feb 6. PMID: 23388380.

66. Baker BC, Heazell AEP, Sibley C, Wright R, Bischof H, Beards F, Guevara T, Girard S, Jones RL. Hypoxia and oxidative stress induce sterile placental inflammation in vitro. Scientific Reports. 2021 Mar 31;11(1):7281. doi: 10.1038/s41598-021-86268-1. PMID: 33790316.

67. Liu X, Cao H, Li J, Wang B, Zhang P, Dong Zhang X, Liu Z, Yuan H, Zhan Z. Autophagy induced by DAMPs facilitates the inflammation response in lungs undergoing ischemia-reperfusion injury through promoting TRAF6 ubiquitination. Cell Death and Differentiation. 2017 Apr;24(4):683-693. doi: 10.1038/cdd.2017.1. Epub 2017 Feb 3. PMID: 28157209.

68. Yang J, Yan H. Mucosal epithelial cells: the initial sentinels and responders controlling and regulating immune responses to viral infections. Cellular and

Molecular Immunology. 2021 Jul;18(7):1628-1630. doi: 10.1038/s41423-021-00650-7. Epub 2021 Apr 29. PMID: 33927362.

69. Jeannin P, Jaillon S, Delneste Y. Pattern recognition receptors in the immune response against dying cells. Current Opinion in Immunology. 2008 Oct;20(5):530-7. doi: 10.1016/j.coi.2008.04.013. Epub 2008 Jun 12. PMID: 18555676.

70. Li D, Wu M. Pattern recognition receptors in health and diseases. Signal Transduction and Targeted Therapy. 2021 Aug 4;6(1):291. doi: 10.1038/s41392-021-00687-0. PMID: 34344870.

71. Surman SL, Penkert RR, Sealy RE, Jones BG, Marion TN, Vogel P, Hurwitz JL. Consequences of Vitamin A Deficiency: Immunoglobulin Dysregulation, Squamous Cell Metaplasia, Infectious Disease, and Death. International Journal of Molecular Sciences. 2020 Aug 4;21(15):5570. doi: 10.3390/ijms21155570. PMID: 32759702.

72. Yoon JH, Koo JS, Norford D, Guzman K, Gray T, Nettesheim P. Lysozyme expression during metaplastic squamous differentiation of retinoic acid-deficient human tracheobronchial epithelial cells. American Journal of Respiratory Cell and Molecular Biology. 1999 Apr;20(4):573-81. doi: 10.1165/ajrcmb.20.4.3127. PMID: 10100988.

73. Puchelle E, Zahm JM, Tournier JM, Coraux C. Airway epithelial repair, regeneration, and remodeling after injury in chronic obstructive pulmonary disease. Proceedings of the American Thoracic Society. 2006 Nov;3(8):726-33. doi: 10.1513/pats.200605-126SF. PMID: 17065381.

74. Whitsett JA. Airway Epithelial Differentiation and Mucociliary Clearance. Annals of the American Thoracic Society. 2018 Nov;15(Suppl 3):S143-S148. doi: 10.1513/AnnalsATS.201802-128AW. PMID: 30431340.

75. Potaczek DP, Miethe S, Schindler V, Alhamdan F, Garn H. Role of airway epithelial cells in the development of different asthma phenotypes. Cellular Signaling. 2020 May;69:109523. doi: 10.1016/j.cellsig.2019.109523. Epub 2020 Jan 2. PMID: 31904412.

76. Zuo WL, Shenoy SA, Li S, O'Beirne SL, Strulovici-Barel Y, Leopold PL, Wang G, Staudt MR, Walters MS, Mason C, Kaner RJ, Mezey JG, Crystal RG. Ontogeny and Biology of Human Small Airway Epithelial Club Cells. American Journal of Respiratory and Critical Care Medicine. 2018 Dec 1;198(11):1375-1388. doi: 10.1164/rccm.201710-2107OC. PMID: 29874100.

77. Pérez B F, Méndez G A, Lagos R A, Vargas M SL. Dinámica y patología del barrido mucociliar como mecanismo defensivo del pulmón y alternativas farmacológicas de tratamiento [Mucociliary clearance system in lung defense]. Revista Médica de Chile.

2014 May;142(5):606-15. Spanish. doi: 10.4067/S0034-98872014000500009. PMID: 25427018.

78. Martinu T, Todd JL, Gelman AE, Guerra S, Palmer SM. Club Cell Secretory Protein in Lung Disease: Emerging Concepts and Potential Therapeutics. Annual Review of Medicine. 2023 Jan 27;74:427-441. doi: 10.1146/annurev-med-042921-123443. Epub 2022 Nov 30. PMID: 36450281.

79. Stauber M, Weidemann M, Dittrich-Breiholz O, Lobschat K, Alten L, Mai M, Beckers A, Kracht M, Gossler A. Identification of FOXJ1 effectors during ciliogenesis in the foetal respiratory epithelium and embryonic left-right organiser of the mouse. Developmental Biology. 2017 Mar 15;423(2):170-188. doi: 10.1016/j.ydbio.2016.11.019. Epub 2016 Dec 1. PMID: 27914912.

80. Dodd DO, Mechaussier S, Yeyati PL, McPhie F, Anderson JR, Khoo CJ, Shoemark A, Gupta DK, Attard T, Zariwala MA, Legendre M, Bracht D, Wallmeier J, Gui M, Fassad MR, Parry DA, Tennant PA, Meynert A, Wheway G, Fares-Taie L, Black HA, Mitri-Frangieh R, Faucon C, Kaplan J, Patel M, McKie L, Megaw R, Gatsogiannis C, Mohamed MA, Aitken S, Gautier P, Reinholt FR, Hirst RA, O'Callaghan C, Heimdal K, Bottier M, Escudier E, Crowley S, Descartes M, Jabs EW, Kenia P, Amiel J, Bacci GM, Calogero C, Palazzo V, Tiberi L, Blümlein U, Rogers A, Wambach JA, Wegner DJ, Fulton AB, Kenna M, Rosenfeld M, Holm IA, Quigley A, Hall EA, Murphy LC, Cassidy DM, von Kriegsheim A; Scottish Genomes Partnership16; Genomics England Research Consortium45; Undiagnosed Diseases Network46; Papon JF, Pasquier L, Murris MS, Chalmers JD, Hogg C, Macleod KA, Urquhart DS, Unger S, Aitman TJ, Amselem S, Leigh MW, Knowles MR, Omran H, Mitchison HM, Brown A, Marsh JA, Welburn JPI, Ti SC, Horani A, Rozet JM, Perrault I, Mill P. Ciliopathy patient variants reveal organelle-specific functions for TUBB4B in axonemal microtubules. Science. 2024 Apr 26;384(6694):eadf5489. doi: 10.1126/science.adf5489. Epub 2024 Apr 26. Erratum in: Science. 2024 May 10;384(6696):eadq2178. doi: 10.1126/science.adq2178. PMID: 38662826.

81. Rusu AD, Georgiou M. The multifarious regulation of the apical junctional complex. Open Biology. 2020 Feb;10(2):190278. doi: 10.1098/rsob.190278. Epub 2020 Feb 19. PMID: 32070233.

82. Buckley CE, St Johnston D. Apical-basal polarity and the control of epithelial form and function. Nature Reviews Molecular Cell Biology. 2022 Aug;23(8):559-577. doi: 10.1038/s41580-022-00465-y. Epub 2022 Apr 19. PMID: 35440694.

83. Osswald M, Morais-de-Sá E. Dealing with apical-basal polarity and intercellular junctions: a multidimensional challenge for epithelial cell division. Current Opinion in Cell Biology. 2019 Oct;60:75-83. doi: 10.1016/j.ceb.2019.04.006. Epub 2019 May 27. PMID: 31153057.

84. Bourke CD, Berkley JA, Prendergast AJ. Immune Dysfunction as a Cause and Consequence of Malnutrition. Trends in Immunology. 2016 Jun;37(6):386-398. doi: 10.1016/j.it.2016.04.003. Epub 2016 May 26. PMID: 27237815.

85. Roth DE, Caulfield LE, Ezzati M, Black RE. Acute lower respiratory infections in childhood: opportunities for reducing the global burden through nutritional interventions. Bulletin of the World Health Organization. 2008 May;86(5):356-64. doi: 10.2471/blt.07.049114. PMID: 18545738.

86. Singh V. The burden of pneumonia in children: an Asian perspective. Paediatric Respiratory Reviews. 2005 Jun;6(2):88-93. doi: 10.1016/j.prrv.2005.03.002. PMID: 15911453.

87. Mendes ACL, De Souza AMG, Nunes ADDS, Jerez-Roig J, Barbosa IR. Frequency of Vitamin a Deficiency in Children Hospitalized for Pneumonia: An Integrative Review. Public Health Reviews. 2022 Dec 13;43:1604500. doi: 10.3389/phrs.2022.1604500. PMID: 36588988.

88. Dickson RP, Erb-Downward JR, Huffnagle GB. Homeostasis and its disruption in the lung microbiome. American Journal of Physiology-Lung Cellular and Molecular Physiology. 2015 Nov 15;309(10):L1047-55. doi: 10.1152/ajplung.00279.2015. Epub 2015 Oct 2. PMID: 26432870.

89. Döring G, Gulbins E. Cystic fibrosis and innate immunity: how chloride channel mutations provoke lung disease. Cellular Microbiology. 2009 Feb;11(2):208-16. doi: 10.1111/j.1462-5822.2008.01271.x. Epub 2008 Dec 2. PMID: 19068098.

90. Harvey C, Weldon S, Elborn S, Downey DG, Taggart C. The Effect of CFTR Modulators on Airway Infection in Cystic Fibrosis. International Journal of Molecular Sciences. 2022 Mar 23;23(7):3513. doi: 10.3390/ijms23073513. PMID: 35408875.

91. Loens K, Van Heirstraeten L, Malhotra-Kumar S, Goossens H, Ieven M. Optimal sampling sites and methods for detection of pathogens possibly causing community-acquired lower respiratory tract infections. Journal of Clinical Microbiology. 2009 Jan;47(1):21-31. doi: 10.1128/JCM.02037-08. Epub 2008 Nov 19. PMID: 19020070.

92. Sul JH, Martin LS, Eskin E. Population structure in genetic studies: Confounding factors and mixed models. PLoS Genetics. 2018 Dec 27;14(12):e1007309. doi: 10.1371/journal.pgen.1007309. PMID: 30589851.

93. Strak M, Janssen N, Beelen R, Schmitz O, Karssenberg D, Houthuijs D, van den Brink C, Dijst M, Brunekreef B, Hoek G. Associations between lifestyle and air pollution exposure: Potential for confounding in large administrative data cohorts.

Environmental Research. 2017 Jul;156:364-373. doi: 10.1016/j.envres.2017.03.050. Epub 2017 Apr 10. PMID: 28395240.

94. Lopez Bernal JA, Upton MN, Henderson AJ, Dedman D, McCarthy A, Davey Smith G, Ben-Shlomo Y. Lower respiratory tract infection in the first year of life is associated with worse lung function in adult life: prospective results from the Barry Caerphilly Growth study. Annals of Epidemiology. 2013 Jul;23(7):422-7. doi: 10.1016/j.annepidem.2013.05.006. PMID: 23790346.

95. Chatterjee G, Negi S, Basu S, Faintuch J, O'Donovan A, Shukla P. Microbiome systems biology advancements for natural well-being. Science of the Total Environment. 2022 Sep 10;838(Pt 2):155915. doi: 10.1016/j.scitotenv.2022.155915. Epub 2022 May 11. PMID: 35568180.

96. Acheson DW, Luccioli S. Microbial-gut interactions in health and disease. Mucosal immune responses. Best Practice and Research Clinical Gastroenterology. 2004 Apr;18(2):387-404. doi: 10.1016/j.bpg.2003.11.002. PMID: 15123077.

97. Beachey EH. Bacterial adherence: adhesin-receptor interactions mediating the attachment of bacteria to mucosal surface. Journal of Infectious Diseases. 1981 Mar;143(3):325-45. doi: 10.1093/infdis/143.3.325. PMID: 7014727.

98. Neish AS. Mucosal immunity and the microbiome. Annals of the American Thoracic Society. 2014 Jan;11 Suppl 1(Suppl 1):S28-32. doi: 10.1513/AnnalsATS.201306-161MG. PMID: 24437401; PMCID: PMC3972979.

99. Ghoul M, West SA, Johansen HK, Molin S, Harrison OB, Maiden MC, Jelsbak L, Bruce JB, Griffin AS. Bacteriocin-mediated competition in cystic fibrosis lung infections. Proceedings: Biological Sciences. 2015 Sep 7;282(1814):20150972. doi: 10.1098/rspb.2015.0972. PMID: 26311664.

100. Tzani-Tzanopoulou P, Skliros D, Megremis S, Xepapadaki P, Andreakos E, Chanishvili N, Flemetakis E, Kaltsas G, Taka S, Lebessi E, Doudoulakakis A, Papadopoulos NG. Interactions of Bacteriophages and Bacteria at the Airway Mucosa: New Insights Into the Pathophysiology of Asthma. Frontiers in Allergy. 2021 Jan 26;1:617240. doi: 10.3389/falgy.2020.617240. Erratum in: Frontiers in Allergy. 2022 Apr 01;3:892908. doi: 10.3389/falgy.2022.892908. PMID: 35386933.

101. Barr JJ, Auro R, Furlan M, Whiteson KL, Erb ML, Pogliano J, Stotland A, Wolkowicz R, Cutting AS, Doran KS, Salamon P, Youle M, Rohwer F. Bacteriophage adhering to mucus provide a non-host-derived immunity. PNAS. 2013 Jun 25;110(26):10771-6. doi: 10.1073/pnas.1305923110. Epub 2013 May 20. PMID: 23690590.

102. Yamada KJ, Kielian T. Biofilm-Leukocyte Cross-Talk: Impact on Immune Polarization and Immunometabolism. Journal of Innate Immunity. 2019;11(3):280-288. doi: 10.1159/000492680. Epub 2018 Oct 22. PMID: 30347401.

103. Mirzaei R, Sabokroo N, Ahmadyousefi Y, Motamedi H, Karampoor S. Immunometabolism in biofilm infection: lessons from cancer. Molecular Medicine. 2022 Jan 29;28(1):10. doi: 10.1186/s10020-022-00435-2. PMID: 35093033.

104. Crabbé A, Jensen PØ, Bjarnsholt T, Coenye T. Antimicrobial Tolerance and Metabolic Adaptations in Microbial Biofilms. Trends in Microbiology. 2019 Oct;27(10):850-863. doi: 10.1016/j.tim.2019.05.003. Epub 2019 Jun 6. PMID: 31178124.

105. Karygianni L, Ren Z, Koo H, Thurnheer T. Biofilm Matrixome: Extracellular Components in Structured Microbial Communities. Trends in Microbiology. 2020 Aug;28(8):668-681. doi: 10.1016/j.tim.2020.03.016. Epub 2020 Apr 21. PMID: 32663461.

106. Donlan RM, Costerton JW. Biofilms: survival mechanisms of clinically relevant microorganisms. Clinical Microbiology Reviews. 2002 Apr;15(2):167-93. doi: 10.1128/CMR.15.2.167-193.2002. PMID: 11932229.

107. Pontes JTC, Toledo Borges AB, Roque-Borda CA, Pavan FR. Antimicrobial Peptides as an Alternative for the Eradication of Bacterial Biofilms of Multi-Drug Resistant Bacteria. Pharmaceutics. 2022 Mar 15;14(3):642. doi: 10.3390/pharmaceutics14030642. PMID: 35336016.

108. Assefa M, Amare A. Biofilm-Associated Multi-Drug Resistance in Hospital-Acquired Infections: A Review. Infection and Drug Resistance. 2022 Aug 31;15:5061-5068. doi: 10.2147/IDR.S379502. PMID: 36068834.

109. Nunez C, Kostoulias X, Peleg A, Short F, Qu Y. A comprehensive comparison of biofilm formation and capsule production for bacterial survival on hospital surfaces. Biofilm. 2023 Jan 22;5:100105. doi: 10.1016/j.bioflm.2023.100105. PMID: 36711324.

110. Hall-Stoodley L, Stoodley P. Biofilm formation and dispersal and the transmission of human pathogens. Trends in Microbiology. 2005 Jan;13(1):7-10. doi: 10.1016/j.tim.2004.11.004. Erratum in: Trends in Microbiology. 2005 Jul;13(7):300-1. PMID: 15639625.

111. Rumbaugh KP, Sauer K. Biofilm dispersion. Nature Reviews Microbiology. 2020 Oct;18(10):571-586. doi: 10.1038/s41579-020-0385-0. Epub 2020 Jun 12. PMID: 32533131.

112. Weaver CM, Miller JW. Challenges in conducting clinical nutrition research. Nutrition Reviews. 2017 Jul 1;75(7):491-499. doi: 10.1093/nutrit/nux026. PMID: 28605476.

113. Picó C, Serra F, Rodríguez AM, Keijer J, Palou A. Biomarkers of Nutrition and Health: New Tools for New Approaches. Nutrients. 2019 May 16;11(5):1092. doi: 10.3390/nu11051092. PMID: 31100942.

114. Martin R, Makino H, Cetinyurek Yavuz A, Ben-Amor K, Roelofs M, Ishikawa E, Kubota H, Swinkels S, Sakai T, Oishi K, Kushiro A, Knol J. Early-Life Events, Including Mode of Delivery and Type of Feeding, Siblings and Gender, Shape the Developing Gut Microbiota. PLoS One. 2016 Jun 30;11(6):e0158498. doi: 10.1371/journal.pone.0158498. PMID: 27362264.

115. Shaw L, Ribeiro ALR, Levine AP, Pontikos N, Balloux F, Segal AW, Roberts AP, Smith AM. The Human Salivary Microbiome Is Shaped by Shared Environment Rather than Genetics: Evidence from a Large Family of Closely Related Individuals. mBio. 2017 Sep 12;8(5):e01237-17. doi: 10.1128/mBio.01237-17. PMID: 28900019.

116. Hornung BVH, Zwittink RD, Kuijper EJ. Issues and current standards of controls in microbiome research. FEMS Microbiology Ecology. 2019 May 1;95(5):fiz045. doi: 10.1093/femsec/fiz045. PMID: 30997495.

117. Carney SM, Clemente JC, Cox MJ, Dickson RP, Huang YJ, Kitsios GD, Kloepfer KM, Leung JM, LeVan TD, Molyneaux PL, Moore BB, O'Dwyer DN, Segal LN, Garantziotis S. Methods in Lung Microbiome Research. American Journal of Respiratory Cell and Molecular Biology. 2020 Mar;62(3):283-299. doi: 10.1165/rcmb.2019-0273TR. PMID: 31661299.

118. Bolger AM, Lohse M, Usadel B. Trimmomatic: a flexible trimmer for Illumina sequence data. Bioinformatics. 2014 Aug 1;30(15):2114-20. doi: 10.1093/bioinformatics/btu170. Epub 2014 Apr 1. PMID: 24695404.

119. Ewing B, Hillier L, Wendl MC, Green P. Base-calling of automated sequencer traces using phred. I. Accuracy assessment. Genome Research. 1998 Mar;8(3):175-85. doi: 10.1101/gr.8.3.175. PMID: 9521921.

120. Ewing B, Green P. Base-calling of automated sequencer traces using phred. II. Error probabilities. Genome Research. 1998 Mar;8(3):186-94. PMID: 9521922.

121. O'Leary NA, Wright MW, Brister JR, Ciufo S, Haddad D, McVeigh R, Rajput B, Robbertse B, Smith-White B, Ako-Adjei D, Astashyn A, Badretdin A, Bao Y, Blinkova O, Brover V, Chetvernin V, Choi J, Cox E, Ermolaeva O, Farrell CM, Goldfarb T, Gupta T, Haft D, Hatcher E, Hlavina W, Joardar VS, Kodali VK, Li W, Maglott D, Masterson P, McGarvey KM, Murphy MR, O'Neill K, Pujar S, Rangwala

SH, Rausch D, Riddick LD, Schoch C, Shkeda A, Storz SS, Sun H, Thibaud-Nissen F, Tolstoy I, Tully RE, Vatsan AR, Wallin C, Webb D, Wu W, Landrum MJ, Kimchi A, Tatusova T, DiCuccio M, Kitts P, Murphy TD, Pruitt KD. Reference sequence (RefSeq) database at NCBI: current status, taxonomic expansion, and functional annotation. Nucleic Acids Research. 2016 Jan 4;44(D1):D733-45. doi: 10.1093/nar/gkv1189. Epub 2015 Nov 8. PMID: 26553804.

122. Liao Y, Smyth GK, Shi W. The R package Rsubread is easier, faster, cheaper and better for alignment and quantification of RNA sequencing reads. Nucleic Acids Research. 2019 May 7;47(8):e47. doi: 10.1093/nar/gkz114. PMID: 30783653.

123. Quiles, K. VADandTheLungMicrobiome: Code used for RNAseq pre-processing and alignment modified for mouse RNAseq data, as well as raw sequencing files from my thesis work. Github. 2024.

124. Zhao Y, Federico A, Faits T, Manimaran S, Segrè D, Monti S, Johnson WE. animalcules: interactive microbiome analytics and visualization in R. Microbiome. 2021 Mar 28;9(1):76. doi: 10.1186/s40168-021-01013-0. PMID: 33775256.

125. Johnson, W., Evan and Jenkins,, David and Khan,, Mohammed, Muzamil and Faits,, Tyler and Zhang,, Yuqing and McFarlane,, Ada and Zhao,, Yue and Campbell,, Joshua, D. Interactive single cell RNA-Seq analysis with Single Cell Toolkit (SCTK). OpenBU. 2019.

126. Ritchie ME, Phipson B, Wu D, Hu Y, Law CW, Shi W, Smyth GK. limma powers differential expression analyses for RNA-sequencing and microarray studies. Nucleic Acids Research. 2015 Apr 20;43(7):e47. doi: 10.1093/nar/gkv007. Epub 2015 Jan 20. PMID: 25605792.

127. Xia, Y., & Sun, J. Bioinformatic and statistical analysis of microbiome data: from raw sequences to advanced modeling with QIIME 2 and R. Springer Nature. 2023.

128. Su X. Elucidating the Beta-Diversity of the Microbiome: from Global Alignment to Local Alignment. mSystems. 2021 Aug 31;6(4):e0036321. doi: 10.1128/mSystems.00363-21. Epub 2021 Aug 17. PMID: 34402645.

129. Lu Y, Zhou G, Ewald J, Pang Z, Shiri T, Xia J. MicrobiomeAnalyst 2.0: comprehensive statistical, functional and integrative analysis of microbiome data. Nucleic Acids Research. 2023 Jul 5;51(W1):W310-W318. doi: 10.1093/nar/gkad407. PMID: 37166960.

130. Manimaran S, Selby HM, Okrah K, Ruberman C, Leek JT, Quackenbush J, Haibe-Kains B, Bravo HC, Johnson WE. BatchQC: interactive software for evaluating sample and batch effects in genomic data. Bioinformatics. 2016 Dec

15;32(24):3836-3838. doi: 10.1093/bioinformatics/btw538. Epub 2016 Aug 18. PMID: 27540268.

131. Zhang Y, Parmigiani G, Johnson WE. ComBat-seq: batch effect adjustment for RNA-seq count data. NAR Genomics and Bioinformatics. 2020 Sep;2(3):lqaa078. doi: 10.1093/nargab/lqaa078. Epub 2020 Sep 21. PMID: 33015620.

132. Liu S, Wang Z, Zhu R, Wang F, Cheng Y, Liu Y. Three Differential Expression Analysis Methods for RNA Sequencing: limma, EdgeR, DESeq2. JoVE Journal of Visualized Experiments. 2021 Sep 18;(175). doi: 10.3791/62528. PMID: 34605806.

133. Simon MM, Greenaway S, White JK, Fuchs H, Gailus-Durner V, Wells S, Sorg T, Wong K, Bedu E, Cartwright EJ, Dacquin R, Djebali S, Estabel J, Graw J, Ingham NJ, Jackson IJ, Lengeling A, Mandillo S, Marvel J, Meziane H, Preitner F, Puk O, Roux M, Adams DJ, Atkins S, Ayadi A, Becker L, Blake A, Brooker D, Cater H, Champy MF, Combe R, Danecek P, di Fenza A, Gates H, Gerdin AK, Golini E, Hancock JM, Hans W, Hölter SM, Hough T, Jurdic P, Keane TM, Morgan H, Müller W, Neff F, Nicholson G, Pasche B, Roberson LA, Rozman J, Sanderson M, Santos L, Selloum M, Shannon C, Southwell A, Tocchini-Valentini GP, Vancollie VE, Westerberg H, Wurst W, Zi M, Yalcin B, Ramirez-Solis R, Steel KP, Mallon AM, de Angelis MH, Herault Y, Brown SD. A comparative phenotypic and genomic analysis of C57BL/6J and C57BL/6N mouse strains. Genome Biology. 2013 Jul 31;14(7):R82. doi: 10.1186/gb-2013-14-7-r82. PMID: 23902802.

134. Hawkins F, Kramer P, Jacob A, Driver I, Thomas DC, McCauley KB, Skvir N, Crane AM, Kurmann AA, Hollenberg AN, Nguyen S, Wong BG, Khalil AS, Huang SX, Guttentag S, Rock JR, Shannon JM, Davis BR, Kotton DN. Prospective isolation of NKX2-1-expressing human lung progenitors derived from pluripotent stem cells. Journal of Clinical Investigation. 2017 Jun 1;127(6):2277-2294. doi: 10.1172/JCI89950. Epub 2017 May 2. PMID: 28463226.

135. Merki, E. Tissue-restricted disruption of retinoid signaling using Cre-LoxP. University of California, San Diego. 2002.

136. Francis R, Lo C. Ex vivo method for high resolution imaging of cilia motility in rodent airway epithelia. JoVE Journal of Visualized Experiments. 2013 Aug 8;(78):50343. doi: 10.3791/50343. PMID: 23963287.

137. Stossi F, Singh PK. Basic Image Analysis and Manipulation in ImageJ/Fiji. Current Protocols. 2023 Jul;3(7):e849. doi: 10.1002/cpz1.849. PMID: 37498127.

138. Humphries MP, Maxwell P, Salto-Tellez M. QuPath: The global impact of an open source digital pathology system. Computational and Structural Biotechnology Journal. 2021 Jan 21;19:852-859. doi: 10.1016/j.csbj.2021.01.022. PMID: 33598100.

139. Flurkey, Currer, and Harrison, 'The mouse in biomedical research.' in James G. Fox (ed.), American College of Laboratory Animal Medicine series (Elsevier, AP: Amsterdam; Boston). 2007.

140. Belyaeva OV, Adams MK, Popov KM, Kedishvili NY. Generation of Retinaldehyde for Retinoic Acid Biosynthesis. Biomolecules. 2019 Dec 18;10(1):5. doi: 10.3390/biom10010005. PMID: 31861321.

141. Korecka JA, van Kesteren RE, Blaas E, Spitzer SO, Kamstra JH, Smit AB, Swaab DF, Verhaagen J, Bossers K. Phenotypic characterization of retinoic acid differentiated SH-SY5Y cells by transcriptional profiling. PLoS One. 2013 May 28;8(5):e63862. doi: 10.1371/journal.pone.0063862. PMID: 23724009.

142. Pai T, Chen Q, Zhang Y, Zolfaghari R, Ross AC. Galactomutarotase and other galactose-related genes are rapidly induced by retinoic acid in human myeloid cells. Biochemistry. 2007 Dec 25;46(51):15198-207. doi: 10.1021/bi701891t. Epub 2007 Dec 4. PMID: 18052213.

143. Kuntz E, Hoeller U, Greatrix B, Lankin C, Seifert N, Acharya S, Riss G, Buchwald-Hunziker P, Hunziker W, Goralczyk R, Wertz K. Beta-carotene and apocarotenals promote retinoid signaling in BEAS-2B human bronchioepithelial cells. Archives of Biochemistry and Biophysics. 2006 Nov 1;455(1):48-60. doi: 10.1016/j.abb.2006.08.023. Epub 2006 Sep 20. PMID: 17034753.

144. Colleoni S, Galli C, Gaspar JA, Meganathan K, Jagtap S, Hescheler J, Sachinidis A, Lazzari G. Development of a neural teratogenicity test based on human embryonic stem cells: response to retinoic acid exposure. Toxicological Sciences. 2011 Dec;124(2):370-7. doi: 10.1093/toxsci/kfr245. Epub 2011 Sep 20. PMID: 21934132.

145. Habib A, Hamade E, Mahfouz R, Nasrallah MS, de Thé H, Bazarbachi A. Arsenic trioxide inhibits ATRA-induced prostaglandin E2 and cyclooxygenase-1 in NB4 cells, a model of acute promyelocytic leukemia. Leukemia. 2008 Jun;22(6):1125-30. doi: 10.1038/leu.2008.59. Epub 2008 Mar 20. PMID: 18354491.

146. Ishii Y, Kasukabe T, Honma Y. Immediate up-regulation of the calcium-binding protein S100P and its involvement in the cytokinin-induced differentiation of human myeloid leukemia cells. Biochimica et Biophysica Acta. 2005 Sep 10;1745(2):156-65. doi: 10.1016/j.bbamcr.2005.01.005. Epub 2005 Feb 9. PMID: 16129123.

147. Alique M, Moreno V, Kitamura M, Xu Q, Lucio-Cazana FJ. Kinase-dependent, retinoic acid receptor-independent up-regulation of cyclooxygenase-2 by all-trans retinoic acid in human mesangial cells. British Journal of Pharmacology. 2006 Sep;149(2):215-25. doi: 10.1038/sj.bjp.0706842. Epub 2006 Aug 7. PMID: 16894348.

148. Baron JM, Heise R, Blaner WS, Neis M, Joussen S, Dreuw A, Marquardt Y, Saurat JH, Merk HF, Bickers DR, Jugert FK. Retinoic acid and its 4-oxo metabolites are functionally active in human skin cells in vitro. Journal of Investigative Dermatology. 2005 Jul;125(1):143-53. doi: 10.1111/j.0022-202X.2005.23791.x. PMID: 15982314.

149. Lachmann A, Xu H, Krishnan J, Berger SI, Mazloom AR, Ma'ayan A. ChEA: transcription factor regulation inferred from integrating genome-wide ChIP-X experiments. Bioinformatics. 2010 Oct 1;26(19):2438-44. doi: 10.1093/bioinformatics/btq466. Epub 2010 Aug 13. PMID: 20709693.

150. Jayaraman S, Pazhani J, PriyaVeeraraghavan V, Raj AT, Somasundaram DB, Patil S. PCNA and Ki67: Prognostic proliferation markers for oral cancer. Oral Oncology. 2022 Jul;130:105943. doi: 10.1016/j.oraloncology.2022.105943. Epub 2022 May 30. PMID: 35653815.

151. Tabula Muris Consortium; Overall coordination; Logistical coordination; Organ collection and processing; Library preparation and sequencing; Computational data analysis; Cell type annotation; Writing group; Supplemental text writing group; Principal investigators. Single-cell transcriptomics of 20 mouse organs creates a Tabula Muris. Nature. 2018 Oct;562(7727):367-372. doi: 10.1038/s41586-018-0590-4. Epub 2018 Oct 3. PMID: 30283141.

152. Nandi D, Cheema PS, Jaiswal N, Nag A. FoxM1: Repurposing an oncogene as a biomarker. Seminars in Cancer Biology. 2018 Oct;52(Pt 1):74-84. doi: 10.1016/j.semcancer.2017.08.009. Epub 2017 Sep 10. PMID: 28855104.

153. Wisdom R, Johnson RS, Moore C. c-Jun regulates cell cycle progression and apoptosis by distinct mechanisms. EMBO Journal. 1999 Jan 4;18(1):188-97. doi: 10.1093/emboj/18.1.188. PMID: 9878062.

154. Liu J, Xia L, Wang S, Cai X, Wu X, Zou C, Shan B, Luo M, Wang D. E2F4 Promotes the Proliferation of Hepatocellular Carcinoma Cells through Upregulation of CDCA3. Journal of Cancer. 2021 Jun 22;12(17):5173-5180. doi: 10.7150/jca.53708. PMID: 34335934.

155. Wen N, Wang Y, Wen L, Zhao SH, Ai ZH, Wang Y, Wu B, Lu HX, Yang H, Liu WC, Li Y. Overexpression of FOXM1 predicts poor prognosis and promotes cancer cell proliferation, migration and invasion in epithelial ovarian cancer. Journal of Translational Medicine. 2014 May 20;12:134. doi: 10.1186/1479-5876-12-134. PMID: 24885308.

156. Gartel AL. FOXM1 in Cancer: Interactions and Vulnerabilities. Cancer Research. 2017 Jun 15;77(12):3135-3139. doi: 10.1158/0008-5472.CAN-16-3566. Epub 2017 Jun 5. PMID: 28584182.

157. Wierstra I, Alves J. FOXM1, a typical proliferation-associated transcription factor. Journal of Biological Chemistry. 2007 Dec;388(12):1257-74. doi: 10.1515/BC.2007.159. PMID: 18020943.

158. Song X, Fiati Kenston SS, Zhao J, Yang D, Gu Y. Roles of FoxM1 in cell regulation and breast cancer targeting therapy. Medical Oncology. 2017 Mar;34(3):41. doi: 10.1007/s12032-017-0888-3. Epub 2017 Feb 8. PMID: 28176242.

159. Manios K, Tsiambas E, Stavrakis I, Stamatelopoulos A, Kavantzas N, Agrogiannis G, C Lazaris A. c-Fos/ c-Jun transcription factors in non-small cell lung carcinoma. Journal of BUON. 2020 Sep-Oct;25(5):2141-2143. PMID: 33277827.

160. Wu L, Wan S, Li J, Xu Y, Lou X, Sun M, Wang S. Expression and prognostic value of E2F3 transcription factor in non-small cell lung cancer. Oncology Letters. 2021 May;21(5):411. doi: 10.3892/ol.2021.12672. Epub 2021 Mar 22. PMID: 33841572.

161. Zhang D, Jiang Q, Ge X, Shi Y, Ye T, Mi Y, Xie T, Li Q, Ye Q. RHOV promotes lung adenocarcinoma cell growth and metastasis through JNK/c-Jun pathway. International Journal of Biological Sciences. 2021 Jun 22;17(10):2622-2632. doi: 10.7150/ijbs.59939. PMID: 34326698.

162. Hollern DP, Honeysett J, Cardiff RD, Andrechek ER. The E2F transcription factors regulate tumor development and metastasis in a mouse model of metastatic breast cancer. Molecular and Cellular Biology. 2014 Sep;34(17):3229-43. doi: 10.1128/MCB.00737-14. Epub 2014 Jun 16. PMID: 24934442.

163. Jayaraman S, Pazhani J, PriyaVeeraraghavan V, Raj AT, Somasundaram DB, Patil S. PCNA and Ki67: Prognostic proliferation markers for oral cancer. Oral Oncology. 2022 Jul;130:105943. doi: 10.1016/j.oraloncology.2022.105943. Epub 2022 May 30. PMID: 35653815.

164. Ng-Blichfeldt JP, Schrik A, Kortekaas RK, Noordhoek JA, Heijink IH, Hiemstra PS, Stolk J, Königshoff M, Gosens R. Retinoic acid signaling balances adult distal lung epithelial progenitor cell growth and differentiation. EBioMedicine. 2018 Oct;36:461-474. doi: 10.1016/j.ebiom.2018.09.002. Epub 2018 Sep 17. PMID: 30236449.

165. Joshi-Tope G, Gillespie M, Vastrik I, D'Eustachio P, Schmidt E, de Bono B, Jassal B, Gopinath GR, Wu GR, Matthews L, Lewis S, Birney E, Stein L. Reactome: a knowledgebase of biological pathways. Nucleic Acids Research. 2005 Jan 1;33(Database issue):D428-32. doi: 10.1093/nar/gki072. PMID: 15608231.

166. Copeland J. Actin-based regulation of ciliogenesis - The long and the short of it. Seminars in Cell and Developmental Biology. 2020 Jun;102:132-138. doi: 10.1016/j.semcdb.2019.12.005. Epub 2019 Dec 18. PMID: 31862221.

167. Yasunaga T, Wiegel J, Bergen MD, Helmstädter M, Epting D, Paolini A, Çiçek Ö, Radziwill G, Engel C, Brox T, Ronneberger O, Walentek P, Ulbrich MH, Walz G. Microridge-like structures anchor motile cilia. Nature Communications. 2022 Apr 19;13(1):2056. doi: 10.1038/s41467-022-29741-3. PMID: 35440631.

168. Bustamante-Marin XM, Ostrowski LE. Cilia and Mucociliary Clearance. Cold Spring Harbor Perspectives in Biology. 2017 Apr 3;9(4):a028241. doi: 10.1101/cshperspect.a028241. PMID: 27864314.

169. Martinu T, Todd JL, Gelman AE, Guerra S, Palmer SM. Club Cell Secretory Protein in Lung Disease: Emerging Concepts and Potential Therapeutics. Annual Review of Medicine. 2023 Jan 27;74:427-441. doi: 10.1146/annurev-med-042921-123443. Epub 2022 Nov 30. PMID: 36450281.

170. Conchola AS, Frum T, Xiao Z, Hsu PP, Kaur K, Downey MS, Hein RFC, Miller AJ, Tsai YH, Wu A, Holloway EM, Anand A, Murthy PKL, Glass I, Tata PR, Spence JR. Regionally distinct progenitor cells in the lower airway give rise to neuroendocrine and multiciliated cells in the developing human lung. PNAS. 2023 Jun 13;120(24):e2210113120. doi: 10.1073/pnas.2210113120. Epub 2023 Jun 6. PMID: 37279279.

171. Vladar EK, Nayak JV, Milla CE, Axelrod JD. Airway epithelial homeostasis and planar cell polarity signaling depend on multiciliated cell differentiation. JCI Insight. 2016 Aug 18;1(13):e88027. doi: 10.1172/jci.insight.88027. PMID: 27570836.

172. Wodarz A, Näthke I. Cell polarity in development and cancer. Nature Cell Biology. 2007 Sep;9(9):1016-24. doi: 10.1038/ncb433. PMID: 17762893.

173. Seeger-Nukpezah T, Little JL, Serzhanova V, Golemis EA. Cilia and cilia-associated proteins in cancer. Drug Discovery Today: Disease Mechanisms. 2013 Dec 1;10(3-4):e135-e142. doi: 10.1016/j.ddmec.2013.03.004. PMID: 24982684.

174. Zhang Y, Jenkins DF, Manimaran S, Johnson WE. Alternative empirical Bayes models for adjusting for batch effects in genomic studies. BMC Bioinformatics. 2018 Jul 13;19(1):262. doi: 10.1186/s12859-018-2263-6. PMID: 30001694.

175. Johnson,, W., Evan and Jenkins,, David and Khan,, Mohammed, Muzamil and Faits,, Tyler and Zhang,, Yuqing and McFarlane,, Ada and Zhao,, Yue and Campbell,, Joshua, D. Interactive single cell RNA-Seq analysis with Single Cell Toolkit (SCTK). OpenBU. 2019.

176. Xia, Y., & Sun, J. Alpha Diversity. In Bioinformatic and Statistical Analysis of Microbiome Data: From Raw Sequences to Advanced Modeling with QIIME 2 and R (pp. 289-333). Springer Nature. 2023.

177. Su X. Elucidating the Beta-Diversity of the Microbiome: from Global Alignment to Local Alignment. mSystems. 2021 Aug 31;6(4):e0036321. doi: 10.1128/mSystems.00363-21. Epub 2021 Aug 17. PMID: 34402645.

178. Janda JM, Abbott SL. 16S rRNA gene sequencing for bacterial identification in the diagnostic laboratory: pluses, perils, and pitfalls. Journal of Clinical Microbiology. 2007 Sep;45(9):2761-4. doi: 10.1128/JCM.01228-07. Epub 2007 Jul 11. PMID: 17626177.

179. Lima A, França A, Muzny CA, Taylor CM, Cerca N. DNA extraction leads to bias in bacterial quantification by qPCR. Applied Microbiology and Biotechnology. 2022 Dec;106(24):7993-8006. doi: 10.1007/s00253-022-12276-4. Epub 2022 Nov 14. PMID: 36374332.

180. Lin H, Peddada SD. Analysis of microbial compositions: a review of normalization and differential abundance analysis. NPJ Biofilms Microbiomes. 2020 Dec 2;6(1):60. doi: 10.1038/s41522-020-00160-w. PMID: 33268781.

181. Aghnatios R, Drancourt M. Gemmata species: Planctomycetes of medical interest. Future Microbiology. 2016 May;11:659-67. doi: 10.2217/fmb-2015-0001. Epub 2016 May 9. PMID: 27158864.

182. Richardson M, Bowyer P, Sabino R. The human lung and Aspergillus: You are what you breathe in? Medical Mycology. 2019 Apr 1;57(Supplement_2):S145-S154. doi: 10.1093/mmy/myy149. PMID: 30816978.

183. Rubio-Portillo E, Orts D, Llorca E, Fernández C, Antón J, Ferrer C, Gálvez B, Esteban V, Revelles E, Pérez-Martín C, Gómez-Imbernón E, Adsuar J, Piqueras P, Amat B, Franco J, Colom MF. The Domestic Environment and the Lung Mycobiome. Microorganisms. 2020 Nov 2;8(11):1717. doi: 10.3390/microorganisms8111717. PMID: 33147738.

184. Belvoncikova P, Splichalova P, Videnska P, Gardlik R. The Human Mycobiome: Colonization, Composition and the Role in Health and Disease. Journal of Fungi (Basel). 2022 Oct 4;8(10):1046. doi: 10.3390/jof8101046. PMID: 36294611.

185. Reimer LC, Sardà Carbasse J, Koblitz J, Ebeling C, Podstawka A, Overmann J. BacDive in 2022: the knowledge base for standardized bacterial and archaeal data. Nucleic Acids Research. 2022 Jan 7;50(D1):D741-D746. doi: 10.1093/nar/gkab961. PMID: 34718743.

186. Hastings J, Owen G, Dekker A, Ennis M, Kale N, Muthukrishnan V, Turner S, Swainston N, Mendes P, Steinbeck C. ChEBI in 2016: Improved services and an expanding collection of metabolites. Nucleic Acids Research. 2016 Jan 4;44(D1):D1214-9. doi: 10.1093/nar/gkv1031. Epub 2015 Oct 13. PMID: 26467479.

187. Rittershaus ES, Baek SH, Sassetti CM. The normalcy of dormancy: common themes in microbial quiescence. Cell Host Microbe. 2013 Jun 12;13(6):643-51. doi: 10.1016/j.chom.2013.05.012. PMID: 23768489.

188. Cockeran R, Dix-Peek T, Dickens C, Steel HC, Anderson R, Feldman C. Biofilm formation and induction of stress response genes is a common response of several serotypes of the pneumococcus to cigarette smoke condensate. Journal of Infection. 2020 Feb;80(2):204-209. doi: 10.1016/j.jinf.2019.10.014. Epub 2019 Oct 26. PMID: 31669377.

189. Olson JA. Benefits and liabilities of vitamin A and carotenoids. Journal of Nutrition. 1996 Apr;126(4 Suppl):1208S-12S. doi: 10.1093/jn/126.suppl_4.1208S. PMID: 8642458.

190. Bollinger N, Hassett DJ, Iglewski BH, Costerton JW, McDermott TR. Gene expression in Pseudomonas aeruginosa: evidence of iron override effects on quorum sensing and biofilm-specific gene regulation. Journal of Bacteriology. 2001 Mar;183(6):1990-6. doi: 10.1128/JB.183.6.1990-1996.2001. PMID: 11222597.

191. Lu Y, Zhou G, Ewald J, Pang Z, Shiri T, Xia J. MicrobiomeAnalyst 2.0: comprehensive statistical, functional and integrative analysis of microbiome data. Nucleic Acids Research. 2023 Jul 5;51(W1):W310-W318. doi: 10.1093/nar/gkad407. PMID: 37166960.

192. Foster ZS, Sharpton TJ, Grünwald NJ. Metacoder: An R package for visualization and manipulation of community taxonomic diversity data. PLoS Computational Biology. 2017 Feb 21;13(2):e1005404. doi: 10.1371/journal.pcbi.1005404. PMID: 28222096.

193. Jurado-Martín I, Sainz-Mejías M, McClean S. Pseudomonas aeruginosa: An Audacious Pathogen with an Adaptable Arsenal of Virulence Factors. International Journal of Molecular Sciences. 2021 Mar 18;22(6):3128. doi: 10.3390/ijms22063128. PMID: 33803907.

194. Tian B, Hua Y. Carotenoid biosynthesis in extremophilic Deinococcus-Thermus bacteria. Trends in Microbiology. 2010 Nov;18(11):512-20. doi: 10.1016/j.tim.2010.07.007. Epub 2010 Sep 9. PMID: 20832321.

195. Rampelotto PH. Extremophiles and extreme environments. Life (Basel). 2013 Aug 7;3(3):482-5. doi: 10.3390/life3030482. PMID: 25369817.

196. Huffnagle GB, Dickson RP, Lukacs NW. The respiratory tract microbiome and lung inflammation: a two-way street. Mucosal Immunology. 2017 Mar;10(2):299-306. doi: 10.1038/mi.2016.108. Epub 2016 Dec 14. PMID: 27966551.

197. Rogers GB, Zain NM, Bruce KD, Burr LD, Chen AC, Rivett DW, McGuckin MA, Serisier DJ. A novel microbiota stratification system predicts future exacerbations in bronchiectasis. Annals of the American Thoracic Society. 2014 May;11(4):496-503. doi: 10.1513/AnnalsATS.201310-335OC. PMID: 24592925.

198. Molyneaux PL, Cox MJ, Willis-Owen SA, Mallia P, Russell KE, Russell AM, Murphy E, Johnston SL, Schwartz DA, Wells AU, Cookson WO, Maher TM, Moffatt MF. The role of bacteria in the pathogenesis and progression of idiopathic pulmonary fibrosis. American Journal of Respiratory and Critical Care Medicine. 2014 Oct 15;190(8):906-13. doi: 10.1164/rccm.201403-0541OC. PMID: 25184687.

199. Winter SE, Winter MG, Xavier MN, Thiennimitr P, Poon V, Keestra AM, Laughlin RC, Gomez G, Wu J, Lawhon SD, Popova IE, Parikh SJ, Adams LG, Tsolis RM, Stewart VJ, Bäumler AJ. Host-derived nitrate boosts growth of E. coli in the inflamed gut. Science. 2013 Feb 8;339(6120):708-11. doi: 10.1126/science.1232467. PMID: 23393266.

200. Winter SE, Bäumler AJ. Why related bacterial species bloom simultaneously in the gut: principles underlying the 'Like will to like' concept. Cell Microbiology. 2014 Feb;16(2):179-84. doi: 10.1111/cmi.12245. Epub 2013 Dec 16. PMID: 24286560.

201. Winter SE, Bäumler AJ. Dysbiosis in the inflamed intestine: chance favors the prepared microbe. Gut Microbes. 2014 Jan-Feb;5(1):71-3. doi: 10.4161/gmic.27129. Epub 2014 Jan 29. PMID: 24637596.

202. Scales BS, Dickson RP, Huffnagle GB. A tale of two sites: how inflammation can reshape the microbiomes of the gut and lungs. Journal of Leukocyte Biology. 2016 Nov;100(5):943-950. doi: 10.1189/jlb.3MR0316-106R. Epub 2016 Jun 30. PMID: 27365534.

203. Larsen JM, Musavian HS, Butt TM, Ingvorsen C, Thysen AH, Brix S. Chronic obstructive pulmonary disease and asthma-associated Proteobacteria, but not commensal Prevotella spp., promote Toll-like receptor 2-independent lung inflammation and pathology. Immunology. 2015 Feb;144(2):333-42. doi: 10.1111/imm.12376. PMID: 25179236.

204. Kovaleva J, Degener JE, van der Mei HC. Methylobacterium and its role in health care-associated infection. Journal of Clinical Microbiology. 2014 May;52(5):1317-21. doi: 10.1128/JCM.03561-13. Epub 2014 Jan 15. PMID: 24430456.

205. Waite RD, Paccanaro A, Papakonstantinopoulou A, Hurst JM, Saqi M, Littler E, Curtis MA. Clustering of Pseudomonas aeruginosa transcriptomes from planktonic cultures, developing and mature biofilms reveals distinct expression profiles. BMC Genomics. 2006 Jun 26;7:162. doi: 10.1186/1471-2164-7-162. PMID: 16800888.

206. Ortiz-Muñoz G, Looney MR. Non-invasive Intratracheal Instillation in Mice. Bio-Protocol. 2015;5(12):e1504. doi: 10.21769/bioprotoc.1504. Epub 2015 Jun 20. PMID: 27390765.

207. Yang J, Yan H. TLR5: beyond the recognition of flagellin. Cellular and Molecular Immunology. 2017 Dec;14(12):1017-1019. doi: 10.1038/cmi.2017.122. Epub 2017 Nov 20. PMID: 29151579.

208. Chao W. Toll-like receptor signaling: a critical modulator of cell survival and ischemic injury in the heart. American Journal of Physiology-Heart and Circulatory Physiology. 2009 Jan;296(1):H1-12. doi: 10.1152/ajpheart.00995.2008. Epub 2008 Nov 14. PMID: 19011041.

209. Pandey S, Kawai T, Akira S. Microbial sensing by Toll-like receptors and intracellular nucleic acid sensors. Cold Spring Harbor Perspectives in Biology. 2014 Oct 9;7(1):a016246. doi: 10.1101/cshperspect.a016246. PMID: 25301932.

210. Arora S, Ahmad S, Irshad R, Goyal Y, Rafat S, Siddiqui N, Dev K, Husain M, Ali S, Mohan A, Syed MA. TLRs in pulmonary diseases. Life Sciences. 2019 Sep 15;233:116671. doi: 10.1016/j.lfs.2019.116671. Epub 2019 Jul 20. PMID: 31336122.

211. Chiang CY, Engel A, Opaluch AM, Ramos I, Maestre AM, Secundino I, De Jesus PD, Nguyen QT, Welch G, Bonamy GM, Miraglia LJ, Orth AP, Nizet V, Fernandez-Sesma A, Zhou Y, Barton GM, Chanda SK. Cofactors required for TLR7- and TLR9-dependent innate immune responses. Cell Host Microbe. 2012 Mar 15;11(3):306-18. doi: 10.1016/j.chom.2012.02.002. PMID: 22423970.

212. Wang R, Ahmed J, Wang G, Hassan I, Strulovici-Barel Y, Salit J, Mezey JG, Crystal RG. Airway epithelial expression of TLR5 is downregulated in healthy smokers and smokers with chronic obstructive pulmonary disease. Journal of Immunology. 2012 Sep 1;189(5):2217-25. doi: 10.4049/jimmunol.1101895. Epub 2012 Aug 1. PMID: 22855713.

CURRICULUM VITAE